University of Cambridge

Doctoral Thesis

Characterisation of a Novel Leukocyte Receptor Complex-encoded Receptor TARM1

Valeria Radjabova
Darwin College

This dissertation is submitted in fulfilment of the requirements for the degree of Doctor of Philosophy in Immunology

June 2018

Abstract

Characterisation of a Novel Leukocyte Receptor Complex-encoded Receptor TARM1

Valeria Radjabova

Cellular immune responses are orchestrated by an intricate balance of activating and inhibitory signals transmitted by cell surface receptors. Perturbations in this balance by overamplified or dysregulated signalling underlie many severe immunopathologies such as sepsis and cancer. In this work I describe the identification and characterisation of a novel, evolutionarily conserved immunoreceptor encoded within the human leukocyte receptor complex and syntenic region of mouse chromosome 7, named T cell–interacting, activating receptor on myeloid cells-1 (TARM1). The transmembrane region of TARM1 contained a conserved arginine residue, consistent with association with a signalling adaptor. Co-immunoprecipitation experiments confirmed that TARM1 associated with the ITAM adaptor FcRγ but not with DAP10 or DAP12. Flow cytometric screening of cells and tissues from pathogen-free mice showed that the TARM1 protein was constitutively expressed on the cell surface of mature and immature CD11b$^+$Gr-1$^+$ neutrophils isolated from bone marrow but not at peripheral sites. Following ip LPS treatment or systemic bacterial challenge, TARM1 protein expression was upregulated by myelocytes, mature neutrophils and inflammatory monocytes and TARM1$^+$ cells were rapidly recruited to sites of inflammation. TARM1 expression was also upregulated by bone marrow–derived macrophages and dendritic cells following stimulation with TLR agonists *in vitro*. Ligation of the TARM1 receptor with specific antibody in the presence of TLR ligands, such as LPS, enhanced the secretion of proinflammatory cytokines by bone marrow–derived macrophages and primary mouse neutrophils, whereas TARM1 stimulation alone had no effect. Finally, an immobilised TARM1 Fc fusion protein suppressed CD4$^+$ T cell activation and proliferation *in vitro*. These results suggest that a putative T cell ligand can interact with TARM1 receptor, resulting in bidirectional signalling and raising the T cell activation threshold while costimulating the release of proinflammatory cytokines by macrophages and neutrophils.

Declaration of Authorship

I declare that this dissertation titled, 'Characterisation of a Novel Leukocyte Receptor Complex-encoded Receptor TARM1' and the work presented in it are my own. I confirm that:

- This dissertation is the result of my own work and includes nothing which is the outcome of work done in collaboration except as declared in the Collaborations and specified in the text.
- It is not substantially the same as any that I have submitted, or, is being concurrently submitted for a degree or diploma or other qualification at the University of Cambridge or any other University or similar institution. I further state that no substantial part of my dissertation has already been submitted, or, is being concurrently submitted for any such degree, diploma or other qualification at the University of Cambridge or any other University or similar institution.
- I have acknowledged all main sources of help.
- It does not exceed the prescribed word limit of 60,000 words.

Valeria Radjabova

Signed: _____

Date: _____

Acknowledgments

I would like to express my immense gratitude to Professor John Trowsdale for allowing me the privilege of undertaking this work and for entrusting me with great freedom to shape my research path and to develop as a scientist.

I am also deeply indebted to Dr. Alex Barrow for stimulating scientific discussions, helpful advice and for being a good friend.

I cannot express enough my appreciation for Professor Jim Kaufman. For sharing his abundant wisdom, experience and advice, for being a caring and supportive mentor who provided continuous encouragement and for humour that so greatly helped in shaping my work and personal development.

I would also like to thank Dr. Piero Mastroeni for training me in *in vivo* Salmonella models and allowing full access to his lab's resources and expertise. With Piero's generous help and care I gained invaluable experience and key experimental data for this work.

I am greatly thankful to Professor Anna Petrunkina-Harrison for giving me the opportunity to gain knowledge and experience in high-dimensional flow cytometry, for the profound care and support she has shown me over the years and for being a wonderful mentor as well as friend.

The completion of this dissertation would not have been possible without the endless patience and support of David Coppard.

Thank you.

Contents

List of Figures

List of Tables

Nomenclature

ALCL Anaplastic large cell lymphoma

APC Antigen-presenting cell

BMDC Bone marrow-derived dendritic cells

BMM Bone marrow-derived macrophages

Col Collagen

DAP12 DNAX activation protein-12

DTT Dithiothreitol

EST Expressed sequence tags

FACS Fluorescence-activated cell sorting

FcRγ Fcϵ Receptor common γ chain

G-MDSC Granulocytic myeloid-derived suppressor cells

GM-CSF Granulocyte-macrophage colony-stimulating factor

GPI Glyco-phosphatidylinositol

GPVI Glycoprotein VI

HDF Human dermal fibroblasts

HMM Hidden Markov Model

HVEM Herpes virus entry mediator

ICOS Inducible co-stimulator

IF Immunofluorescent

IgSF Immunoglobulin Superfamily

ILC Innate lymphoid cells

iNOS Inducible nitric oxide synthase

ip Intraperitoneally

IPCs Interferon producing cells

ITAM Tyrosine-based activation motif

ITAMi Inhibitory ITAM

ITIM Tyrosine-based inhibition motifs

ITSM immunoreceptor tyrosine-based switch motif

iv Intravenously

KIRs Killer cell immunoglobulin–like receptors

LAIR Leukocyte-associated Ig-like receptors

LN Lymph nodes

LPS Lipopolysaccharide

LRC Leucocyte receptor complex

MLN Mesenteric lymph nodes

NETs Neutrophil extracellular traps

NJ Neighbour-joining

ORF Open reading frame

OSCAR Osteoclast-associated receptor

PD-1 Programmed cell death 1

PD-L1 Programmed cell death 1 ligand

pDC plasmacytoid DC

PEC Peritoneal exudate cells

PPR Proline rich repeats

PTN Post-translational modifications

qPCR Quantitative polymerase chain reaction

RA Rheumatoid arthritis

RT Room temperature

SDS Sodium dodecyl sulfate

SLE Systemic lupus erythematosus

SP-D Surfactant protein D

Syk Spleen tyrosine kinase

TANs Tumour associated neutrophils

TREM Triggering receptor expressed on myeloid cells

wpi Weeks post infection

Collaborations

Animal immunisations and the generation of hybridomas secreting monoclonal anti-human and mouse TARM1 antibodies were performed in the laboratory of Professor Karsten Skjødt (Department of Immunology and Microbiology, Institute for Molecular Medicine, University of Southern Denmark, DK-5000 Odense.)

Salmonella cultures were prepared and maintained in the laboratory of Dr Piero Mastroeni, who also assisted with all animal inoculations.

Research aims

Previous work by Dr. Alex Barrow and Dr. Bernard de Bono resulted in the identification of the *TARM1* gene, a novel member of IgSF encoded within the human LRC. I set out to perform a complete characterisation of *TARM1* including genomics, phylogenetics and protein function. The work pursued the following aspects of TARM1 biology.

- **Genomics of TARM1** The starting step was to perform an extensive bioinformatic study of *TARM1* gene structure and expression using databases of expressed sequence tags and to establish a predicted amino-acid sequence of the full-length protein.
- **Phylogenetics of TARM1** It was of interest to elucidate the phylogenetic relationship of the predicted TARM1 DNA and amino-acid sequences to other members of IgSF within the LRC of the mouse and human as well as to establish whether TARM1 is present in the genomes of other species.
- **Expression of TARM1 mRNA in cells and tissues** The next step was to identify the cells and tissues with constitutive and/or inducible TARM1 gene expression and to validate the predicted TARM1 DNA sequence.
- **Generation of soluble TARM1 Fc proteins and the development of monoclonal anti-TARM1 antibodies** Once the full-length transcripts of the human and mouse TARM1 were identified, it was necessary to develop monoclonal antibodies to enable the study of TARM1 protein. I generated secreted human and mouse TARM1 Fc fusion proteins to serve as immunogens. Several cell lines expressing full-length FLAG- or HA-tagged TARM1 protein were also established to facilitate further biochemical analysis.

- **Biochemical analysis of TARM1 protein** I investigated the glycosylation status of human and mouse TARM1 proteins as well as their ability to associate with signalling adaptor molecules DAP10, DAP12 and the FcRγ.

- **Characterisation of TARM1 protein expression *in vivo* during inflammatory responses.** Based on the finding that TARM1 expression was induced by TLR signalling, I characterised the expression of TARM1 in mice during LPS-induced inflammatory response and during infection with live Salmonella typhimurim.

- **Characterisation of TARM1 protein function** In the final chapter I addressed the question of whether TARM1 protein could function as a bona fide receptor either by signalling through as yet unidentified ligand or by transducing intracellular signals that modulate the function of TARM1-expressing cells. I generated 2B4-TARM1-CD3ζ-NFAT-GFP reporter cell lines to screen for TARM1 ligand. I also used TARM1 Fc fusion protein to study the effects of TARM1 ectodomain on activation and proliferation of primary T cells. And established whether TARM1-crosslinking with monoclonal antibodies could modulate the function of TARM1-expressing cells.

Chapter 1

Introduction

Cellular function, in particular that of immune cells, is tightly controlled through the integration of signals from a large array of cell surface receptors. Therefore, the search for and characterisation of as yet unidentified immune receptors encoded within our genomes is a prerequisite for understanding immune cell function and genetic diseases. The present work adds a new member to the growing family of immune regulators belonging to the Immunoglobulin Superfamily (IgSF).

The IgSF is the largest and most functionally diverse protein family in the human genome. Ancestral genes for IgSF proteins existed more than 300 million years ago, before the divergence of birds and mammals. The evolution of the Ig-like fold can be traced back all the way to nematodes, as evidenced by the presence of large number of IgSF members (80 validated) in *C. elegans* (Vogel, Teichmann, and Chothia 2003) and in every multicellular eukaryote studied to date.

The majority of IgSF proteins are cell surface receptors with diverse tissue and cellular distributions, although secreted forms such as immunoglobulins, β_2m and a number of other soluble molecules represent rare exceptions. Despite their functional diversity, the common feature of all IgSF members is the presence of at least one or more structurally conserved Ig-like fold in their extracellular domains.

1.1 IgSF domain structure

The signature domain of the IgSF proteins, the Ig-like fold, is formed by approximately one hundred amino acid residues arranged into two anti-parallel amphipathic β-sheets, whose hydrophobic sides face each other. This arrangement is often stabilised by a disulphide bond between two conserved cysteines in the centre of each β-sheet. The stretches of amino acids joining the two β-sheets are not structurally constrained and loop outward which allows them to accommodate a high variety of sequence compositions. These intervening loops are the main sites that determine ligand specificity and allow for a large ligand diversity of IgSF proteins without compromising their conserved structural domains (A. Williams and Barclay 1988).

Although the emergence of the Ig fold long predates the evolutionary events that gave rise to its role in the adaptive immune system of jawed vertebrates (Agrawal, Eastman, and Schatz 1998), the IgSF domains are classified into four distinct sets based on their structural similarity to the immunoglobulin constant and variable domains. Thus, the IgSF fold where the number of the β strands and their relative position resemble immunoglobulin variable or constant region is termed the V-set, the C1 or C2-set, respectively. An intermediate structure between the V-set and the C-set is termed the I-set and is suggested to represent the ancestral Ig domain family (A. Williams and Barclay 1988; Harpaz, Chothia, et al. 1994).

Domains from the same set are more phylogenetically and structurally related to each other than to members of a different set (Teichmann and Chothia 2000) and form distinct clades on a phylogenetic tree. Different sets are variously represented among organisms, with the I-set being the most prevalent in lower organisms (Harpaz, Chothia, et al. 1994). C and V-sets dominate the structural repertoire of immune receptors in higher vertebrates.

The next section discusses the evolutionary origin of the LRC and describes the IgSF members comprising the human LRC.

1.2 Signaling by immune receptors through tyrosine-based activation, inhibition and switch motifs ITAMs, ITIMs and ITSMs.

The initiation and resolution of immune responses are orchestrated through a complex interplay between activating and inhibitory signals transmitted by an array of cell surface receptors. The immune system has co-opted a large number of such cell surface receptors belonging to the IgSF. Two distinct, evolutionarily conserved signalling motifs encoded within the cytoplasmic domains of many of these receptors are responsible for the initiation of inhibitory or activating signalling cascades.

The inhibitory class of immune cell receptors contains long cytoplasmic domains bearing one or more immunoreceptor tyrosine-based inhibition motifs (ITIM) with a consensus sequence defined as I/V/L/SxYxxL/V (where x denotes any amino acid) (Ravetch and Lewis L Lanier 2000). Ligand engagement of ITIM-bearing receptors results in tyrosine phosphorylation of the ITIM by Src kinase. Phosphorylated ITIM sequences are the docking sites for SH2 domain-containing lipid or protein-tyrosine phosphatases (PTPs) such as SHP-1 (Src homology region 2 domain-containing phosphatase 1), SHP-2, or the inositol-5'-phosphatase SHIP.

ITIM-recruited phosphatases SHP-1 or SHP-2 dephosphorylate key signalling components of activating receptors positioned in close proximity to the inhibitory ITIM-containing receptor leading to the dampening of cellular responses (Ravetch and Lewis L Lanier 2000). SHIP acts by translocating to the cell membrane and hydrolysing the phosphatidylinositol-3-kinase (PI3K)-generated second messenger PI-3,4,5-P3 (PIP_3) to PI-3,4-P2 (PIP_2) resulting in the suppression of cell proliferation and survival (Sly et al. 2007).

Immunoreceptor tyrosine-based switch motif (ITSM) is an ITIM-like motif with the consensus sequence TxYxxV/I (where x denotes any amino acid) that can mediate both inhibitory and activating signals depending on the associated signalling components (Cannons, Tangye, and Schwartzberg 2011). It was initially characterised in cell-surface receptors belonging to the signalling lymphocyte activation molecule family (SLAMF) with a broad expression in immune cells. Each member of the family contains one or more ITSM motifs in the cytoplasmic domain, which, when phosphorylated in humans,

serve as docking sites for SH2 domain-containing small adaptor molecules SAP and EAT-2 and enzymes such as Src-related protein tyrosine kinase (PTK), phosphatases SHP-2, SHP-1, SHIP and the inhibitory kinase Csk (Latour et al. 2003; Chemnitz et al. 2004; Feng, Garrity, et al. 2005; Eissmann et al. 2005).

2B4, a SLAM family member, is expressed on T cells and NK cells and contains four consecutive ITSMs in its cytoplasmic tail. Ligation of 2B4 on NK cell leads to the phosphorylation of tyrosines within ITSMs and the recruitment of SAP adaptor that initiates an activating signalling cascade resulting in triggering of cytolytic activity and cytokine release. However, in the absence of SAP, as seen in patients suffering from X-linked lymphoproliferative disease, the phosphorylated ITSMs recruit the inositol phosphatase SHIP-1, which inhibits signalling by activating ITAM adaptor-associated receptors (Eissmann et al. 2005).

The ITSM motifs have been identified in other receptors such as programmed death 1 (PD-1), a critical co-inhibitory receptor on T cells. The cytoplasmic tail of PD-1 contains an ITIM followed by a single ITSM (Chemnitz et al. 2004). ITIM and ITSM were shown to perform distinct but overlapping functions in PD-1 signalling. Mutagenesis of the tyrosines in these motifs indicated that ITSM is indespensable for PD-1 mediated inhibition of T cell activation (Sheppard et al. 2004; Chemnitz et al. 2004). PD-1 engagement leads to ITSM tyrosine phosphorylation and the recruitment of phosphatases SHP-1 or SHP-2 enabling the receptor to signal in an inhibitory manner (Chemnitz et al. 2004).

As opposed to the inhibitory receptors whose signalling motif-containing domain is located on the same polypeptide as the ligand-binding domain, the activating receptors usually have a modular architecture where several protein subunits with distinct roles are associated non-covalently into a functional receptor. The ligand-binding subunits have short cytoplasmic portions and are incapable of independent signal transduction. Instead, they encode a charged amino acid in the transmembrane (TM) domain, usually an arginine or a lysine, that facilitates the association with a dimeric signalling subunit of the receptor via a complementary charged TM residue. The signalling subunits contain a cytoplasmic Immunoreceptor Tyrosine-based Activation Motif (ITAM).

Two main ITAM-bearing adaptors, the FcϵR common γ chain (Fc$R\gamma$) and the DNAX activation protein 12 (DAP12) are shared by numerous immunoreceptors expressed on

NK and myeloid cells. Signalling cascades initiated by the ITAM motif have been studied extensively since its identification by Reth et al. over two decades ago. ITAM sequences contain two conserved tyrosines according to the consensus YxxL/I-$(x)_{6\text{-}8}$-YxxL/I (where x represents any residue) (Reth 1989) where the tyrosines are phosphorylated by Src family kinases upon the engagement of the ligand-binding subunit. The phosphorylated tyrosines become a docking site for a number of kinases which initiate an activating cascade culminating in, among others, calcium flux and the activation of transcription factor NF-κB (J. A. Hamerman and Lewis L Lanier 2006).

The paradigm of ITAM as a transducer of activating signals originated from studies of ITAM signalling properties in the context of high-avidity antibody cross-linking of the associated antigen receptors. Under these conditions a strong induction of the NF-κB and MAP kinases leading to cell activation was observed. Mounting evidence suggests, however, that the functional outcome of ITAM mediated signalling is strongly influenced by the cellular and molecular context and can result in either activation or inhibition of cellular responses as discussed below.

This functional ITAM heterogeneity provides an explanation for the behaviour of the IgA. The IgA receptor FcαRI associates with an ITAM-bearing adaptor FcRγ and can elicit cellular activation but can also suppresses cytokine secretion (Wolf et al. 1994) and signalling by a variety of activating receptors such as TLRs, cytokine receptors and TNF receptors (Pasquier et al. 2005; Kanamaru et al. 2008). Ligation of the FcαRI by a monomeric IgA in the absence of an antigen or by an anti-FcαRI Fab delivers an inhibitory signal and can attenuate a plethora of cellular functions such as phagocytosis, oxidative burst and cytokine secretion (Nikolova and Russell 1995; Pasquier et al. 2005; Kanamaru et al. 2008). Conversely, co-aggregation of FcαRI by multimeric IgA immune complexes initiates an activating signalling cascade (Kanamaru et al. 2008; Pasquier et al. 2005).

Bifunctional signalling is also described for a number of DAP12-associated receptors. DAP12 was initially identified as a signalling subunit of several activating NK cell receptors in humans and mice (Lewis L Lanier et al. 1998; K. M. Smith et al. 1998). Several recent studies described DAP12 associated receptors including triggering receptor expressed on myeloid cells (TREM)-2 (J. Hamerman et al. 2006; Turnbull et al. 2006), NKp44 (Fuchs et al. 2005) and Siglec-H (Blasius et al. 2006) where DAP12 was

involved in an inhibitory pathway and where the absence of DAP12 led to enhanced cellular responses to TLR ligands (J. A. Hamerman, Tchao, et al. 2005).

For example, ligation of Siglec-H, a sialic acid-binding Ig-like lectin, expressed on interferon producing cells (IPCs), was shown to reduce IFN-α secretion in response to TLR9 agonist (Blasius et al. 2006). A similar outcome was shown for NKp44 ligation on IPCs. NKp44, an IgSF member, that was originally identified on human activated NK cells, where it triggered the release of IFN-γ and cytotoxicity against tumour and virus-infected cells (Vitale et al. 1998; Arnon et al. 2001), was shown to suppress TLR9 signalling and production of IFN-α (Fuchs et al. 2005). Macrophage activation by TLR ligation can be inhibited by DAP-12 associated TREM-2. Macrophages in which TREM-2 was knocked down with shRNA construct secreted more TNF in response to TLR ligands (J. Hamerman et al. 2006). This phenotype is reproduced in DAP-12 deficient macrophages that produce higher concentrations of proinflammatory cytokines TNF, IL-6 and IL-12 p40 in response to TLR stimulation than wild type cells (J. A. Hamerman, Tchao, et al. 2005).

The signalling dichotomy of the ITAM motif led to the adoption of the term inhibitory ITAM (ITAMi).

1.2.1 Inhibitory ITAM

The molecular mechanism responsible for the dual action of ITAMs is only beginning to be unravelled. In the classical model of ITAM signalling, the dually phosphorylated tyrosines in the ITAM recruit kinases spleen tyrosine kinase (Syk) and/or Zap-70 which bind doubly phosphorylated ITAMs through their tandem SH2 domains, leading to cellular activation (J. A. Hamerman and Lewis L Lanier 2006). However, suboptimal activation of ITAM adaptor as in the case of monovalent antibodies and low-avidity ligands results in an inhibitory ITAM signalling (Pasquier et al. 2005; Kanamaru et al. 2008).

The study of the FcαRI inhibitory signalling revealed that a suboptimal receptor ligation, with either monovalent IgA or an anti-FcαRI Fab, results in ITAM phosphorylation on one of the two tyrosines and leads to the preferential recruitment of SHP-1 phosphatase instead of Syk (Kanamaru et al. 2008; Ganesan et al. 2003; Pfirsch-Maisonnas

et al. 2011). Syk is nevertheless important in the inhibitory signalling pathway as demonstrated in Syk deficient macrophages. In the absence of Syk macrophages exhibit identical phenotype to DAP-12 deficiency and are more sensitive to activation by TLR ligation (J. A. Hamerman, Tchao, et al. 2005).

In addition to FcαRI, TREM2, NKp44 and Siglec-H, ITAMi is described for a large number of immunoreceptors among which are FcγRIII (Da Silva et al. 2007), LILRA (D. J. Lee et al. 2007), ILT7 (Cao et al. 2006), MHC class II (Liang et al. 2008) and others, that will act as inhibitors of cellular activation in certain contexts.

It was also found that pathogens such as *E. coli* can exploit ITAMi to achieve immune evasion during infection. For example, non-opsonised *E. coli* can evade phagocytosis through macrophage class A scavenger receptor MARCO by binding with low avidity to the FcγRIII. Under these conditions, the tyrosines in the FcγRIII associated ITAM adaptor Fcγ are not fully phosphorylated which leads to a strong recruitment of the phosphatase SHP1. In turn, SHP1 proceeds to dephosphorylate downstream signalling mediators such as PI3 kinase and inhibits phagocytosis (Da Silva et al. 2007).

1.3 Regulation of T cell responses

T cell populations act both as powerful effectors of immune function and as a safeguard against inappropriate immune activation thus ensuring tolerance. Maintenance of this balance is the result of a delicate interplay between a plethora of co-stimulatory and co-inhibitory signals transduced by T cell receptors. Continuous integration of these signals determines the functional outcome of T cell responses.

This section reviews the immunoregulatory mechanisms that shape T cell function and fate during immune homeostasis and disease.

1.3.1 Families of T cell co-signalling IgSF molecules

Our understanding of T cell activation originates from the early findings that led to the development of a two-signal model of B and T cell activation (Lafferty and Cunningham 1975). The first signal in the T cell activation requires the engagement of the T cell receptor (TCR) by a specific ligand-bound MHC. This interaction is highly sensitive and

requires only a few MHC molecules (Sykulev et al. 1996). The second signal, delivered by a co-stimulatory receptor, is required for a productive initiation of T cell responses. CD28 was identified as one of the most effective constitutively expressed co-stimulatory receptors on T cells. Engagement of CD28 by its ligands B7-1 (CD80) or B7-2 (CD86) expressed on antigen presenting cells (APCs) simultaneously with TCR engagement provides the necessary second stimulus. In the absence of CD28 ligation, T cells enter a state of anergy characterised by hyporesponsiveness to subsequent activating stimuli or undergo apoptosis (Harding, Gross, et al. 1992). As our understanding of T cell regulation is improving and more co-signalling receptors are being characterised, the two-signal paradigm of B7-CD28 is being expanded.

A majority of co-signalling receptors characterised to date belong to the IgSF and tumour necrosis factor receptor families. Within the IgSF, several subfamilies have been identified. The most well-characterised are the CD28 and B7 families. With some exceptions, B7 related receptors interact with receptors related to CD28. Exceptions include the receptor B and T lymphocyte attenuator (BTLA), a negative regulator of lymphocytes that interacts with a member of the tumour necrosis factor receptor family and herpes virus entry mediator (HVEM) (Sedy et al. 2005). HVEM has a broad expression pattern and is present on T cells. Although numerous studies implicated HVEM as a co-stimulatory molecule, T cells isolated from HVEM deficient animals are hyper-reactive to activating stimuli and the animals are more susceptible to autoimmune conditions (Yang Wang et al. 2005). Recently, the interaction of HVEM on T cells with BTLA-expressing DCs was shown to drive the conversion to Foxp3$^+$ T regulatory cells and the establishment of tolerance (A. Jones et al. 2016).

Butyrophilin (BTN) and BTN-like (BTNL) family molecules resemble B7 family members in their extracellular domains and carry a B30.2 domain in the cytoplasmic tails. BTN and BTNL proteins have a complex tissue and cell expression patterns and their function and the mechanism of action are only beginning to be understood. *In vitro* assays have demonstrated that some BTN proteins inhibit T cell activation and proliferation via an unidentified ligand on T cells (I. A. Smith et al. 2010). The isoforms of BTN3 have been shown to play a critical role in the activation of $\gamma\delta$ TCR by phosphoantigens via a novel antigen presentation mechanism (Vavassori et al. 2013; Sandstrom et al. 2014).

Inducible co-stimulator (ICOS) is another important co-stimulating member of IgSF related to CD28 (Hutloff et al. 1999). As the name indicates, ICOS expression is induced on the surface of CD4 and CD8 T cells following antigen-specific TCR signalling and/or CD28 co-stimulation (Hutloff et al. 1999). Similarly to its homologue CD28, ICOS binds to a B7-like ligand expressed predominantly by B cells, macrophages and DCs but also by some endothelial cells (Yoshinaga et al. 1999; Aicher et al. 2000; Khayyamian et al. 2002). Early studies in ICOS and ICOS ligand (ICOSL) deficient mice indicated that ICOS is involved in thymus dependent antibody responses and regulates various T helper cell subsets in the context of infection, mainly by promoting or inhibiting Th1 and Th2 responses. More recently, ICOS signalling was found to play a role in controlling the responses of germinal centres by directing functional differentiation and maintenance of follicular helper T cells and follicular regulatory T cells (Leavenworth et al. 2015).

One of the most critical and well-studied negative co-regulators of T cells is CTLA-4. CTLA-4 expression is upregulated on conventional T cells following activation, where it competes with CD28 for binding to CD80 and CD86 on APCs. This interaction leads to inhibition of T cell activation and safeguards against T cell hyperactivation (Walunas et al. 1994). The critical role of CTLA-4 in maintaining T cell homeostasis is illustrated by the fact that a genetic disruption resulting in the loss of CTLA-4 expression is fatal within weeks after birth due to a severe autoimmune organ failure (Tivol et al. 1995).

PD-1 is another important co-inhibitory receptor that regulates the balance between T cell activation and tolerance (Keir et al. 2008). PD-1 is a member of the IgSF and contains an ITIM and ITSM in its intracellular domain. PD-1 expression is not detected on resting T cells but can be induced by TCR ligation and T cell activation. PD-1 ligands, PD-L1 and PD-L2 are related to the B7 family members and are expressed on lymphoid and nonlymphoid tissue. PD-L1 expression is observed on activated T cells and there is evidence for a bi-directional signalling for PD-L1. T cell expressed PD-L1 has been shown to bind B7-1 (CD80) with affinity intermediate to B7-1 interaction with CTLA-4 and CD28. B7-1/PD-L1 binding inhibits T cell activation and cytokine secretion (Butte et al. 2007).

ITMS of PD-1 can associate with both SHP-1 and SHP-2 following T cell stimulation, although, the ligation of PD-1 by its ligand favours the recruitment of SHP-2 (Chemnitz

et al. 2004). During TCR engagement by an APC, PD-1 accumulates at the immunological synapse (Pentcheva-Hoang et al. 2007). Engagement of PD-1 in proximity to the antigen receptor complex and the recruitment of SHP-2 results in the preferential dephosphorylation of the CD28 (Hui et al. 2017; Kamphorst et al. 2017) and potentially TCR (Bennett et al. 2003; Sheppard et al. 2004) signalling intermediates. The effectiveness of PD-1 mediated inhibition is inversely related to the extent of T cell activation and can be overcome by CD28 engagement or high exogenous IL-2 (Bennett et al. 2003).

PD-1 and CTLA-4 inhibit T cell activation through distinct and potentially synergistic pathways. CTLA-4 acts primarily at the very early stages of T cell activation and regulates the magnitude of the response by competing with the co-stimulatory CD28 molecule and by transducing an inhibitory signal to the T cell. PD-1 regulates ongoing immune responses and is responsible for T cell exhaustion during chronic viral infections (Kaufmann and Walker 2009) and in the tumour microenvironment (R. H. Thompson et al. 2007). High levels of PD-L1 expression are seen on a variety of tumours and on many tumour-associated APCs and T cells. PD-L1 expression is induced and maintained by a number of pro-inflammatory cytokines. It is thought that tumour-associated effector T cell-derived IFN-γ is partially responsible for high expression levels of PD-L1 in this setting, which contributes to the establishment of an immunosuppressive microenvironment and tumour immune-evasion (Curiel et al. 2003; Ghebeh et al. 2006; Kuang, Zhao, Peng, et al. 2009; Taube et al. 2012). PD-1/PD-L1 pathway blockage has shown varied success in reversing tumour immune-suppression in a number of clinical trials and a variety of solid and hematologic malignancies. Current clinical data indicates that PD-1 pathway blockade resulted in significant antitumor activity in patients with, among others, advanced melanoma and metastatic bladder cancer (Hamid et al. 2013; Powles et al. 2014).

Many T cell co-regulatory receptors have been identified in recent years. As our knowledge and understanding of the complexity of their interplay increases, every receptor with immunomodulatory function may represent a potential target for therapeutic intervention.

Besides adaptive immune cells, such as T- and B-lymphocytes, coactivating and coinhibitory IgSF receptors are expressed on innate cells e.g. monocytes, macrophages, neutrophils and dendritic cells, innate lymphoid cells (ILCs), Natural Killer cells, and

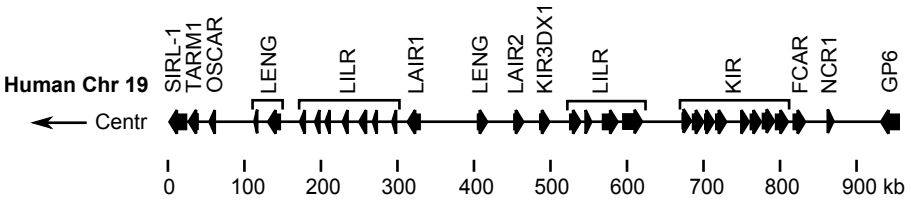

FIGURE 1.1: Human LRC located on chromosome 19q13.4

even on non-classical immune cells, such as platelets and osteoclasts, where they are predicted to play critical immunoregulatory roles during tissue homeostasis and disease.

Many of such coactivating and coinhibitory receptors that typify this broad expression profile on innate and adaptive immune cells are encoded in a large conserved cluster present in all mammalian genomes termed the leucocyte receptor complex (LRC). The LRC is particularly important since many of the receptors encoded within this region recognise MHC class I molecules strongly associated with disease. This region also contains other IgSF members critical for osteoclastogenesis (e. g. OSCAR) and platelet function (e. g. GPVI).

1.4 The LRC and its genes

In humans, the LRC is located on chromosome 19q13.4 (Fig. 1.1). A number of key findings point to the origin of the LRC in the distant evolutionary past, before the divergence of mammalian and avian lineages. Syntenic LRC regions have been identified in every mammalian genome studied so far, with many LRC-encoded genes well conserved across species. The notion of a single evolutionary origin of the LRC genes is also supported by the identification of a number of homologous Ig-like sequences in chickens (Dennis, Kubagawa, and Cooper 2000; Nikolaidis, J. Klein, and M. Nei 2005), amphibians (Guselnikov et al. 2010) and teleosts (Stafford et al. 2006; Yoder et al. 2001).

The LRC region in humans spans roughly 1Mb of genomic DNA and, until recently, the boundaries for the canonical LRC region were set at osteoclast-associated receptor (*OSCAR*) on the centromeric side and glycoprotein VI (GPVI) on the telomeric side. The work in our group and by Steevels et al (Steevels, Lebbink, et al. 2010) led to the identification and characterisation of additional genes encoding Ig-like receptors *TARM1* and *SIRL-1* located at the centromeric side of the LRC adjacent and related to OSCAR.

These genes mark the new centromeric boundary of and are likely the last remaining Ig-like immunoreceptors in the LRC.

1.4.1 OSCAR

OSCAR is a key costimulatory receptor expressed on osteoclasts where it regulates osteoclastogenesis in human and mouse (A. Barrow, N. Raynal, et al. 2011). In mouse OSCAR expression is restricted to osteoclasts, in human, OSCAR is also expressed on monocytes, macrophages, neutrophils and dendritic cells where it plays a role in innate immune responses by supporting cell activation and differentiation, antigen presentation and the release of pro-inflammatory mediators (Merck, Gaillard, Scuiller, et al. 2006; Merck, Gaillard, Gorman, et al. 2004).

The function of OSCAR on monocytes has been addressed by several groups showing that ligation of OSCAR by cross-linking antibodies promoted cell survival and induced the release of multiple chemokines, while cross-linking of OSCAR in conjunction with TLR stimulation, enhanced the secretion of TLR-induced proinflammatory cytokines (Merck, Gaillard, Scuiller, et al. 2006). Barrow et al. demonstrated that collagens (Col) I, II and III (A. Barrow, N. Raynal, et al. 2011) and the collagenous protein Surfactant Protein D (SP-D)(A. D. Barrow et al. 2015) are the physiological ligands for OSCAR. In vitro treatment of human peripheral blood monocytes or monocyte-derived DCs with ColII promoted their survival in the absence of growth factors and the effect was dependent on OSCAR signalling (Schultz, Nitze, et al. 2015; Schultz, L. Guo, et al. 2016). OSCAR-ColII interaction on monocytes induced upregulation of activation markers and secretion of 14 proinflammatory mediators including TNF-α, IL-8, IL-1β and MIP-1α (Schultz, L. Guo, et al. 2016). OSCAR-Col interaction has been implicated in the pathogenesis of rheumatoid arthritis (RA). Fragments of ColII are present in the synovial fluid of RA patients with ongoing disease. Monocytes of these patients express elevated levels of OSCAR, have activated phenotype and infiltrate the synovium inflamed joints. Schultz et al. hypothesize that OSCAR signalling on monocytes may contribute to the sustained inflammation and joint damage in RA patients (Schultz, L. Guo, et al. 2016). Barrow et al. also showed that OSCAR is expressed on the cell surface of inflammatory interstitial lung and blood $CCR2^{+}$ monocytes from patients with chronic obstructive pulmonary disease. Engagement of OSCAR on these cells by SP-D,

a secreted product of alveolar epithelial cells, induced TNF-α release (A. D. Barrow et al. 2015).

Telomeric to OSCAR is the Leukocyte Ig-Like Receptors (LILR) comprised of 13 members, that, due to an inverted duplication (Wende, Volz, and Ziegler 2000), are separated into two clusters flanking the Leukocyte-Associated Ig-like Receptors (LAIR)-1 and -2, LENG (an unrelated, non IgSF encoding gene) and the KIR3DX1 gene.

1.4.2 LILRs

LILRs are expressed on the surface of cells in the lymphoid and myelomonocytic lineages. Ligation of these receptors has been shown to have profound immunomodulatory effects such as regulation of classical and non-classical HLA class I (Marco Colonna, Navarro, et al. 1997; Allan et al. 1999; Lepin et al. 2000; Navarro et al. 1999; Shiroishi, Tsumoto, et al. 2003; Marco Colonna, Samaridis, et al. 1998). LILRs are grouped into two functional categories; the inhibitory receptors, termed LILRB, and the activating variants, denoted LILRA. The importance of LILR immunomodulatory capacity came to prominence when Chang *et al.* demonstrated that LILRB2 and LILRB3 lie at the heart of DC functional plasticity by providing the inhibitory signalling necessary for the acquisition of tolerogenic properties by immature DCs(C.-C. Chang et al. 2002).

Moreover, the activating LILRA1 was shown to bind to a β_2m-free HLA-B27 allele, while the inhibitory LILRB2 can engage both the unfolded, β_2m-free HLA-B27 and the non-classical HLA-G (Shiroishi, Kuroki, et al. 2006; Allen, Raine, et al. 2001).

Classical HLA molecules are highly polymorphic and a recent comprehensive analysis of LILR binding to over 90 HLA class I antigens demonstrated that the binding affinity was strongly influenced by the HLA allelic variation (D. C. Jones et al. 2011). This represents a significant finding as unfolded HLA is a hallmark of activated lymphocytes (Schnabl et al. 1990; Allen, O'Callaghan, et al. 1999; Madrigal et al. 1991), thus certain HLA genotypes may underlie the perturbations in the balance between the activating and inhibitory LILR signalling and may influence disease outcomes. This scenario is exemplified by recent findings pointing to an important role for LILRs in the progression of HIV-1 infection. LILRB2 interaction with HLA in patients was found to correlate with the ability of the immune system to control the virus (Lichterfeld and G. Y. Xu 2012;

Bashirova et al. 2014). A recent study found a novel function for an orphan activating receptor LILRA2. Hirayasu et al. showed that LILRA2 acts as innate immune receptor that detects microbially cleaved immunoglobulins associated with bacterial infections (Hirayasu et al. 2016).

1.4.3 Leukocyte-associated immunoglobulin-like receptor I and II (LAIR-I and -II)

LAIR-I and -II are located in the middle of the LILR cluster and contain a single C2-type Ig-like domain. The characterisation of LAIRs revealed a previously unrecognised immunoregulatory mechanism effected through binding to collagen in the extracellular matrix (Lebbink, Nicolas Raynal, et al. 2009) and to the collagenous C-type lectin surfactant protein D (SP-D) present at mucosal surfaces where it is involved in host defense against infections (Nordkamp et al. 2014). LAIR-I is an inhibitory receptor constitutively expressed by the majority of peripheral blood mononuclear leukocytes (Linde Meyaard, Adema, et al. 1997) and during early osteoclast development. LAIR-II is its soluble counterpart that acts as a LAIR-I antagonist by competing for the collagen binding sites (Lebbink, Berg, et al. 2008; L. Meyaard 2008).

Although the precise nature of LAIR-I mediated immune regulation *in vivo* remains poorly defined, numerous studies using antibodies cross-linking LAIR-I showed its ability to inhibit the function of many immune cells *in vitro* such as NK (Linde Meyaard, Adema, et al. 1997), T cells (Maasho et al. 2005; Linde Meyaard, Hurenkamp, et al. 1999), plasmacytoid DC (Bonaccorsi et al. 2010) and the differentiation of hematopoietic progenitors (Poggi et al. 1998).

For instance, heterogeneous expression of LAIR-I has been reported for T cells, where naive T cells express the highest level. Crosslinking of LAIR-I on human peripheral blood naive (Maasho et al. 2005) or cytotoxic T effector cells (Linde Meyaard, Hurenkamp, et al. 1999) attenuates T cell function such as TCR signalling and cytotoxic responses suggesting LAIR-I signalling may provide an important regulatory input during both the very early T cell activation and later at the effector stage.

Similarly, LAIR-I, highly expressed on plasmacytoid dendritic cells, was found to inhibit IFN-α production in response to TLR stimulation (Bonaccorsi et al. 2010).

1.4.4 Killer cell immunoglobulin–like receptors (KIRs)

KIRs are a large family of highly polymorphic receptors that have been intensively studied over the past decades. KIRs are thought to represent a relatively recent evolutionary development as no KIR homologues have as yet been identified in non-mammalian vertebrates. The KIR receptors are expressed on natural killer (NK) cells and cytotoxic T cells and have been implicated as major players in the regulation of a wide range of cell functions, from anti-tumour activity to human reproduction (Parham and Moffett 2013). KIRs exhibit a striking haplotype and gene copy number diversity as well as a high degree of allelic polymorphism and have been shown to recognise HLA class I molecules with each KIR exhibiting strong preference for a specific HLA-C allotype (Yawata et al. 2008). Some KIRs containing three Ig-like domains bind certain HLA-A and -B alleles (L. Moretta and A. Moretta 2004).

Binding of the inhibitory KIRs expressed by NK cells to cognate HLA class I ligands on target cells safeguards against non-specific NK cell-mediated cytotoxicity against healthy cells and is the fundamental principle behind missing self recognition. Many pathogenic states are characterised by the downregulation of HLA class I expression on the cell surface as seen during viral infections or cancer. This serves to relieve the inhibitory signals normally conferred by the KIR receptors and primes NK cells for cytotoxic killing of target cells. Several classes of stimulatory receptors expressed by NK cells can then either recognise virally encoded epitopes or stress ligands expressed by diseased cells and initiate NK cytotoxic responses (Raulet 2006).

KIR genes are comprised of two functional haplotype groups, A and B, and are present in all human populations at varying frequencies. KIR A haplotypes encode alleles that are strongly inhibitory in the presence of HLA-C2 and alleles that are weakly inhibitory HLA-C1 receptors. In contrast, KIR B haplotypes encode weak inhibitory HLA-C2 receptors and strong inhibitory HLA-C1 receptors (Yawata et al. 2008). Numerous studies have demonstrated that the different possible combinations of KIRs and HLA and the high degree of polymorphism within both molecules is associated with susceptibility or resistance to disease such as viral infections, autoimmunity and cancer (Purdy and Campbell 2009). Moreover, the mismatch between the maternal KIR genotype and fetal HLA-C has been shown to influence the risk of developing pre-eclampsia and affect the reproductive success (Hiby et al. 2004).

1.4.5 FcaR, NCR1 and GpVI

Telomeric to the KIR gene cluster are the Fc receptor for IgA (FCAR), the natural cytotoxicity receptor (NCR1, also known as Nkp46 receptor in humans), and the platelet collagen receptor, Glycoprotein VI (GpVI) (A. Barrow and J. Trowsdale 2008). NCR1 is an activating member of the IgSF with two C2-type Ig-like domains in the extracellular portion, a short cytoplasmic tail and a charged arginine in the transmembrane domain. NCR1 is well-conserved in mammals and is expressed on the surface of all mature NK cells where it mediates NK cytotoxic activity against target cells by recruiting ITAM-bearing adaptors (Walzer et al. 2007).

GpVI is a major signalling receptor for collagen expressed by platelets (Kehrel et al. 1998). It is triggered by binding to collagen present in the exposed extracellular matrix in the context of blood vessel injury. The interaction leads to a rapid platelet activation and the formation of platelet plug followed by coagulation cascade. Similarly to other activating members of the LRC, GPVI recruits ITAM-bearing adaptor for signal transduction (Nieswandt and Watson 2003).

1.4.6 SIRL-1

A new immune receptor, Signal Inhibitory Receptor on Leukocytes-1 (also known as VSTM-1), was recently identified at the telomeric boundary of the LRC. SIRL-1 contains a single Ig-like V-set domain and encodes two ITIMs in the cytoplasmic tail. Steevels et al showed that it is highly expressed on human neutrophils and monocytes where it plays a role in the negative regulation of cell functions such as oxidative burst and release of neutrophil extracellular traps (NETs) (Steevels, Lebbink, et al. 2010; Steevels, Avondt, et al. 2013; Van Avondt et al. 2013). Numerous recent findings suggest a role for neutrophils in the regulation of adaptive immune responses and implicate dysregulation of neutrophil function in a variety of autoimmune conditions such as Systemic lupus erythematosus (SLE) (Lande et al. 2011). SLE is characterised by the presence of antibodies to self-antigens such as double-stranded DNA. Abberant NET formation by neutrophils is thought to contribute to the disease pathogenesis by exposing nuclear DNA within the NETs to self-reactive B cells leading to production of autoantibodies (Lande et al. 2011). Cross-linking of SIRL-1 on neutrophils from SLE patients was shown

to inhibit NETs formation and can represent a target for therapeutic intervention in the treatment SLE (Steevels, Lebbink, et al. 2010; Steevels, Avondt, et al. 2013; Van Avondt et al. 2013).

1.5 Neutrophil-mediated immune regulation

Neutrophils have long been viewed as short-lived, terminally differentiated, innate effector cells specialised for antimicrobial responses. Evidence accumulated over the past two decades puts into question this long-standing view and tells a new fascinating story of this underappreciated cell type.

It is now clear that under certain conditions the neutrophil life-span is extended and new neutrophil subsets are generated through hematopoietic proliferation or recruited from the pool of tissue-resident neutrophils. These cells can then actively modulate innate and adaptive immune responses by engaging in complex bi-directional interactions with a variety of immune cells (Mantovani et al. 2011; Pelletier et al. 2010). Another aspect that has recently emerged from studies of various immune pathologies is the presence of heterogeneous neutrophil populations composed of mature and immature cells with distinct, and often opposing, functions. It has proven extremely difficult to study this heterogeneity due to the lack of unique markers that would define discrete neutrophil subsets and their functions. The matter is further complicated by the fact that different neutrophil populations emerge under different pathological states. It is, however, now firmly accepted that neutrophils play an important role in conditions ranging from sepsis and autoimmunity to cancer.

Neutrophil cross-talk with immune cells The ability of neutrophils to interact with other immune cells, whether through cell-to-cell contact or through soluble mediators, has been demonstrated in multiple studies of *ex vivo* cells. For instance, *ex vivo* culture of human or murine neutrophils in the presence of IFN-γ, GM-CSF and IL-3 causes neutrophils to acquire a DC-like phenotype, become less susceptible to apoptosis and to be able to prime antigen-specific T cell responses (Brach, Gruss, Herrmann, et al. 1992; Colotta et al. 1992; Gosselin et al. 1993; Fanger et al. 1997; Oehler et al. 1998). Other studies show that even in the absence of exogenous cytokines, antigen-pulsed neutrophils can present in an MHC II-dependent manner to antigen-specific T cells and induce their

polarisation towards a proinflammatory Th1 or Th17 phenotype (Abdallah et al. 2011; Radsak et al. 2000).

In vivo, neutrophils were found to traffic antigens or live bacilli to draining lymph nodes (Abadie et al. 2005; Chtanova et al. 2008) and cross-present to prime naive $CD8^+$ T cells (Tvinnereim, S. E. Hamilton, and Harty 2004; Beauvillain et al. 2007). Neutrophil-DC cross-talk was shown to either enhance or inhibit the function and survival of both cell types depending on the tissue localisation and the immune status. This interaction was found to be mediated through direct cell contact (Gisbergen, Sanchez-Hernandez, et al. 2005; Gisbergen, Ludwig, et al. 2005) and/or through the release of immune mediators.

Activated neutrophils are known to release reactive oxygen species, cytokines, chemokines and extracellular vesicles containing immunoregulatory factors that are chemotactic for other immune cells and regulate their responses. For instance, *in vitro* stimulated neutrophils enhance DC maturation and their ability to stimulate T cell proliferation and polarisation through the release of TNF-α and direct cell contact (Gisbergen, Sanchez-Hernandez, et al. 2005; Gisbergen, Ludwig, et al. 2005). In co-culture, DCs upregulate CD40, CD86 and HLA-DR and acquire antigens from live neutrophils in a cell-contact dependent manner (Megiovanni et al. 2006). *In vitro* findings have been corroborated *in vivo* where inflammatory sites in the colonic mucosa of Crohn's disease patients were found to contain neutrophils interacting with DCs (Gisbergen, Sanchez-Hernandez, et al. 2005). Neutrophil-DC interactions have been implicated in the pathogenesis of other autoimmune and inflammatory diseases such as SLE (Lande et al. 2011), RA (Khandpur et al. 2013) and T1D (Diana et al. 2013). In the context of autoimmune conditions, activated neutrophils were found to be more prone to undergo NETosis, a process whereby neutrophils extrude large quantities of nuclear DNA bound to a variety of autoantigens in the form of web-like structures called neutrophil extracellular traps (NETs). This self-DNA-autoantigen complexes were found to activate plasmacytoid DC (pDC) to produce type I interferons and to trigger aberrant adaptive immune responses, such as activation of autoreactive B cells, culminating in the production of autoantibodies to both the self-DNA and the autoantigen peptides present within the NETs (Lande et al. 2011; Khandpur et al. 2013).

Numerous studies have also demonstrated neutrophil-mediated regulation of other immune cells. In recent years research interest has focused on the neutrophil-mediated

regulation of T cells particularly during tumourigenesis and sepsis. Cytotoxic T cells are the major effector cells in the anti-tumour immunity but are rendered non-functional by the suppressive tumour microenvironment. In murine models of cancer and later in human patients, neutrophils were shown to infiltrate the tumour mass, pre-metastatic and metastatic tissues where they took an active part in either limiting tumour growth through the release of soluble factors and by supporting anti-tumour immune responses or promoting tumourigenesis by enhancing tumour-driven inflammation, angiogenesis and contributing to T cell suppression (Tazzyman, Lewis, and Murdoch 2009; Fridlender et al. 2009).

Neutrophils with T cell regulatory properties are often referred to as granulocytic myeloid-derived suppressor cells (G-MDSC). Initially, MDCSs were described in murine models of cancer and characterised as a heterogeneous population of mainly immature neutrophils and monocytes capable of T cell suppression. This population has since been described in late stage human cancers and is associated with unfavourable prognosis.

Conflicting data on the role of neutrophils in cancer comes from studies of murine models and human patients. This stems from the great phenotypic and functional heterogeneity of neutrophils and the differences in murine and human pathologies. Mouse tumours are routinely induced using aggressive, rapidly growing tumour cell lines that, most likely, represent advanced stages of tumour development in humans where the immune-suppressive microenvironment is fully established. In contrast, human tumours develop very slowly while undergoing repeated rounds of immune selection (Eruslanov 2017).

Although the majority of research on neutrophils in human cancer uses peripheral blood, a few recent high quality studies using human early-stage lung tumour tissue provide fascinating insight into the role of tumour associated neutrophils (TANs). In these studies, small, early-stage tumours showed infiltration with immature neutrophils that differentiated into a hybrid cell population exhibiting characteristics of canonical neutrophils and APCs (APC-like hybrid TANs). The differentiation was driven by low amounts of tumour-derived IFNγ and GM-CSF. The APC-like hybrid TANs acquired new functions such as the ability to augment or directly stimulate antigen-dependent and independent memory and effector T cell responses, and capture and cross-present tumour antigens. This cell subset was only found in small early-stage tumours and was not present in

larger, more advanced tumours (Eruslanov et al. 2014; Singhal et al. 2016). These findings are in agreement with previous data reported by other groups showing that both mouse and human neutrophils can be induced to acquire APC-like functions when cultured in the presence of IFN-γ, GM-CSF and IL-3 (Gosselin et al. 1993; Fanger et al. 1997; Oehler et al. 1998; Abdallah et al. 2011; Radsak et al. 2000).

In contrast to human data, a recent study of murine model of invasive breast cancer demonstrated that early in the malignant conversion, tumour-secreted G-CSF triggers myeloid expansion in the bone marrow and drives the hematopoietic cells towards an alternative differentiation generating T cell suppressive neutrophils (Casbon et al. 2015).

Neutrophils were shown to modulate T cell function in other contexts such as transplantation and acute systemic inflammatory reactions. Acute inflammation is known to be associated with a rapid mobilisation of mature and immature neutrophils. Pillay et al identified a unique population of mature human neutrophils that are released into the circulation in patients with severe injury or following intravenous (iv) LPS challenge in healthy volunteers. These cells showed a hypersegmented nuclear morphology characteristic of more mature neutrophils, were $CD62L^{dim}$ and were able to strongly suppress T cell proliferation *in vitro*. This suppression was mediated by a localised release of H_2O_2 into the immunological synapse between neutrophils and T cells. The synapse formation depended on the integrin Mac-1 and the suppression could be relieved with blocking anti-Mac-1 antibodies (Pillay et al. 2012). Peripheral blood neutrophils from healthy donors could not be induced to acquire suppressive phenotype *in vitro* suggesting that the mature suppressive population is recruited from the tissues under particular conditions of systemic inflammation (Pillay et al. 2012).

It is now beyond any doubt that neutrophils are important players in shaping both innate and adaptive immune responses. Our understanding of the mechanisms employed by the variety of neutrophil/G-MDSC and the specific conditions that lead to the emergence of the functional heterogeneity is still rudimentary.

The work presented in this dissertation describes the identification and characterisation of TARM1, a novel IgSF member expressed by activated neutrophils/G-MDSC. TARM1 expressing cells are mobilised during acute inflammatory responses and TARM1 protein is capable of suppressing T cell activation and proliferation *in vitro*. TARM1 may

represent a novel receptor employed by G-MDSC to control T cell proliferation during inflammation.

Chapter 2

Materials and methods

2.1 Bioinformatics

2.1.1 Novel gene identification

The *TARM1* gene was identified in the NCBI human genome database (NCBI 2009) using the Hidden Markov Model (HMM) designed by Dr Bernard de Bono in collaboration with Dr Alexander Barrow. The algorithm parameters were adjusted to identify novel IgSF members that contained the following elements: a) a leader peptide sequence for surface expression, b) at least one immunoglobulin-like domain, and c) either a charged transmembrane residue and/or one of the following signaling motifs in the cytoplasmic tail: an immunoreceptor tyrosine-based inhibition motif (ITIM), proline rich repeats (PRR) or an immunoreceptor tyrosine-based switch motif (ITSM). This approach was successful in identifying a number of novel genes among which was VSTM1 (also known as SIRL-1) encoding a single Ig-like fold, a transmembrane domain and an ITIM containing cytoplasmic tail. Further search for homologous genes using the VSTM1 nucleotide sequence revealed a closely related gene,TARM1, encoded in close vicinity to VSTM1 on the human chromosome 19.

2.1.2 Genomics and Sequence analysis

Full-length human and mouse TARM1 nucleotide sequences were predicted by analysing the database of expressed sequence tags (ESTs). NCBI Position-Specific Iterated (PSI)-BLAST and tBLASTn search methods were used to search the High Throughput Genomic Sequences (HTG) database with the putative TARM1 consensus sequences. A tBLASTn search enables a comparison of the query protein sequence to the six-frame translation of a nucleotide sequence database such as EST or to an unannotated draft genome sequence such as HTG and thus allows the identification of homologous protein coding regions. PCR primers were designed to verify TARM1 gene expression in human and mouse tissues and to confirm the nucleotide sequence (as described in 2.2.1). Validated TARM1 nucleotide and amino-acid sequences were analysed using bioinformatics software resources (see Table 2.1 below) available from the Expasy proteomics server (www.expasy.org)

Prediction type	Software	Reference
N-glycosylation	NetNGlyc	www.cbs.dtu.dk/services/NetNGlyc/
O-glycosylation	NetOGlyc	www.cbs.dtu.dk/services/NetOGlyc/
Signal peptide	SignalIP	www.cbs.dtu.dk/services/SignalP/
Transmembrane region	Phobius	http://phobius.sbc.su.se/
Molecular weight	Compute pI/Mw	http://web.expasy.org/compute_pi/
Structure, homology	HHpred	http://toolkit.tuebingen.mpg.de/hhpred

Table 2.1: Expasy bioinformatics software resources used for TARM1 sequence analysis

2.1.3 Phylogenetic analysis

To establish the molecular evolutionary relationship of *TARM1* gene to other members of the LRC, amino acid sequences encoding Ig-like domain 1 and 2 were aligned separately and the phylogenetic tree was constructed using the neighbour-joining (NJ) method with the *p*-distance. All multiple sequence alignments were conducted at the amino acid level using CLC Main Workbench software (CLC Bio, Qiagen) and ClustalW (J. Thompson, Higgins, and Gibson 1994). All resulting alignments were inspected by eye to ensure best accuracy. MEGA v5.0 (Tamura et al. 2011) was used to construct phylogenetic

trees based on the NJ method with the *p*-distance. Bootstrap analysis was performed on 1000 runs and bootstrap values are indicated for each node. The multiple sequence alignment parameters set in the ClustalW are outlined in the table 2.2 below. The *p*-distance method was chosen as it generates small standard errors and is thus considered to produce a good resolution of branching topology (M. Nei and S. Kumar 2000).

Parameter	Setting
Gap Open Penalty	10.0
Gap Extension Penalty	0.1
Weight Matrix	Blosum
Clustering type	NJ

TABLE 2.2: ClustalW parameters used for multiple sequence alignments

2.2 Molecular biological methods

2.2.1 Primer design for molecular cloning and TARM1 gene expression studies

Predicted DNA sequences were initially used to design forward and reverse primers to amplify the full-length human and mouse TARM1 transcripts for cloning into pCR2.1-TOPO vector (Invitrogen). All primers were designed using the Primer3 (Untergasser et al. 2012) software taking into account self-complementarity, 3' stability, internal repeats, GC content (40-60%) and a theoretical annealing temperature of 62-65 ℃. qPCR primers were designed to span an exon-exon junction to prevent genomic DNA amplification. The specificity of primer pairs was validated by performing a Primer-BLAST search (http://www.ncbi.nlm.nih.gov/tools/primer-blast/) on the mouse or human reference genome databases. Primers used for cloning were designed to contain a restriction enzyme cite preceded by three additional nucleotides to allow the formation of a stable DNA restriction enzyme complex. The integrity of the resulting open reading frame was validated using CLC Main Workbench software (CLC Bio, Qiagen). Sequences of primers used in this work are listed in Table 2.3.

		Sequences 5'−3'		
Primer ID, F / R	Target	Forward	Reverse	Amplicon
HA01233987 / HA01089345	mTARM1 full-length	AGACCTGCTGAAGACCTTTG	TTCAACCAGGAAGCCTCCCACTATTA	864 bp
full-F1 / full-R2	hTARM1 full-length	GAGCCATCATGATCCCTAAG	AGCCCCGGTTCAAGATGGAG	844 bp
HA03927386 / full-R2	hTARM1 exons 2-5	CACAAGGGGAGATGGGTCAC	AGCCCCGGTTCAAGATGGAG	780 bp
HA01286330 / HA01286331	mGapdh	GCAGTGCCAGCCTCGTCC	TGAGGTCAATGAAGGGGTCGT	143 bp
HA01252576 / HA01252577	hGapdh	GAAGGTGAAGGTCGGAGTC	CATCACGCCACAGTTTCCC	590 bp
HA00778803	hTARM1 XhoI		GCC**CTCGAG**TCACTCTGGTTTGAAG	
HA00778802	mTARM1 XhoI		GCC**CTCGAG**TTACCAGGGTTTATTTGG	
HA04544210 / HA04544216	mTARM1 qPCR	TCTGTGATAGACAACCATCTGCCTC	ACACCGACCCGGATGAGATT	
HA01782199 / HA01782200	hTARM1 qPCR	TTCACAGCGCAGTGACGTCCTT	ATTGGTCTCGCTTCTGGCACTG	131 bp

TABLE 2.3: Sequences of primers used for TARM1 gene expression studies and molecular cloning. Nucleotide sequences are given in a 5' to 3' orientation. Restriction sites are in bold font. Amplicon size produced by each primer pair is given in base pairs (bp). h, human; m, mouse

2.2.2 Polymerase chain reaction (PCR) and quantitative PCR (qPCR)

Colony PCR Routine PCR screening of transformed DH5α *E. coli* was performed in 10 μl reactions using GoTaq Flexi (Promega) according to the setup in Table 2.5. The reaction mix was inoculated with bacterial colony of interest and overlaid with 10 μl PCR-grade mineral oil. Template amplification was carried out after a "hot start" of 2 min at 95 ℃ and then followed by 30 cycles of denaturation at 94 ℃ for 30 sec, annealing at 60 ℃ for 30 sec and extension at 72 ℃ for 1 min with a final extension step of 72 ℃ for 5 min. The resulting PCR product was resolved by electrophoresis on 1% agarose gel and visualised under UV light.

RT-PCR analysis of TARM1 mRNA expression in tissues Mouse tissue total RNA panel was prepared in-house as follows. Total RNA was extracted from tissues of 8-10 week old C57BL/6 female mice with TRIzol reagent (Invitrogen) following the manufacturer's instructions. cDNA was synthesised from 2 μg total RNA using oligo dT primer and Superscript III (Invitrogen). PCR screening was performed using primer pairs that amplified a full-length TARM1 and are listed in Table 2.3. Forward primer HA01233987 was specific to 5' UTR region and reverse primer HA01089345 was specific to exon 6. Mouse Gapdh was used as a reference gene using primer pair HA01286330 and HA01286331.

Human total RNA Master Panel II was purchased from Clontech (cat. 636643). cDNA was synthesised from 2 μg total RNA using oligo-dT primer and Superscript III (Invitrogen). Forward primer HA03927386 was specific to the junction of exons 2 and 3. Reverse primer full-R2 was specific to exon 5. Human *GAPDH* was used as a reference gene with the primer pair HA01252576 HA01252577 (see Table 2.3). RT-PCR reaction was carried out using GoTaq Flexi RT-PCR kit (Promega) as shown in Table 2.4.

Quantitative PCR analysis of tissue mTARM1 expression following Salmonella infection Mouse tissues were harvested at indicated time points following Salmonella infection and stored in RNAlater (Qiagen) at -20 ℃ until further processing. Total RNA was extracted using RNeasy kit (Qiagen) and cDNA was synthesised from 2.5 μg total RNA using oligo dT primer and Superscript III (Invitrogen). qPCR was performed using GoTaq qPCR Master Mix (Promega), according to the manufacturer's instructions on an ABI 7500 Fast Real-Time PCR System. Forward primer HA04544210 was designed to span the junction of exons 4 and 5. Reverse primer HA04544216 was specific for

exon 6 (see Table 2.3). Gapdh was used as a reference gene using Gapdh QuantiTect 156 Primer mix (Qiagen, cat QT01658692). Primer amplification efficiencies (E=1.9 for both TARM1 and Gapdh) were calculated from the slope of a standard curve prepared with a 2-fold serial dilution of splenic cDNA. TARM1 gene expression levels were calculated as fold change over the levels detected in control animals using *fold change=2-*$\Delta\Delta CT$ method. Primer specificity was verified by melt curve analysis of the product and amplicon sequencing.

2.2.3 Molecular cloning

The DNA sequences of interest were amplified by PCR using primer pairs containing appropriate restriction sites and the products were purified using QIAquick PCR Purification Kit (Qiagen) according to the manufacturer's instructions.

Restriction digestion of DNA All DNA digestion reactions were performed with restriction enzymes from New England Biolabs (NEB) according to the manufacturer's instructions. In brief, the reactions were set up in a volume of 50 μl in 0.25 ml PCR tubes using 1-2 units of appropriate enzymes per 1 μg of DNA substrate in a compatible buffer. The reactions were allowed to proceed for 4 hours at 37 ℃ with a final inactivation step of 20 min at 85 ℃. Following restriction digest, PCR products were purified using QIAquick PCR Purification Kit (Qiagen). For restriction digest of plasmids 2-5 μg DNA were used. To purify the digested plasmid DNA, the reaction was mixed with gel loading buffer and separated on 1.5% agarose gel in 1xTBE buffer. 1 kb DNA ladder (Promega) was used as DNA size reference marker. The band corresponding to the linearised plasmid was excised and the DNA was extracted as described below.

Gel extraction DNA fragments to be gel-extracted were visualised with long-wavelength UV light and excised with a scalpel blade. Agarose slices were either extracted immediately using the QIAquick Gel Extraction kit (Qiagen) or stored in 1.5 ml eppendorf tubes at -20 ℃ until extraction. The concentration of the purified DNA was determined on Nanodrop 1000 apparatus.

Ligation reactions 50 ng of linearised plasmid DNA was ligated to a four fold molar excess of insert DNA with compatible ends in the presence of 1 unit of T4 DNA Ligase (NEB) and manufacturer's buffer in a final volume of 20 μl for 15 min at RT. The

ligation reaction product was either used immediately to transform competent *E. coli* or stored at -20 ℃.

2.2.4 Transformation of competent *E. coli*

Subcloning efficiency DH5α competent *E.coli* (Invitrogen) were transformed with ligation product according to manufacturer's instructions. Briefly, competent *E.coli* were thawed on ice, ligation product was added and the cells were incubated for 30 min on ice. Following incubation, the bacteria were heat-shocked at 42 ℃ for 30 s and allowed to cool on ice for 2 min. Pre-warmed SOC medium was added and the cells were allowed to recover on a shaking heat-block at 37 ℃ for 1 hour. To select for successfully transformed bacteria, the cells were streaked onto LB agar plates containing 100 μg/ml ampicillin and incubated at 37 ℃ overnight. Single cell colonies were screened by PCR as described in section 2.2.2 for the presence of plasmid with the insert of expected size. Several clones were picked for sequencing of the transformed DNA.

2.2.5 Plasmid DNA extraction from *E. coli*

Small and large-scale plasmid DNA extractions were performed using the Qiagen Plasmid Mini or Maxi kits, respectively, following the manufacturer's protocol. Briefly, LB broth supplemented with ampicillin (100 μg/ml) was inoculated with a single bacterial colony that was previously confirmed to contain the cloned DNA sequence. The bacterial culture was expanded overnight at 37 ℃ in a shaking incubator. To extract the DNA plasmid, the bacterial culture was centrifuged at 4000 $\times$ g for 20 min, LB broth was discarded and the pelleted cells were lysed.

2.2.6 Transient transfection

All transient transfections were carried out in 6-well plates using either FugeneHD (Promega) or jetPEI™ (Polyplus). Cells were seeded at optimal densities into 6-well plates the day before transfection and allowed to adhere. Immediately prior to the transfection, growth medium was changed to 1 ml/well of either serum-free, antibiotics-free medium for FugeneHD or complete medium for jetPEI transfection. 2 μg of plasmid DNA was used per well for transfection according to the manufacturer's protocol. Cells

	x1 reaction (μl)
5x Green buffer	4
$MgCl_2$ (25 mM)	1.2
dNTP (10 mM)	0.5
Forward primer	1
Reverse primer	1
PEG	0.37
GoTaq (5 U/μl)	0.1
Template	1
Water	10.83
Total	20

TABLE 2.4: Composition of PCR master mix

	x1 reaction (μl)
5x Green buffer	2
$MgCl_2$ (25 mM)	1
dNTP (10 mM)	0.2
Forward primer	0.5
Reverse primer	0.5
GoTaq (5 U/μl)	0.05
Template	solid colony
Water	5.75
Total	10

TABLE 2.5: Composition of PCR master mix for colony PCR

were then incubated for 6 h to overnight and the medium was exchanged to normal growth medium. The expression of transfected construct was assayed 48 h following the transfection.

2.2.7 Stable transfections to generate TARM1-Fc fusion protein

DNA sequences encoding the extracellular portions of murine (aa 16-255) and human (aa 16-233) TARM1 were cloned into the mammalian expression vector Signal pIg Plus (R&D Systems) carrying a neomycin resistance gene, CD33 signal sequence and a human IgG_1 Fc tail. For stable transfections, the vector was linearised to facilitate the integration into genomic DNA. HEK293 cells were prepared in the same manner as for the transient transfections (see section 2.2.6) and transfected with 2 μg of plasmid DNA using FugeneHD according to the manufacturer's protocol. The cells were passaged under G418 selection (1 mg/ml) until stable cell lines secreting soluble TARM1-Fc fusion protein were established.

2.3 Protein biochemistry

2.3.1 SDS-PAGE

The mini-Protean3 system (BioRad) was used to perform all SDS-PAGE. The gels were prepared to contain a 10% resolving and 4% stacking layers. Samples were mixed with reducing sample buffer containing DTT and denatured at 90 ℃ for 5 min, vortexed and allowed to cool prior to loading. Prestained SDS-PAGE molecular weight standard was loaded alongside the samples and the gel was run at 100 V in Tris-glycine buffer (see section 2.3.6). Protein bands were visualised by either coomassie stain or western blot.

2.3.2 Coomassie staining

Proteins resolved on the SDS-PAGE gels were visualised by incubation with Coomassie blue stain for 1 h and cleared in a de-stain solution (see section 2.3.6 on page 32 for recipes).

2.3.3 Western blotting

Proteins were resolved on a 10% SDS-PAGE gel and wet transferred in Towbin buffer (see section 2.3.6) onto a methanol-activated PVDF membrane (Immobilon-P, Millipore) for 1 h at 100 V on a BioRad Mini Transblot system (BioRad). Following transfer, the membrane was blocked in 5% milk, 0.05% Tween-20 (Sigma) for 1 h at RT on a rocking platform. After the blocking step, primary antibody diluted in PBS-T 5% milk was added to the membrane and incubated for 1 h at RT on a rocking platform. Thereafter, the membrane was washed 5 min × 5 times in PBS-T and the secondary HRP-conjugated antibody diluted in PBS-T 5% milk was added and incubated for 1 h at RT on a rocking platform. The membrane was washed 5 min × 5 times in PBS-T then soaked in chemiluminescent ECL™ Detection Reagents (GE Healthcare) and the protein bands were visualised by exposing an X-ray film (GE Healthcare). The X-ray film was developed on a Kodak compact X4 X-ray developer (Kodak).

2.3.4 PNGase F and Endo H treatment of TARM1

Hek293T cells were transiently transfected with full-length FLAG-tagged TARM1 using FugeneHD (Promega). Two days post transfection total cell lysates were prepared in ice-cold Nonidet P-40 (NP-40) lysis buffer for 20 min on ice. Insoluble cell fragments were removed by centrifugation at 14,000 × g for 15 min. Proteins were denatured at 90 ℃ for 5 min and the samples were treated with either Endo H or PNGase F (both from NEB) for 4 h at 37 ℃. Control samples were incubated without the addition of enzymes. All samples were stored at -80 ℃ until further analysis by Western blotting.

2.3.5 Co-immunoprecipitation

Hek293 cells stably expressing HA-tagged ITAM-adaptors Dap10, Dap12 and FcRγ were transiently transfected with full-length Flag-tagged human TARM1 and cells were lysed in 1% Triton X-100 lysis buffer (see section 2.3.6) for 25 min on ice. Lysates were centrifuged at 10,000 × g and 4 ℃ for 5 min to remove debris. Supernatants were collected and incubated with monoclonal anti-TARM1 antibody or isotype control for 1 h at 4 ℃ on a rotor. Washed protein A agarose FastFlow beads (Sigma) were added to the samples and incubated on a rotor for 1 h at 4 ℃. The agarose beads were then washed three times in lysis buffer and two times in TBS. Proteins were eluted from the beads by heating at 70 ℃ for 10 min in lithium dodecyl sulphate (LDS) (Invitrogen) sample buffer and separated by SDS-PAGE. Co-immunoprecipitated proteins were resolved on a 10% agarose gel and analysed by Western blotting. The membrane was probed with anti-HA monoclonal antibody (Roche) to detect the co-immunoprecipitated adaptor protein.

2.3.6 Recipes

Name	**Composition**
PBS-T	1 ml Tween-20
	1 L PBS
NP-40 lysis buffer	50 mM Tris-HCl pH 8.0
	150 mM NaCl
	1% NP-40
	1.0 mM AEBSF (Sigma)
Co-IP lysis buffer	20 mM Tris-HCl pH 8.0
	150 mM NaCl
	1% Triton X-100
	0.5 mM AEBSF (Sigma)
	ProteoBlock (Fermentas)
Laemmli sample buffer×2	4% SDS
	0.125 M Tris-HCl pH 6.8
	0.004% Bromophenol blue
	20% Glycerol
	0.7 M DTT added prior to use
	dH_2O
Tris-glycine buffer×10	0.25 M Tris
	1.92 M Glycine (pH 8.6)
	1% SDS

	dH_2O
Towbin transfer buffer×10	0.25 M Tris
	1.92 M Glycine (pH 8.6)
	1% SDS
	20% Methanol
	dH_2O
Coomassie stain	0.05% Coomassie Blue R, (Sigma)
	10% Acetic acid
	50% Methanol
	dH_2O
Coomassie de-stain	9% Acetic acid
	25% Methanol
	1% Glycerol
	dH_2O

2.4 Confocal microscopy of spleen sections

Spleen fragments from control or Salmonella-infected mice were harvested at 2 wpi and fixed in 4% paraformaldehyde, paraffin-embedded and stored until analysis. Tissue sections were deparaffinised, and heat-induced epitope retrieval was performed in citrate buffer pH 5.5. Sections were blocked with goat serum and sequentially stained with rat anti-mouse TARM1 and goat $F(ab')_2$ anti-rat FITC (AbD Serotec) secondary Ab. Nuclei were visualised with DAPI. Multiple images of each section were taken to ensure accurate representation.

2.4.1 Flow cytometric cell-surface phenotyping

For flow cytometric cell phenotyping, 0.5 - 1.0 $\times$ 10^6 cells were stained per well. Flow cytometry was performed on BD FACScan with CyTek DxP three laser setup (Table 2.7) and data analysis was carried out using FlowJo 10 software (Tree Star).

Laser	Excitation (nm)	Fluorochrome conjugates
Blue argon	488	Fitc
Red diode	635	Alexa Fluor647
Green-Yellow	561	Pe

TABLE 2.7: Lasers and optical configuration

Unless otherwise stated, all incubation steps were performed on ice and all commercial antibodies were diluted to working concentrations in FACS buffer. FACS buffer was also used for all washing steps. All immunostaining was performed in v-bottomed 96-well plates (Sterilin).

- Fc receptors were blocked by resuspending cell pellets in 40 μl of 5% normal mouse serum and incubated for 20 min.
- 20 μl of anti-TARM1 monoclonal antibody-containing hybridoma supernatant or isotype control were added to appropriate wells and incubated for 1 h.
- Cells were washed twice and fluorochrome conjugated anti-Rat secondary antibody was added to the wells and incubated for 1 h.
- Cells were washed twice and unbound anti-Rat antibodies were blocked with 50 μl of 5% normal rat serum for 25 min.
- Rat serum was removed and appropriately diluted antibodies to lineage markers were added to the wells and incubated for 1 h.
- Cells were washed twice, fixed in 2% paraformaldehyde solution and stored at 4 ℃ over night.

2.5 Generation and purification of TARM1-Fc fusion proteins

2.5.1 Collection of TARM1-Fc containing supernatants

Hek293 cells stably transfected with TARM1-Fc construct (see section 2.2.7) were maintained in DMEM supplemented with 2 mM L-Glutamine, 100 U/ml penicillin/streptomycin, 2% ultra-low IgG FCS (Invitrogen) and 1 mg/ml G418. TARM1-Fc fusion protein secretion was assessed by Western blotting and ELISA assays. The culture supernatant containing the fusion proteins was collected every four days and exchanged for fresh medium until 5 L of each fusion-containing supernatant were collected. The supernatants were stored at 4 ℃ until further processing. For storage, the medium was clarified by centrifugation, Tris buffer was added to adjust the pH to 8 and 1 mM phenylmethane sulfonyl fluoride (PMSF) was added to inhibit proteolytic protein degradation.

2.5.2 Purification of TARM1-Fc fusion proteins

TARM1-Fc fusions were purified by affinity chromatography over protein-A agarose FastFlow (Sigma-Aldrich) packed columns. Glass columns (Millipore) were packed with 2 ml of 50% protein-A agarose slurry and washed with 0.1 M Tris-HCl pH8. The column assembly was kept at 4℃ during the entire purification process. TARM1-Fc containing supernatants were allowed to enter the column by gravity flow. The columns were washed with 50 ml 0.1 M Tris-HCl pH8 and then with 20 ml 0.1 M Citrate buffer pH5.5. Thereafter, the fusion proteins were eluted from the columns with 0.1 M Glycine at pH2.5. The eluate was collected into tubes containing 2.0 M Tris-HCl pH8. The eluted Fc fusion proteins were concentrated using Amicon Ultra-0.5 mL Centrifugal Filters (Millipore) with a molecular weight cutoff of 10 kDa. The concentrated solutions were filter-sterilised and the protein concentration was measured on a Nanodrop 1000 spectrophotometer (Fisher Scientific). Aliquots of TARM1-Fc fusion proteins (1 mg/ml) were stored at -80 ℃.

2.6 Generation of TARM1 reporter lines

2.6.1 Retroviral transduction

2B4-NFAT-GFP T cell lymphoma cell line was retrovirally transduced with chimeric TARM1 construct bearing the extracellular portion of TARM1 fused to the transmembrane domain of PDGFR and the cytoplasmic tail of human CD3ζ.

Phoenix™-E ecotropic retroviral packaging system was used to stably transduce 2B4-NFAT-GFP cell line following previously published protocol (Pear et al. 1993). Packaging cells were seeded into 6-well plate and transiently transfected with 3 μg pMXs-TARM1 vector DNA per well using FugeneHD reagent (Promega). 24 h post transfection the cells were transferred to 32 ℃ for additional 2 days to increase the stability of secreted viral particles. On day 3 post transfection, retroviral supernatants were harvested and applied to 2B4-NFAT-GFP cells in the presence of 4 μg/ml of Polybrene (Sigma-Aldrich). The cells were then placed a six-well plate and centrifuged at 1200 *times* g at 32 ℃ for 1 h. Following the spin, the cells were incubated at 32 ℃ overnight. The medium was then exchanged for normal growth medium and grown at 37 ℃. 72 h following transduction the expression of TARM1 was analysed by flow cytometry using anti-HA monoclonal antibody.

2.7 Antibodies

2.7.1 Generation and screening of anti-TARM1 monoclonal antibodies

mAb production

Monoclonal mouse anti-humanTARM1 and rat anti-mouse TARM1 Abs were raised against the ectodomain of mouse and human TARM1 proteins using TARM1-Fc as immunogens. The work was performed by the laboratory of Professor Karsten Skjødt (Dept. Cancer & Inflammation, Institute for Molecular Medicine, University of Southern Denmark).

mAb screening

To eliminate the clones specific for the IgG_1 Fc tail, hybridoma supernatants were screened by ELISA using the TARM1-Fc fusion proteins whereby the mouse anti-human

TARM1 clones were screened against mouse TARM1-Fc fusion, and the rat anti-mouse TARM1 clones were screened against the human TARM1-Fc fusion protein. The performance and specificity of monoclonal anti-TARM1 Ab clones selected by ELISA were further evaluated by flow cytometry and Western blot against transfected and primary cells.

2.7.2 Antibodies used in this work

Antibody	**Clone**	**Isotype**	**Supplier**
Ly6C APC	HK1.4	Rat IgG2c, κ	BioLegend
Ly6G FITC	1A8	Rat IgG2a, κ	BioLegend
Gr-1 FICT	RB6-85C	Rat IgG2b, κ	eBioscience
CD19 APC	1D3	Rat IgG2a, κ	eBioscience
CD11c FITC	N418	Armenian hamster IgG	eBioscience
CD11b APC	M1/70	Rat IgG2b, κ	eBioscience
CD69 PE	H1.2F3	Armenian hamster IgG	eBioscience
CD62L PE-Cy5	MEL-14	Rat IgG2a, κ	eBioscience
CD3 FITC	145-2C11	Armenian hamster IgG	eBioscience
CD4 APC	GK1.5	Rat IgG2b	eBioscience
CD25 APC	PC61.5	Rat IgG1, λ	eBioscience
Annexin V FITC	-	-	BD Pharmingen
		Secondary	
anti-Rt IgG (H+L) PE	Polyclonal	Goat Ig	Southern Biotech
anti-Ms Alexa Fluor 647	Polyclonal	Goat Ig	Molecular Probes

Continues on next page

Table 2.8 – continued from previous page

Antibody	Clone	Isotype	Supplier
Western blot			
anti-Rt HRP ms-ads	Polyclonal	Goat Ig	Southern Biotech
anti-Hu IgG (Fc) HRP	Polyclonal	Goat Ig	Sigma-Aldrich
anti-HA HRP	3F10	Rat IgG1	Roche
anti-FLAG HRP	M2	Mouse IgG1	Sigma-Aldrich
Cell activation			
anti-CD3	145-2C11	Armenian hamster IgG	eBioscience
anti-CD28	37.51	Syrian Hamster IgG	Miltenyi
anti-human IgG (Fc)	GtxHu-004-D	Goat Ig	ImmunoReagents

2.8 Cell isolation, manipulation and culture

2.8.1 General tissue culture

All cell lines were maintained in either RPMI-1640 or Dulbecco's Modified Eagle medium (DMEM, both from Gibco) supplemented with 10% heat inactivated fetal calf serum (FCS), 2 mM L-glutamine, 50 U/ml penicillin and 50 μg/ml streptomycin (all from PAA). Primary cells were maintained in RPMI-1640 supplemented with all the above plus 50 μM 2-Mercaptoethanol. For cryopreservation, cells were resuspended in 10% dimethylsulfoxide (DMSO) diluted in FCS and stored in liquid nitrogen.

2.8.2 Preparation of primary murine cells

Mice were sacrificed and tissues collected into ice-cold RPMI supplemented with 10% FCS. Single cell suspensions of liver, spleen and lymph nodes were prepared by gently forcing the tissues through a 70 μm nylon cell strainer.

Splenocytes The resulting cell suspension was pelleted by centrifugation at 400 × g for 10 min at 4 ℃ and resuspended in 2 ml of ammonium chloride buffer per spleen to lyse red blood cells. The lysis was allowed to proceed for 20 seconds on ice with occasional swirling. Thereafter, 40 ml FACS buffer was added to the cell suspension to stop the reaction and cells were washed twice.

Liver mononuclear cells (MNC) Cells were pelleted by centrifugation at 400 × g, resuspended in 10 ml of Percoll (GE Healthcare) 33% (vol/vol) and centrifuged at 800 × g for 20 min at RT. MNC were collected and washed once with FACS buffer.

Bone marrow (BM) Femur and tibia of both legs were thoroughly cleaned from surrounding tissue, epiphyses were cut and bone marrow was flushed with ice-cold FACS buffer using a 24 gauge needle attached to a syringe. Cellular aggregates were dissociated by pipetting and the cells were then passed through 70 μm nylon cell strainer, pelleted by centrifugation and red blood cells were lysed with ammonium chloride buffer as described above.

2.8.3 Isolation of peripheral blood mononuclear cells (PBMC)

Blood samples were collected from healthy adult volunteers into heparin containing tubes (Sarsted) and processed immediately. PBMC were isolated by density centrifugation over Histopaque-1077 (Sigma) according to the manufacturer's instructions. Briefly, 20 ml freshly drawn blood was diluted 1:1 in PBS and overlaid onto Histopaque-1077 in 50 ml Falcon tubes equilibrated to RT. The samples were centrifuged at 700 × g with low acceleration and no breaks for 20 min at RT. The PBMC layer was transferred into a fresh 50 ml tube and washed in PBS 2 mM EDTA once at 700 × g 10 min and once at 300 × g 10 min.

2.8.4 Isolation of human peripheral blood neutrophils

Peripheral blood was collected from healthy volunteers and circulating neutrophils were purified using Dextran sedimentation and discontinuous plasma-Percoll gradients as previously described (Haslett et al. 1985). Briefly, 40 ml of blood was collected into 50 ml tubes (containing 4 ml 3.8% (w/v) sodium citrate) using a 19 gauge needle, and centrifuged for 20 minutes at 300 × g. Platelet-rich plasma upper layer was removed for

later use. Red blood cells were removed from the leukocyte/erythrocyte pellet by dextran sedimentation. The upper leukocyte-rich layer was collected and centrifuged at 275 × g for 5 minutes. The cell pellet was resuspended in platelet-poor plasma and neutrophils were isolated by discontinuous plasma-Percoll gradient centrifugation. Neutrophil purity as determined by cytospins was routinely greater than 95% using this method.

2.8.5 Immunomagnetic T cell isolation

Spleen and lymph nodes of 6-8 week old mice were pooled and single cell suspension was prepared by gentle mechanical disruption through a 70 μ nylon cell strainer. Total T cell population was isolated by immunomagnetic selection with either negative selection Mouse T Cell Enrichment Kit (StemCell Technologies) or EasySep CD4 positive selection magnetic beads (StemCell Technologies) in accordance with the manufacturer's protocol. The purity of isolated T cells was assessed by staining with fluorescently labelled anti-CD3 antibody and flow cytometric analysis. The purities were routinely at or above 96%.

2.8.6 Plates for T cell stimulation inhibition assay with TARM1-Fc

96-well flat-bottomed plates were coated in two layers. First layer was the anti-human IgG Fc-specific antibody 10 μg/ml (ImmunoReagents) and 1 μg/ml anti-CD3 (clone 145-2C11, eBioscience) together with 0.25 μg/ml anti-CD28 (clone 37.51, Miltenyi) over night at 4 ℃. The plates were then washed with PBS and coated with a second layer of mouse TARM1-Fc or human IgG1 control both at 10 μg/ml for 2 h at 37 ℃ washed with complete growth medium and used in either CFSE dilution assay or MTT metabolic assay of T cell proliferation (see section 2.8.7).

2.8.7 T cell proliferation assays

CFSE For CFSE dilution assay $CD4^+$ T cells were purified from naive NOD female mice using EasySep positive selection magnetic beads (StemCell Technologies) to 95–98% purity as determined by flow cytometric analysis. Cells were loaded with 1 μM CFSE (Molecular Probes) in PBS for 15 min at 37 ℃ washed three times in complete growth

medium and seeded into a 96-well plate coated as described in 2.8.6. A total of 1.5 × 10^5 T cells were added to each well in a volume of 200 μl RPMI-1640 supplemented with 10% FCS, penicillin/streptomycin and 50 μM 2-mercaptoethanol. CFSE dilution was assessed after 90 h of culture.

MTT For metabolic MTT assay, $CD4^+$ T cells were purified using EasySep negative selection magnetic beads (StemCell Technologies) and activated in precoated plates as described above in section 2.8.6, but omitting the anti-CD28 antibody. Cells were cultured for 20 h, 40 h and 80 h. Two hours prior to each time point, MTT (Sigma) stock solution was added directly to the wells to give 500 μg/ml final concentration and following 2 h incubation at 37 ℃, DMSO was used to dissolve formazan crystals. Absorbance (570 nm) was measured on a Synergy HT plate reader. Human T cells were isolated from peripheral blood of healthy donors (n=2) using CD4 positive selection magnetic beads (Miltenyi) to 95-98% purity and activated with plate-bound anti-CD3 (1.2 μg/ml, clone OKT3) in the presence of plate-bound human TARM1-Fc (10 μg/ml) or hIgG1 (10 μg/ml). Recombinant human IL-2 (50 U/ml) was added to some wells as indicated. T cells were cultured for 3 days and the expression of CD25 and CD69 was analysed by flow cytometry.

2.8.8 Generation of bone marrow-derived dendritic cells and macrophages

Bone marrow was isolated as described in section 2.8.2. Single cell suspension was prepared in IMDM supplemented with 10% FCS, 2 mM L-glutamine, 50 U/ml Penicillin, 50 μg/ml Streptomycin (all from PAA) and 50 μM 2-Mercaptoethanol and transferred into tissue culture dishes. For bone marrow-derived dendritic cell (BMDC) differentioation cells were allowed to adhere for 30 min at 37 ℃ and the nonadherent cells were reseeded into new plates in IMDM complete growth medium supplemented with GM-CSF (20 ng/ml, Peprotech) and IL-4 (10 ng/ml, Peprotech). For bone marrow-derived macrophage (BMM) differentiation the medium was supplemented with 10% L-cell conditioned medium as a source of M-CSF. On day 10 (BMDC) or on day 5-6 (BMM) non-adherent cells were washed out from the plates with PBS, adherent cells were detached non-enzymatically and the cellular phenotype was confirmed by flow cytometry using CD11b and F4/80 markers for BMMs and CD11c and CD80 for BMDCs.

TLR	Agonist	Final concentration
TLR1/2	Pam3CSK4	100 ng/ml
TLR3	Poly(I:C)	50 μg/ml
TLR4	LPS Ultrapure from E. coli R515	100 ng/ml
TLR5	Flagellin from S. Typhimurium	50 ng/ml
TLR2/6	MALP-2	80 ng/ml
TLR7	Imiquimod	1 μg/ml
TLR9	CpG ODN 1585	2 μg/ml
TLR11	Profilin from Toxoplasma gondii	250 ng/ml

TABLE 2.9: TLR agonists and their final concentrations used for cell stimulation.

2.8.9 TLR stimulation and measurement of cytokine secretion

For the analysis of TARM1 cell-surface expression, BMM and BMDC were stimulated for 24h with the TLR agonists (all from Apotech) listed in Table 2.9. For analysis of cytokine secretion, 1×10^5 of BMM or 1.3×10^5 sorted neutrophils were cultured in 96-well tissue culture plates coated with goat anti-rat capture Ab and rat anti-TARM1 crosslinking Ab or a rat IgG2a isotype control Ab (all at 10 μg/ml). Neutrophils were stimulated in the presence or absence of 10 ng/ml Ultrapure LPS from E. coli K12 (InvivoGen) for 8 h at 37 ℃. BMM were stimulated in the presence or absence of either 0.5 μg/ml Pam3CSK4, 0.5 μg/ml PolyI:C, 1 ng/ml LPS, or 10 μM Imiquimod for 16 h at 37 ℃. Tissue culture supernatants were collected and cytokine production determined using the Cytometric Bead Array mouse inflammation kit (Becton Dickinson).

DuoSet sandwich ELISA (R&D) was used in accordance with manufacturer's protocol to determine IL-2 secretion by stimulated mouse T cells.

2.9 Induction of sterile inflammation and Salmonella infection

2.9.1 Sterile inflammation and S. Typhimurium infection

To induce sterile inflammation, 8-10 week old C57BL/6 mice were injected with 3 mg per mouse of ultrapure LPS (InvivoGen) intraperitoneally (ip), and tissues were harvested for immunophenotyping 24 h later. Systemic infection was induced with an *aroA* attenuated strain of Salmonella enterica serovar Typhimurium, SL3261. Bacteria were grown overnight in Luria–Bertani (LB) broth until stationary phase and C57BL/6 mice were injected into a lateral tail vein with 1×10^6 CFU diluted in PBS. At indicated times following infection, mice were euthanised and TARM1 expression in cells and tissues was analysed by flow cytometry, qPCR, and confocal microscopy.

2.9.2 Enumeration of bacterial load within organ homogenates

Inocula were enumerated by pour-plating in LB agar as follows. Mice were euthanised by cervical dislocation one week post infection, spleens and livers were removed and homogenised in 5 ml of sterile water in a Stomacher 80 Lab System (Seward). The resulting homogenate was 10-fold serially diluted in PBS and pour-plated in LB agar. The plates were incubates at 37 ℃ for 24-48 h and the number of CFU determined by counting.

Chapter 3

Bioinformatics

3.1 TARM1 gene-structure analysis

The human *TARM1* gene maps to chromosome 19q13.42, at the centromeric portion of the LRC, in the identical position to the mouse gene within the syntenic region of chromosome 7A1 (Fig. 3.1). Using the data on the genomic location of predicted TARM1 open reading frame (ORF) I validated its exon-intron structure and investigated the existence of alternative splice variants and homologs in human and mouse using the bioinformatics tools described below.

Prediction of gene structure from genomic sequence is a computationally challenging problem. The most reliable results are achieved by aligning a spliced cDNA sequence of the gene of interest to the genomic sequence. In the absence of cDNA sequence, computational analysis of expressed sequence tags (EST) can be used as a starting point for the gene structure prediction. ESTs are short, single-pass sequencing products that represent partial cDNAs. Aligning EST sequences to the genomic DNA is complicated due to the short length and inherently low quality of the EST sequence, which often contains abundant deletions and chimerism. The analysis could be further confounded by the presence of non-canonical splice site, very short exons (∼20 bp), paralogous genes and/or complex patterns of alternative splicing (Brendel, Xing, and W. Zhu 2004) . A number of computational tools have been developed to address this problem.

Unlike other species, human and mouse GenBank EST databases have a large sampling of sequences. I was able to retrieve ESTs that originated within the genomic region of

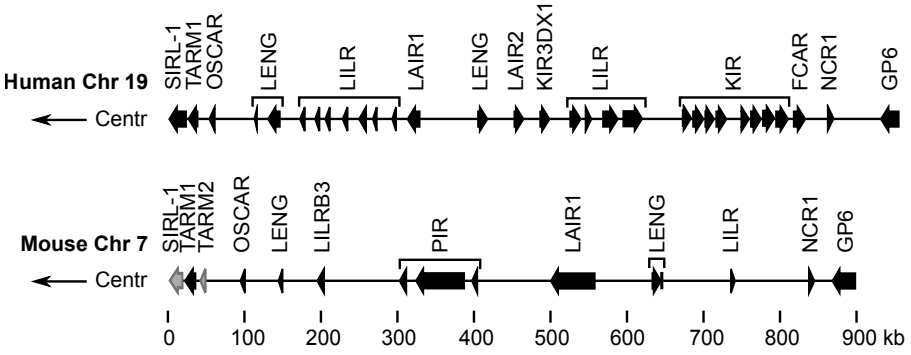

FIGURE 3.1: TARM1 and TARM1-related genes are encoded at the centromeric boundary of the LRC in mouse and human. Genomic organisation of the human LRC (top) on chromosome 19q.13.42 and the syntenic mouse LRC (bottom) on chromosome 7A1. Gene orientation is indicated by arrows. Black - transcriptionally active genes. Grey - pseudogenes. Centr - centromeric.

Tarm1 and that had at least $\geq 90\%$ sequence identity with *Tarm1* nucleotide sequence. I used the Geneseqer software (Brendel, Xing, and W. Zhu 2004) to perform EST alignment to the genomic DNA and to establish the initial exon structure. Although the availability of high-identity sequences meant the prediction was relatively accurate, the existence of splice variants could not be established using this method. Hence, it was necessary to adopt a more direct experimental approach. To this end, I cloned a full-length *Tarm1* cDNA from a total RNA of mouse bone marrow and human spleen (purchased from ClonTech) and the nucleotide sequence was aligned using GeneSeqer to the corresponding genomic region alongside previously retrieved ESTs. Resulting alignments were checked by eye to ensure correct assignment of exonic boundaries. This approach confirmed the computationally derived exon number and structure of *Tarm1* gene in human and mouse and identified putative splice variants.

The analysis of murine ESTs and cDNA revealed a six-exon organisation with a combined sequence length of 867 bp (Fig. 3.2**A**). The analysis also suggested there may exist a putative protein coding splice variant lacking exon 5 (Clone 5), which encodes a 22 amino-acid stem region. ESTs BY748165, BY178134, BY210189 and BY189575 lack exon 2 which destroys a portion of the signal peptide and would most likely result in an aberrant protein translocation along the secretory pathway.

Tarm1 coding sequence gives rise to a protein of 288 amino acids, which contains a hydrophobic signal peptide split between exons 1 and 2; two Ig-like domains encoded by exon 3 and 4, respectively; a stem, exon 5-encoded low complexity polypeptide

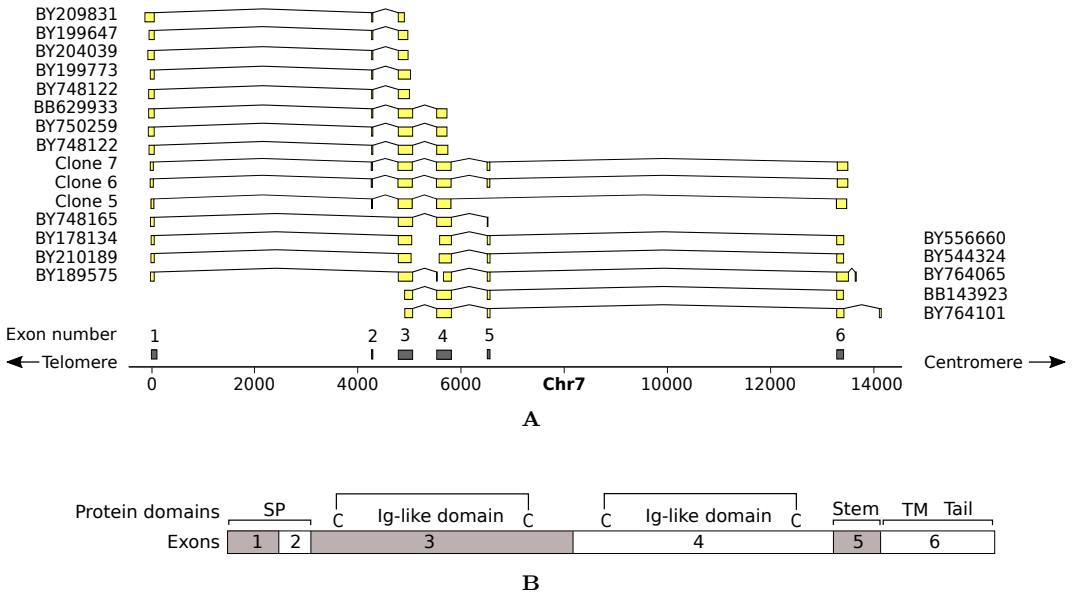

FIGURE 3.2: Analysis of mouse *Tarm1* gene exon structure and alternative splicing. The analysis was performed by aligning mouse *Tarm1* full-length clone and EST sequences to the reference genomic DNA. Full-length *Tarm1* transcripts were amplified by PCR from mouse bone marrow mRNA using primer pair specific to the exons 1 and 6. EST sequences were obtained by searching the NCBI EST database with *Tarm1* cDNA sequence. The data showed a six-exon organisation and suggested the existence of one splice variant lacking exon 5.

separating the proximal Ig-like fold and the transmembrane domain; a short cytoplasmic tail following the transmembrane region is encoded within exon 6 (Fig. 3.2**B**).

The human *TARM1* resembles closely its murine ortholog both in sequence and exon structure. However, human *TARM1* lacks the region homologous to exon 5 (the stem) present in its murine counterpart and is thus comprised of a total of five exons (Fig. 3.3**A**). Analysis of human *TARM1* full-length transcripts identified a splice variant which, like murine *Tarm1*, would result in an incomplete signal peptide due to the lack of exon 2. Additionally, an alternative exon 1 is located within the intronic region upstream of exon 2 and encodes a non-canonical lysine-rich signal peptide MKERKKKERK-ERKRKKERN (AK301730).

Both Ig-like domains of TARM1 contain two characteristic conserved cysteines in identical positions. The predicted TM region contains a conserved arginine, often seen in activating receptors, where it serves as an association site for ITAM-bearing signalling adaptors such as FcϵRγ chain.

Six kb upstream of *TARM1* on human chromosome 19 is a closely related *VSTM1* gene (also known as *SIRL-1*) with a 10-exon structure. I analysed full-length cDNA

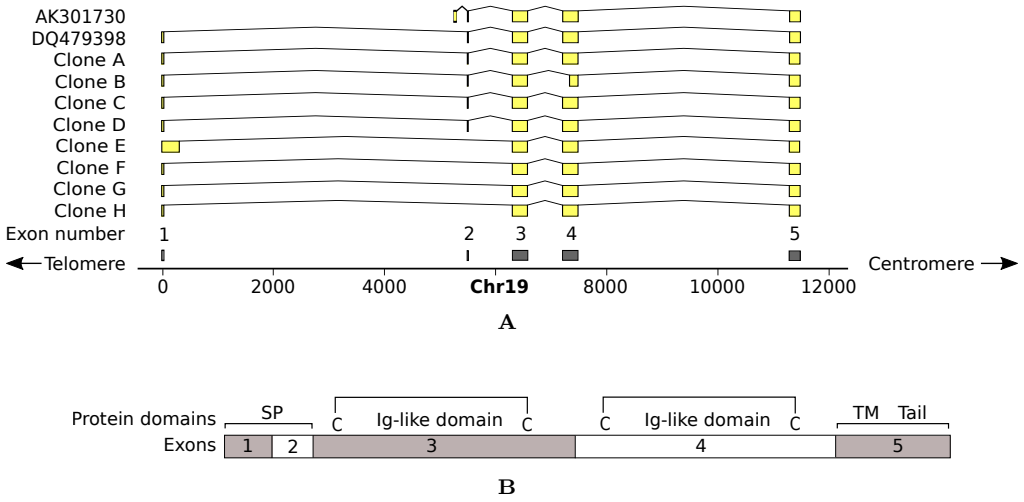

FIGURE 3.3: Analysis of human *TARM1* gene exon organisation and alternative splicing. The analysis was performed by aligning human *TARM1* full-length clone and EST sequences to the reference genomic DNA. Full-length *TARM1* transcripts were amplified by PCR from human spleen mRNA (purchased from Clontech) using primer pair specific to the exons 1 and 5. EST sequences were obtained by searching the NCBI EST database with *TARM1* cDNA sequence. The data showed a five-exon organisation and an alternatively spliced transcript containing a non-canonical signal peptide.

clones and VSTM-1 transcripts contained in the NCBI EST database (Fig. 3.4**A**) and found that several possible *SIRL-1* isoforms could exist. Particularly interesting was the isoform lacking exon 6 which encodes the TM region and which suggested the existence of a soluble form of SIRL-1 receptor.

At the time this work was performed (2009) there were no published studies describing the *VSTM-1* gene. In 2010, Steevels et al. reported the identification and characterisation of *VSTM1* (Steevels, Lebbink, et al. 2010), which they named signal inhibitory receptor on leukocytes-1 (SIRL-1). In 2012 Guo et al. published a more detailed transcriptional profiling of human *VSTM1* splice variants confirming the existence of a soluble isoform expressed predominantly within immune tissues such as bone marrow, spleen, lymph node and thymus (X. Guo et al. 2012).

SIRL-1 cDNA encodes a 236 amino-acid protein, which, in contrast to TARM1, contains a single Ig-V domain and lacks the conserved arginine within its TM. Instead, a long cytoplasmic tail contains two ITIMs, implying inhibitory potential through SHP-1 recruitment (L. Meyaard 2008; Marco Colonna, Navarro, et al. 1997; Burshtyn et al. 1996). The single Ig-V domain of SIRL-1 is closely related to the membrane distal Ig-like domain of TARM1 sharing 58.1% amino acid similarity and 48.4% identity.

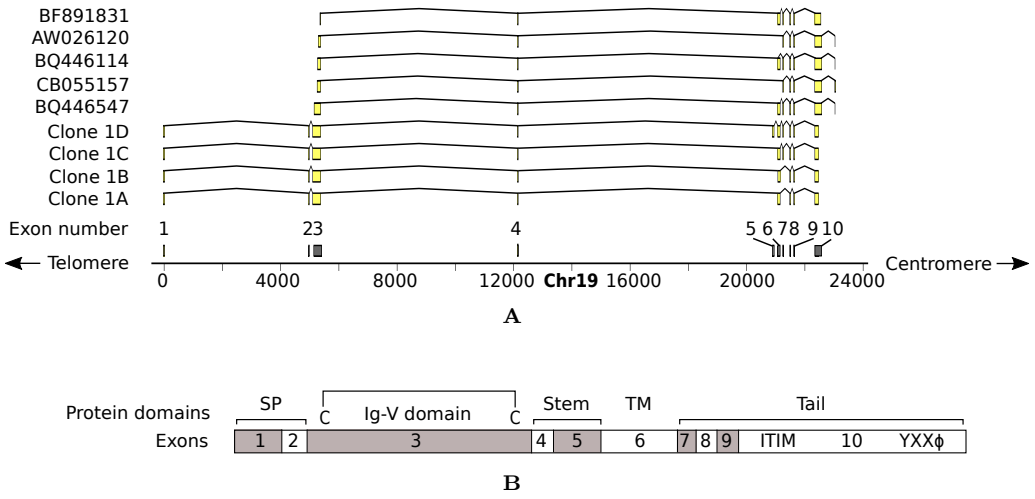

FIGURE 3.4: Alignment of human *SIRL-1* full-length clone and EST sequences to the reference genomic DNA. Full-length *SIRL-1* transcripts were amplified by PCR from human spleen RNA (purchased from Clontech) using primer pair specific to the 3' and 5' UTR. EST sequences were obtained by searching the NCBI EST database with *SIRL-1* cDNA sequence.

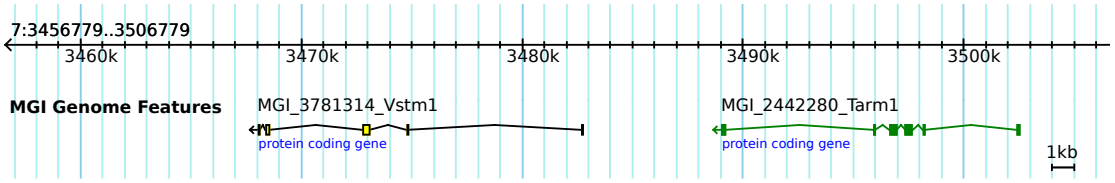

FIGURE 3.5: Mouse chromosome 7 with annotation of the predicted *Sirl-1* (*Vstm1*) ORF and *Tarm1* gene. Genome build 38, MGI Mouse genome browser.

The ORF of the putative murine *Sirl-1* gene (XM_001475796) can be computationally deduced and is located, as expected, approximately 6 kb upstream of the *Tarm1* gene (Fig 3.5). It encodes a single Ig-like domain and the amino-acid sequence of the extracellular portion bears similarity to human SIRL-1. Similarly, the rat genome contains a closely related gene sequence (XM_002728681) in the syntenic region on Chr 1 just upstream of *Tarm1*. The alignment of this predicted rat *Sirl-1* transcript to the mouse genomic sequence produces a high similarity (over 85% nucleotide identity) match to the region of the predicted mouse *Sirl-1* ORF. However, in contrast to *SIRL-1* in human, it is unclear whether the murine or rat orthologs are functional. It appears that the ITIM-bearing cytoplasmic tail found in human SIRL-1 is not encoded within either mouse or rat ORFs. Instead, their cytoplasmic tails are short and do not seem to be evolutionarily conserved. Moreover, neither mouse nor rat putative *Sirl-1* genes show evidence of transcriptional activity as the NCBI database lacks mRNAs or ESTs that originate from these genes. It is thus likely that both mouse and rat *Sirl-1* are pseudogenes.

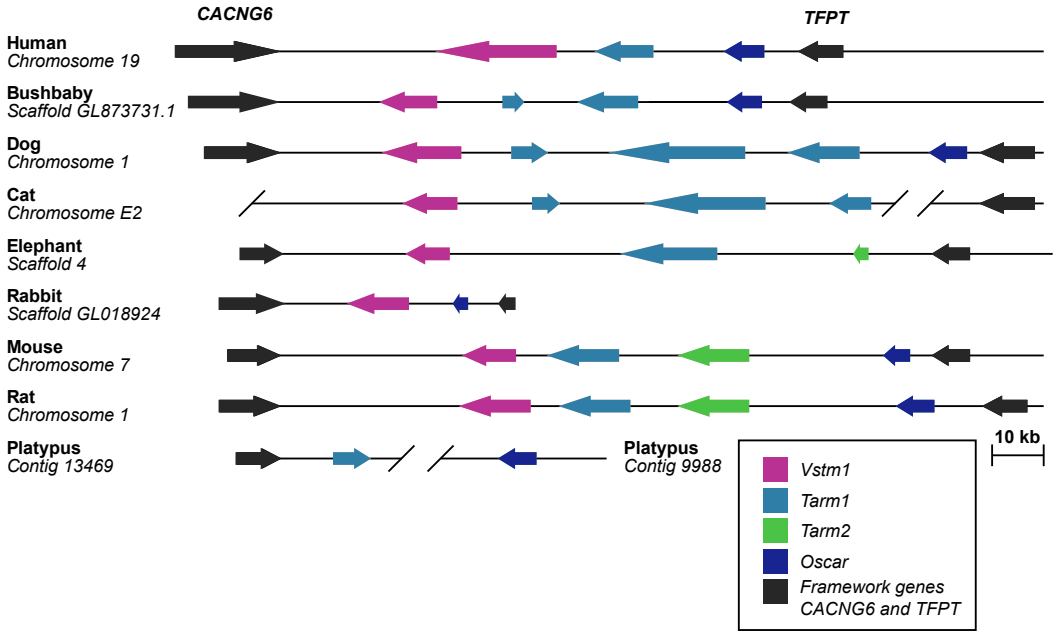

FIGURE 3.6: To scale comparison of TARM1 genomic region of mammals. Framework genes *CACNG6* (black arrow on the left) and *TFPT* (black arrow on the right) were used to identify *Tarm1* genomic regions in bushbaby, dog, cat, elephant, rabbit, mouse, rat and platypus. Amino-acid sequences of predicted ORFs and annotated genes encoded between the framework genes were aligned to the known human and mouse TARM1 and OSCAR protein sequences. Phylogenetic tree was then constructed to infer orthology to SIRL-1, TARM1 and Tarm2. Arrows indicate the gene coding orientation. Orthologs are color-coded.

The genomic distance between *Tarm1* and *Oscar* genes is approximately 60 Kbp in the mouse LRC (reference sequence NT_039413.7), which is considerably larger than the corresponding region between human genes ($\sim$ 17 Kbp) and could potentially contain additional unannotated TARM1 related genes. I performed a more detailed computational analysis of this genomic region in human, mouse and rat using nucleotide alignment of TARM1 transcript to the genomic sequence in these species. This approach identified a TARM1 related gene in mouse (Gm3144) and rat (RGD1564272), but not human, encoded directly downstream of *Tarm1* that I have termed *Tarm-2*.

The position of *Tarm-2*.

BLASTn alignment of the rat predicted *Tarm-2* ORF to the whole mouse genomic sequence returns mouse *Tarm-2* ORF with over 80% nucleotide identity. Phylogenetic analysis of *Tarm-2* predicted protein sequence places it closer to TARM1 than any other *Tarm1*-related gene suggesting a potential gene duplication event (see next section Fig. 3.9).

Bearing in mind the species-specific differences in *Tarm1*-related gene number and conservation, it was of interest to investigate this family in other mammalian lineages. Using two evolutionarily conserved genes, *CACNG6* and *TFPT*, as framework genes, I identified the genomic region encoding OSCAR and TARM1 in elephant, rabbit, dog, cat, bushbaby and platypus (Fig. 3.6). Genscan (Burge and Karlin 1997) was used to predict the location and intron-exon structure of unannotated *Tarm1*-related genes encoded within this genomic region. The translated peptide sequence of each predicted ORF was used as a query in NCBI tBLASTn (Altschul et al. 1997) search of non-redundant translated nucleotide sequences database for matches to annotated and predicted genes across all species. The positions and order of the predicted ORFs together with phylogenetic analysis of the encoded proteins were used to infer orthology to VSTM1, TARM1 and Tarm2.

Oscar and *Tarm1*-related sequences appear early in mammalian evolution as evidenced by their presence in the platypus genome. Interestingly, the genomes of bushbaby, dog and cat contain *Tarm1*-like gene located in close proximity to *Tarm1* but encoded in the opposite orientation (Fig. 3.6). An additional *Tarm1*-like gene is encoded downstream of *Tarm1* in dog and cat. This suggests that the *Tarm1* region may have undergone an expansion by inverse duplication in the common ancestor of early primates and carnivores with a subsequent contraction in hominoids, which eliminated all but one of the *TARM1* genes. In lagomorphs (rabbit) this genomic region has undergone a contraction, which completely eliminated the *Tarm1* locus.

A more detailed computational analysis of the human and mouse TARM1 amino-acid sequences was performed to map the boundaries of all structural domains in order to facilitate molecular cloning and further phylogenetic analysis. Signal peptide cleavage site was predicted with SignalP (Petersen et al. 2011) (available here: www.cbs.dtu.dk/services/SignalP) to lie between the positions 16 and 17 in TARM1 of both species (Fig. 3.7). Amino-acid alignment of human and mouse TARM1 orthologs shows an extensive residue conservation with 47% sequence identity and 62% sequence similarity (Fig. 3.8). Conserved cysteines of TARM1 Ig-like domains are separated by 47 residues in the first domain (membrane distal) and by 49 residues in the second domain (membrane proximal) of both orthologs. In order to determine the type and the span of the domains, Pfam-A database (http://pfam.sanger.ac.uk) of HMM-profiles representing protein domain families was searched with TARM1 amino-acid sequence. HMM-based analysis established

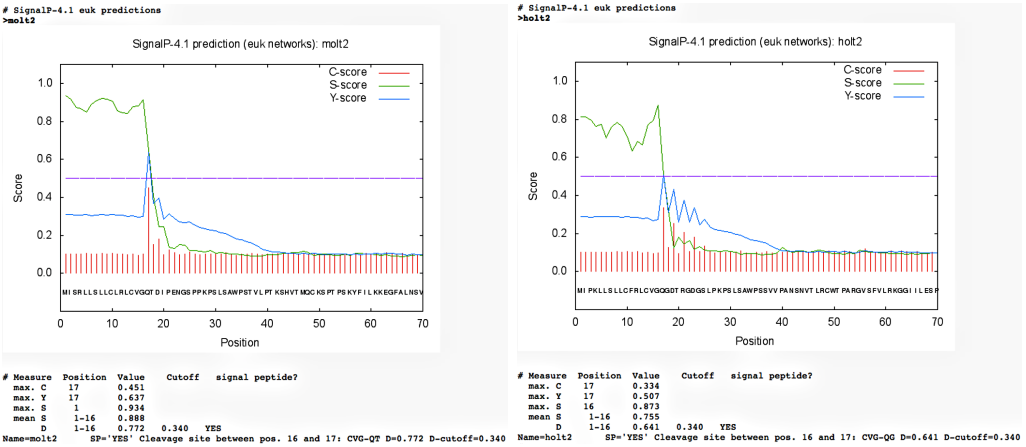

A **B**

FIGURE 3.7: Prediction of TARM1 signal peptide cleavage site. Full-length amino-acid sequence of mouse and human TARM1 was analysed on SignalP 4.0 server(Petersen et al. 2011). A) Mouse Tarm1, B) Human TARM1

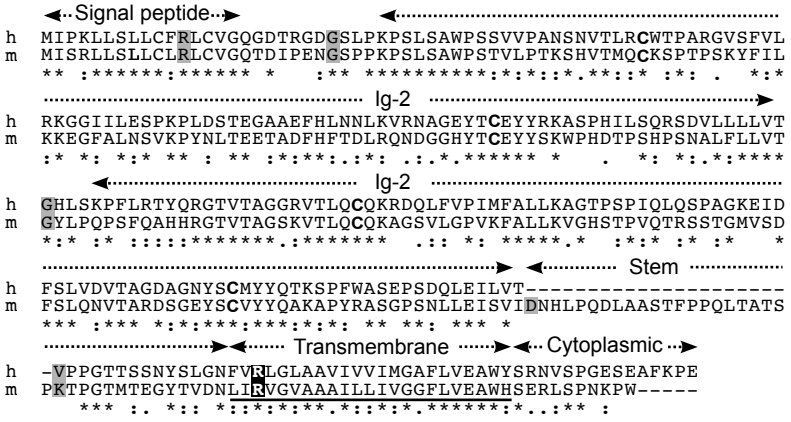

FIGURE 3.8: Amino-acid sequence alignment of human (h) and mouse (m) TARM1 orthologs. Structural protein domains are labeled above the alignement. Grey-shaded amino-acids are encoded at exonic splice junctions. Conserved cysteines that form the Ig-fold intra-chain disulfide bridge are in bold font. Transmembrane region is underscored and contains a conserved arginine (highlighted) predicted to mediate FcRγ association.

the boundaries of both domains and identified them as belonging to the Ig_2 family (PF13895) with E-values of 2e-10 and 2.9e-09 (hTARM1), 4e-09 and 1.3e-10 (mTARM1) for domain one and two respectively. The first domain spans 92 residues (28-119) and the second 94 residues (125-218) in both orthologs (Fig. 3.8)

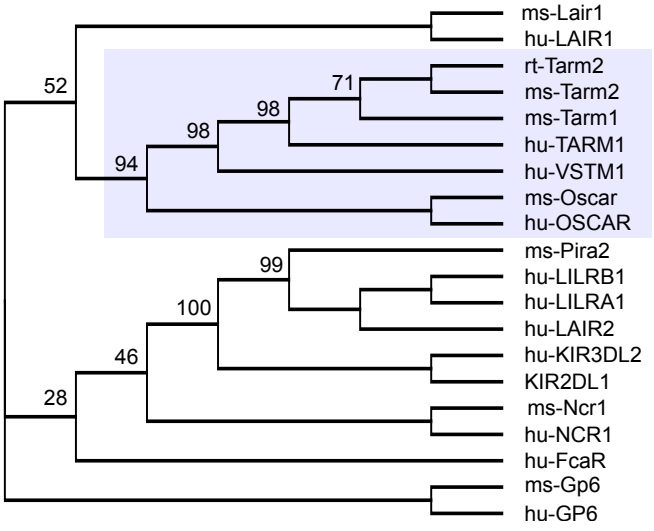

FIGURE 3.9: Phylogenetic tree constructed using amino acid sequences of the extracellular portions of LRC-encoded proteins. Amino acid sequences were aligned with Clustalw and the phylogenetic tree was constructed using the Neighbor-Joining method (Saitou and Masatoshi Nei 1987). The percentage of replicate trees in which the associated taxa clustered together in the bootstrap test (100 replicates) are shown next to the branches (Felsenstein 1985). The evolutionary distances were computed using the *p*-distance method (M. Nei and S. Kumar 2000) reflecting the number of amino acid differences per site. All positions containing gaps and missing data were not included in the analysis. The analysis was performed in MEGA5 (Tamura et al. 2011).

3.2 Phylogenetic analysis

SIRL-1 and TARM1 are members of the broad immunoglobulin superfamily (IgSF) and are evolutionarily related to other members of the LRC. However, within this set of genes TARM1 and SIRL-1 are most closely related to OSCAR. A neighbour-joining (NJ) phylogenetic tree constructed from the multiple protein sequence alignment of the extracellular portions of human and mouse LRC genes places TARM1, SIRL-1 and OSCAR into a well-defined clade with a high bootstrap value (Fig. 3.9).

The majority of the LRC-encoded receptors are composed of two or more Ig-like domains, each encoded within a separate exon. This arrangement facilitates gene evolution by the exchange of encoded domains through exon shuffling. Indeed, exon shuffling was demonstrated to underlie the emergence of new KIR genes in hominoids (Rajalingam, Parham, and Abi-Rached 2004). In order to account for potential exon duplication and shuffling events, multiple sequence alignment of TARM1-related genes and other LRC members was repeated using amino-acid sequences of each Ig-like fold separately.

This approach produced a clear grouping of the first and the second domains of TARM1-related proteins into separate clades. SIRL-1, which has a single Ig-like domain, grouped with the domain-1 clade of TARM1 (Fig. 3.10). Although OSCAR Ig-domain sequences did not group within the TARM1 clades, OSCAR Ig1 and OSCAR Ig2 formed sister clades to the respective Ig-clades of TARM1-related genes.

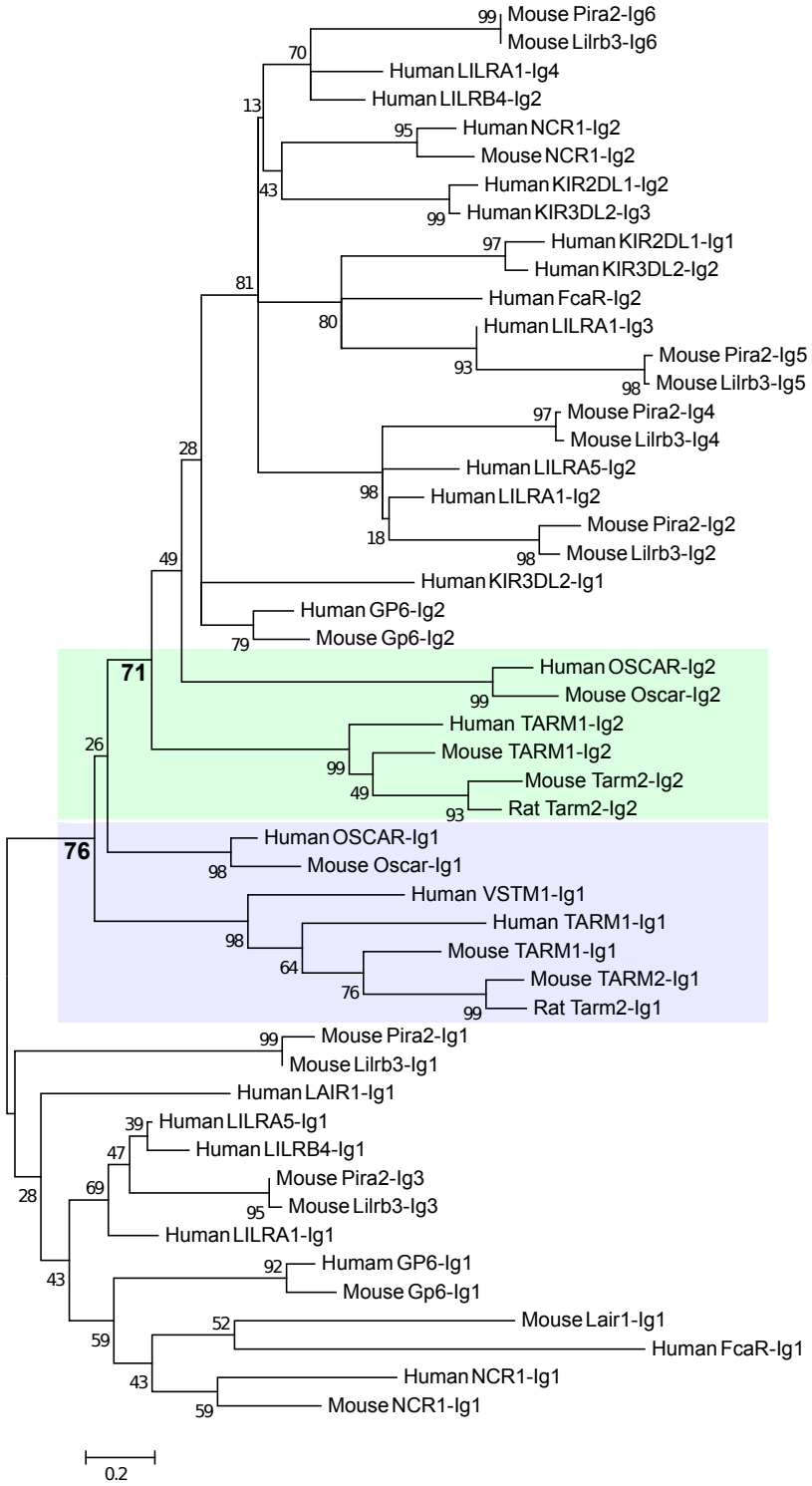

FIGURE 3.10: Phylogenetic tree constructed using amino acid sequences of the Ig-like domains of LRC-encoded proteins. Ig-like domain amino acid sequences were aligned in Clustalw and the phylogenetic tree was constructed using the Neighbor-Joining method (Saitou and Masatoshi Nei 1987). The percentage of replicate trees in which the associated taxa clustered together in the bootstrap test (100 replicates) are shown next to the branches (Felsenstein 1985). The evolutionary distances were computed using the *p*-distance method (M. Nei and S. Kumar 2000) reflecting the number of amino acid differences per site. All positions containing gaps and missing data were not included in the analysis. The analysis was performed in MEGA5 (Tamura et al. 2011).

3.3 Summary

The LRC encodes sets of paired activating and inhibitory receptors that modulate the function of classical innate and adaptive immune cells, such as NK, CTL and myeloid cells in addition to non-classical immune cells, such as platelets and osteoclasts. This chapter described the comparative genomics and evolutionary characterisation of two novel paired OSCAR-related genes, *Vstm1* and *Tarm1*, encoded on the centromeric boundary of the human and mouse LRC regions.

Mouse and human *Tarm1* genes encode proteins belonging to the immunoglobulin superfamily. Their extracellular portions are comprised of two Ig-like domains and are well conserved both in sequence and exon structure. The transmembrane regions contain a conserved arginine, often seen in activating receptors where it serves as an association site for ITAM-bearing signalling adaptors such as FcϵRγ. An additional, *Tarm1*-related gene, which I termed *Tarm2* is encoded just downstream of *Tarm1* in mouse, rat and elephant but is not present in human.

Human SIRL-1, in contrast to TARM1, contains only a single Ig-like domain and lacks the conserved arginine within its TM. Instead, a long cytoplasmic tail contains two ITIMs, implying inhibitory potential through SHP-1 recruitment. Murine *Sirl-1* is not conserved as only a partial ORF, lacking the inhibitory cytoplasmic tail, is found with no evidence of transcriptional activity.

This disparity in gene conservation and number between human and mouse extends to several mammalian orders studied. I analysed the genomic region of *Tarm1*-related genes in Primates (human and bushbaby), Carnivora (cat and dog), Rodentia (mouse and rat), Lagomorpha (rabbit), Proboscidea (elephant) and Monotremata (platypus).

Based on this analysis, it appears that the earliest mammalian OSCAR-related sequence is found in platypus and is orthologous to *Tarm1*. Further, the comparison of *Tarm1* genomic region showed evidence of its expansion and contraction resulting in the birth and death of the members of *Tarm1* family in different mammalian orders. In early primates (represented here by the bushbaby) and the genomes of cat and dog, but not human, *Tarm1* seems to have undergone rounds of duplication events including an inverse duplication giving rise to two additional *Tarm1*-like genes.

This duplication event does not however explain the emergence of SIRL-1 which contains a single Ig-like domain and a long cytoplasmic tail with inhibitory ITIMs. To investigate a potential acquisition of the inhibitory tail from another LRC-encoded gene through exon shuffling, BLAST search was performed with the SIRL-1 tail amino-acid sequence. The search did not identify any significant hits other than SIRL-1 orthologs. A more in-depth analysis would thus be required to establish the origins of SIRL-1. Interestingly, the single Ig domain of SIRL-1 clusters with high confidence values with the Ig1 domains of human and mouse TARM1 and TARM2 proteins indicating common evolutionary origin.

The clustering of gene families within the LRC suggests a common ancestral relationship and a closely linked functional role as has been demonstrated for KIRs and LILRs. It is likely that SIRL-1 and TARM1 evolved to function antagonistically in primates and other mammals with functional SIRL-1 and TARM1 proteins. The lack of conservation of *Sirl-1* gene in rodents may be due to the differential cell and tissue distribution of its activating counterparts *Tarm1* and *Oscar*. OSCAR is expressed on osteoclasts in human and mouse where it plays a central role in the regulation of osteoclastogenesis (A. Barrow, N. Raynal, et al. 2011). In human, but not mouse, OSCAR is also expressed on monocytes, neutrophils, macrophages and DCs where it modulates innate and adaptive immune responses (Merck, Gaillard, Scuiller, et al. 2006; Merck, Gaillard, Gorman, et al. 2004). In order to study TARM1 protein cell and tissue distribution, monoclonal anti-human and -mouse TARM1 antibodies had to be developed. The next chapter describes the development and characterisation of these reagents.

Chapter 4

Generation and validation of anti-TARM1 monoclonal antibodies

At the onset of this project, the *TARM1* gene was a newly identified and as yet an uncharacterised member of the LRC. This presented a particular challenge as new immunological tools, such as monoclonal antibodies, had to be developed and validated in order to permit further characterisation and functional analysis of TARM1 protein.

This chapter describes the development of reagents that enabled me to undertake further characterisation of TARM1 receptor expression and function.

4.1 Generation and characterisation of monoclonal antibodies against mouse and human TARM1

Multiple approaches are available for generating monoclonal antibodies, each with its own advantages and drawbacks. Characterisation of TARM1 required antibodies that would be suitable for a wide range of immunological techniques where the antibodies would recognise both linear and conformational epitopes, such as in Western blot and flow cytometry respectively.

I decided to develop a chimeric TARM1 protein comprised of TARM1 ectodomain fused to the Fc region of human IgG_1 for use as an immunogen. This approach provided a dual advantage, both enabling the generation of a large number of monoclonal antibodies to a variety of TARM1 epitopes and provided a fusion protein tool which could be used in its own right to study functional aspects of TARM1 receptor and its putative ligand.

Soluble fusion proteins composed of the constant region of human or murine IgG_1 fused to the extracellular portion of a protein of interest are used extensively in both research and therapeutic applications. A number of receptor ligand interactions have been identified using such soluble Fc fusions (Latchman, McKay, and Reiser 1998).

Besides the apparent advantage of producing a secreted form of an otherwise transmembrane protein, the presence of an Fc portion confers additional valuable properties to the fusion protein. It acts as a tag, allowing easy visualisation in the absence of monoclonal antibodies against the protein of interest. The Fc portion also makes it possible to purify the fusion proteins using standard chromatography with protein A or G columns. Moreover, due to the natural propensity of the IgG heavy chain constant region to dimerise, Fc fusion proteins form homodimers that display higher avidity for their ligand than monomeric forms.

Thus, construction of TARM1 fusion proteins equipped me with a valuable tool to study TARM1 protein function as well as to serve as an immunogen for generating a panel of monoclonal anti-TARM1 antibodies. This section describes how TARM1 fusion proteins were generated, expressed, purified and validated.

4.1.1 Cloning of TARM1 into Signal pIG vector.

Using bioinformatics tools such as protein secondary structure prediction, domain identification and multiple sequence alignment with other LRC-encoded proteins, I established the amino acid sequence of the two Ig-like folds of TARM1 and the membrane proximal "stem" region to be between the following amino acids: mouse QTDIPE...GYTVDN and human QGDTRG...NYSLGN. Next, the DNA sequence encoding this extracellular portion was amplified by PCR introducing restriction enzyme sites compatible with the multiple cloning site of the Signal pIG plus vector. A detailed cloning procedure

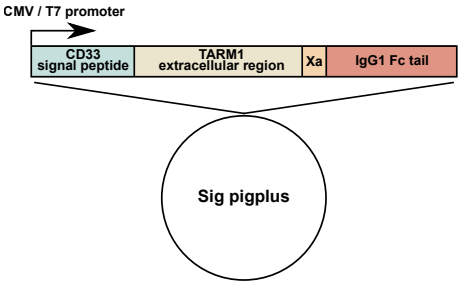

FIGURE 4.1: Schematic representation of TARM1-Fc construct. TARM1 sequence encoding two Ig-like domains and the stem region was cloned into Sig pIG plus vector placing TARM1 extracellular portion downstream of CD33 signal peptide and upstream of human IgG_1 C region. The resulting construct is under control of two promoters T7 and CMV. A factor Xa site is encoded within the vector sequence between TARM1 and IgG_1 Fc tail.

is described in *Materials and Methods* section. Briefly, TARM1 amplicons were digested, purified and ligated into a linearised Signal pIG plus vector. Ligation products were transformed into competent *E. coli* DH5α cells. The resulting construct is under transcriptional control of a dual promoter T7 and CMV allowing for vector expression in both bacterial and mammalian cells respectively. The construct places TARM1 sequence downstream of the CD33 signal peptide, ensuring efficient protein secretion, and is followed by a human IgG_1 Fc region (Fig. 4.1). A factor Xa site is included in the vector sequence between TARM1 and IgG_1 Fc tail which, if necessary, permits enzymatic removal of the Fc portion from the fusion protein.

The sequences of human and mouse TARM1 Signal pIG plus constructs were validated by sequencing and transfected into Hek293 cells for a large-scale protein secretion as described next.

4.1.2 Expression, purification and validation of human and mouse TARM1 Fc proteins

Hek293 cells were chosen for the expression of TARM1 Fc fusion proteins. Initially, transient transfections were performed in a 6-well format, and cell culture medium was collected to confirm the presence of secreted fusion proteins by Western blot using anti-human IgG_1 Fc-specific antibody. As mentioned earlier, Fc fusion proteins tend to form covalently-linked dimers; it was, therefore, important to establish whether:

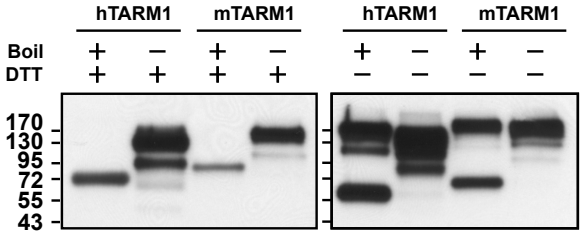

FIGURE 4.2: Western blot analysis of TARM1 Fc fusion-containing supernatants. Confluent Hek293 cells stably expressing human (h) or mouse (m) TARM1 Fc fusion proteins were grown for 5 days. Supernatants were collected and cell debris removed by centrifugation. 10 μl of 20 times concentrated supernatants were treated as indicated and analysed by Western blot. The PVDF membranes were probed with anti-human IgG_1 Fc-specific antibody conjugated to HRP.

1) Human and mouse TARM1 Fc fusion proteins were efficiently expressed as soluble molecules

2) formed dimers, remained as monomers or were expressed as a mixture of the two, and

3) whether any potential dimerisation was mediated by covalent bonds

Fusion protein-containing cell culture supernatants were concentrated 20 times and analysed by Western blot following different treatments. The supernatants were either reduced with dithiothreitol (DTT) or left untreated, with or without concomitant heat treatment in the presence of sodium dodecyl sulfate (SDS). Figure 4.2 (*left panel*) shows that a complete reduction of the disulphide bridges (*samples with DTT and heat treatment*) resulted in a single band of approximately 70 kDa for human TARM1 Fc fusion protein and 90 kDa for mouse. In the absence of DTT and heat treatment (*right panel*) the bulk of both human and mouse TARM1 Fc fusion proteins were expressed as dimers. However, heat treatment alone caused partial dissociation of the dimers into monomers (*non-reduced plus heat treatment*) indicating that some of the dimerisation is not mediated by covalent linkage between the Fc domains.

These results confirmed that both human and mouse TARM1 Fc fusion proteins were indeed secreted predominantly as covalently linked dimers enabling me to move on to a large-scale protein expression and purification. To this end, Hek293 cells were transfected with TARM1 Fc constructs and grown under neomycin selection until stable cell lines were established for each fusion construct. Following selection, stably transfected cells were expanded and seeded into triple-bottom tissue culture flasks. Cell culture supernatants were collected over the course of 3 weeks and fusion proteins were purified on protein-A columns.

To test the purification efficiency and the Fc fusion protein quality, samples of the column flow-through from each purification step were denatured, reduced and separated on a 10% polyacrylamide gel. Protein bands were visualised with Coomassie stain Figure 4.3**A**. The lane containing the cell culture supernatant (sup) prior to the purification contains bands corresponding to protein constituents of the cell culture medium, with the most abundant being BSA ($\sim$ 66 kDa). In the first and second column washes (lanes w1 and w2) the irrelevant proteins were removed. The final eluted TARM1 Fc fusion fraction (eluate) displayed the expected size.

Next, the integrity and stability of the purified fusion proteins was examined by Western blot after two rounds of freeze-thaw cycles. Samples were either treated under reducing or non-reducing conditions with or without heating and analysed by Western blot. The membrane was probed with HRP-conjugated anti-human IgG_1 Fc specific antibody (Fig. 4.3**B**). Under non-reducing conditions (*right panel*) both mouse and human TARM1-Fc fusion proteins were present as dimers, although heat-treatment caused a small fraction of the dimers, not linked covalently, to dissociate into monomers (*lanes 1 and 3*). Hence, purified TARM1-Fc fusions retained their integrity and exhibited good stability under storage conditions (1 mg/ml in Tris-neutralised elution buffer, pH7.5, at -80 ℃) even after repeated freeze-thaw cycles. This made them suitable for use as immunogens for development of monoclonal antibodies against human and mouse TARM1 extracellular domains and for further study of TARM1 function.

4.2 Immunisation and characterisation of monoclonal antibodies

All immunisations with TARM1 Fc fusion proteins, cell fusion and the initial enzyme-linked immunosorbent assay (ELISA)-based antibody screen were performed in collaboration with Professor K. Skjødt laboratory as described in *Materials and Methods*.

I performed further characterisation of two panels of monoclonal antibodies, 31 rat anti-mouse TARM1 and 91 mouse anti-human TARM1. The performance and specificity of individual clones were tested by flow cytometry, Western blot and immunofluorescent microscopy.

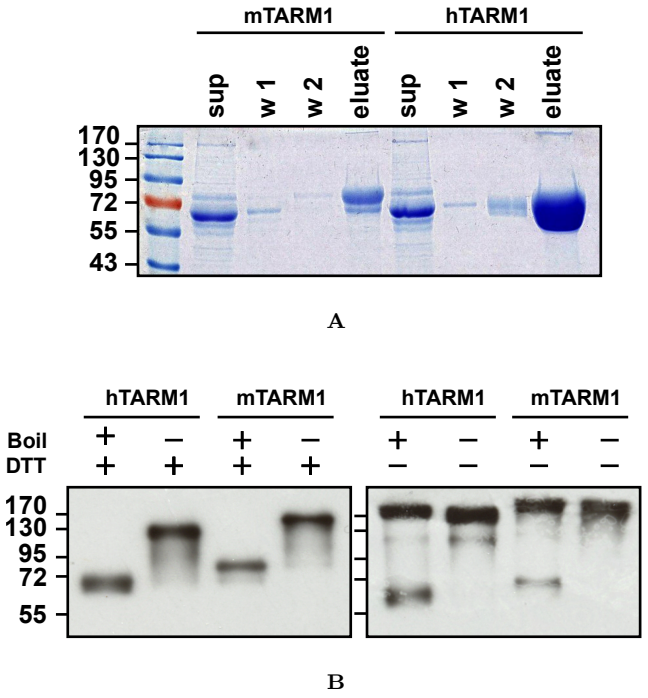

FIGURE 4.3: TARM1 Fc protein purification and validation. (A) Coomassie stain of denatured and reduced samples of column flow-through taken at different stages of TARM1 Fc purification. sup, 20 times concentrated cell culture supernatant; w1, first wash; w2, second wash; eluate, eluted TARM1 Fc fusion proteins. (B) Western blot analysis of purified TARM1 Fc fusion proteins after two repeated freeze-thaw cycles. Human and mouse fusion proteins were stored at -80 ℃ until analysis. Samples were treated as indicated and analysed by Western blot, ∼40 ng of protein were loaded per lane. Membranes were probed with anti-human IgG_1 Fc specific antibody conjugated to HRP

To determine the antibody reactivity, I expressed full-length FLAG-tagged human and mouse TARM1 proteins in Hek293T cells as well as HA-tagged versions were retrovirally transduced into 2B4 cells. Mouse TARM1-expressing cells were stained with rat anti-mouse TARM1 monoclonal antibodies; cells transduced with human TARM1 were used as a negative control. A representative screening panel for flow cytometry using 2B4 cells is shown in Figure 4.4. Median fluorescence intensity (MFI) of staining normalised to control MFI was plotted for each clone (*see the bar chart*). The same strategy was used to screen anti-human TARM1 monoclonal antibodies using mouse TARM1 expressing 2B4 cells as a negative control.

Hek293T cells transiently transfected with full-length FLAG-tagged TARM1 were screened with antibodies for use in Western blot. Rat anti-mouse TARM1 clone 13 (mAb13) and mouse anti-human TARM1 clone 4 (mAb4) were chosen for use in flow cytometry applications. Clones mAb2 (mouse-specific) and mAb74 (human-specific) performed well

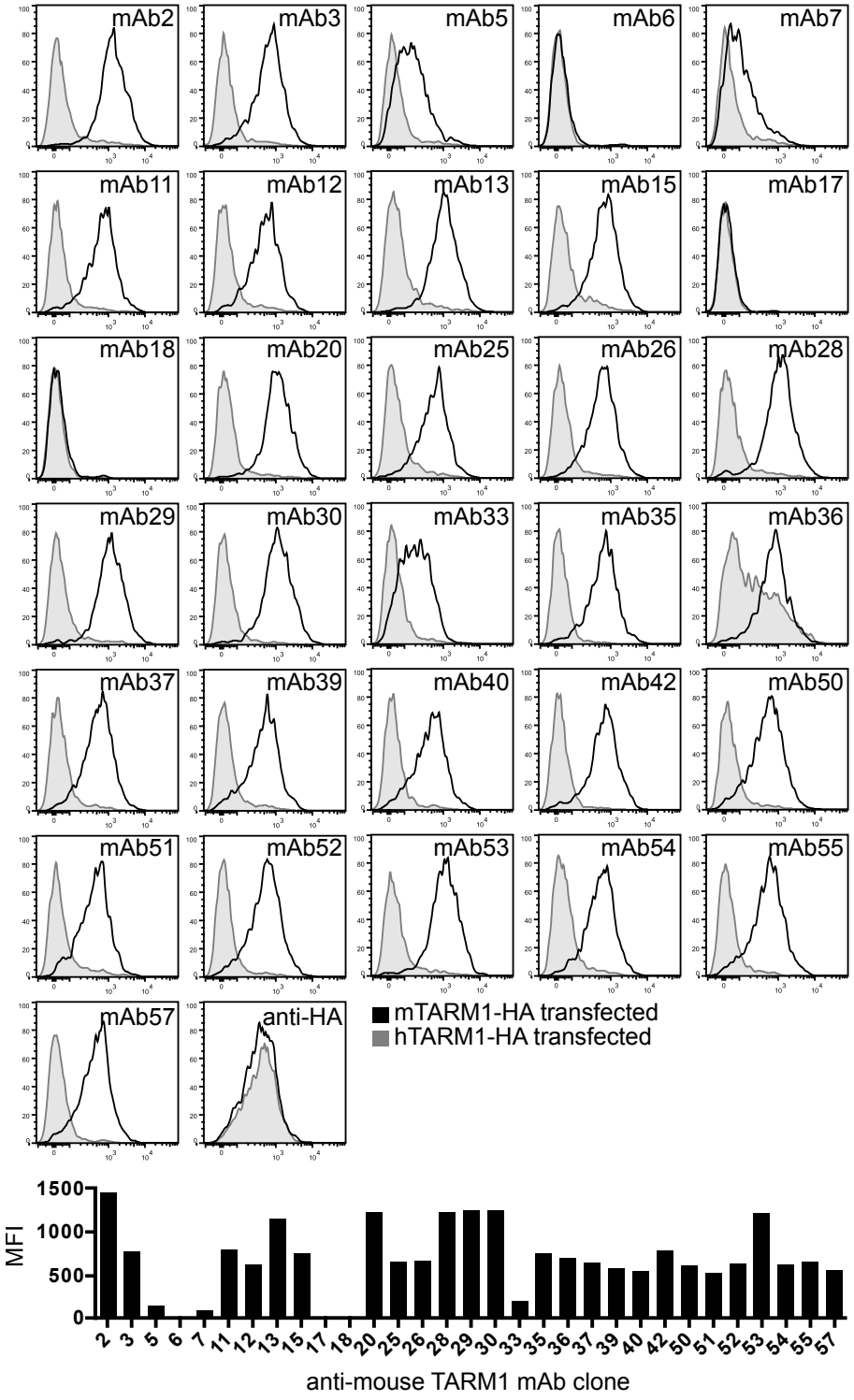

FIGURE 4.4: Anti-mouse TARM1 monoclonal antibody screen. 2B4 cells were transduced with HA-tagged human (grey filled histograms) or mouse TARM1 (black line) and stained with rat anti-mouse TARM1 antibodies. Normalised median fluorescence intensity (MFI) of staining was compared for all antibody clones. Similar levels of cell-surface expression of both mouse and human TARM1 was confirmed by staining with anti-HA antibody.

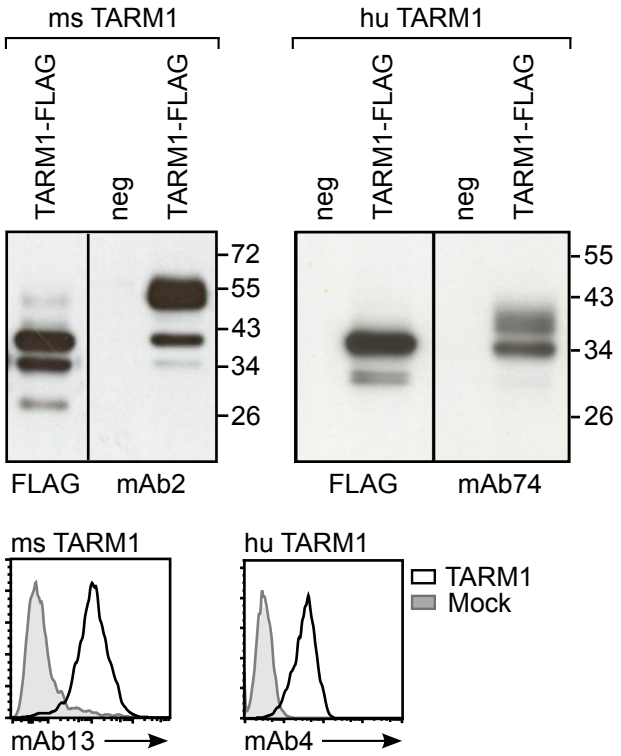

FIGURE 4.5: Anti-TARM1 monoclonal antibodies bind specifically to TARM1. Hek293T cells transiently transfected with TARM1 (open histograms) or mock transfected (filled histograms)were stained with monoclonal anti-mouse TARM1 mAb13 (left panel) or anti-human TARM1 mAb4 (right panel) and fluorescently labelled secondary Abs and analysed by flow cytometry. (B)Western blot analysis of the total lysate from TARM1-transfected cells. Hek293T cells were transfected with full-length Flag-tagged TARM1 and the specificity of anti-TARM1 Abs was determined by Western blot. Anti-Flag and anti-TARM1 mAbs detected bands of ∼40 kDa for mouse TARM1 (left panel,mAb2) and ∼34 kDa for human TARM1 (right panel, mAb74). Anti-Flag Ab failed to detect the higher molecular mass band of both mouse and human TARM1 proteins. No bands were detected in untransfected (neg) cell lysates.

in Western blot (Figure 4.5). Surprisingly, the anti-Flag antibody failed to detect the higher molecular mass (Mr) band detected by the TARM1-specific antibodies in both human and mouse blots. This discrepancy may be due to the steric occlusion of the Flag epitope caused by TARM1 glycosylation and/or tertiary structure.

Next, It was crucial to validate that the anti-TARM1 antibodies were reactive against both the recombinant and the endogenously expressed protein. The observation that *Tarm1* mRNA was abundant in the mouse bone marrow prompted me to investigate whether anti-TARM1 antibodies could detect the endogenous TARM1 on the cell surface of bone marrow-derived dendritic cells (BMDC).

I selected a panel of antibody clones with the highest MFI of TARM1 staining on

transduced 2B4 cells (as shown in Fig. 4.4. Additionally, it was of interest to establish whether TARM1 expression on the cell surface of resting BMDC was altered following their stimulation with LPS. For this purpose, bone marrow cells were isolated from a C57BL/6 mouse and differentiated into BMDC for 7 days as described in *Materials and Methods*. On day 8, cells were stimulated with ultra-pure LPS (100 ng/ml) for 24 h or left untreated. BMDC were stained for flow cytometric analysis of TARM1 expression with a panel of selected antibody clones or a Rat $IgG2_a$ isotype control antibody. Figure 4.6 shows that selected clones (except mAb18 which was used as a negative control) stained with high MFI and detected the presence of TARM1 protein on the cell surface of both resting and LPS-stimulated BMDCs. Comparison of staining MFI for control (PBS) and LPS-treated cells revealed a strong upregulation of TARM1 cell-surface expression following LPS-induced BMDC maturation.

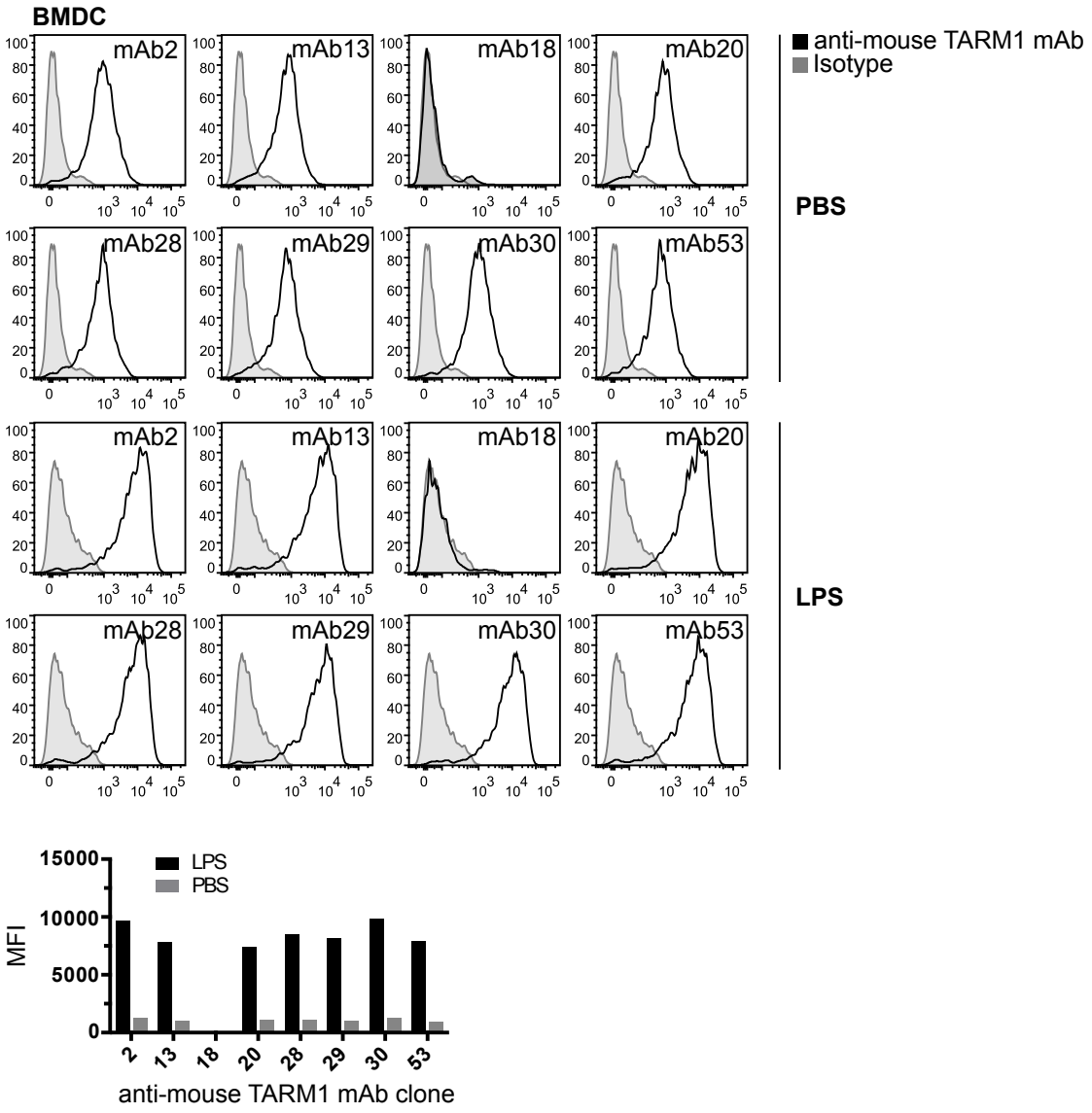

FIGURE 4.6: Anti-mouse TARM1 monoclonal antibodies detect endogenous protein expression in resting and LPS-stimulated BMDC. C57BL/6 bone marrow cells were differentiated into BMDC as described in *Materials and Methods*. BMDC were plated into 6-well plates and stimulated with LPS (100 ng/ml) for 24 h or left untreated (PBS). Following stimulation cells were detached and stained with a panel of selected anti-mouse TARM1 monoclonal antibodies (black lines) or isotype control (grey filled histograms). MFI (median) of TARM1 stain was plotted for each antibody clone.

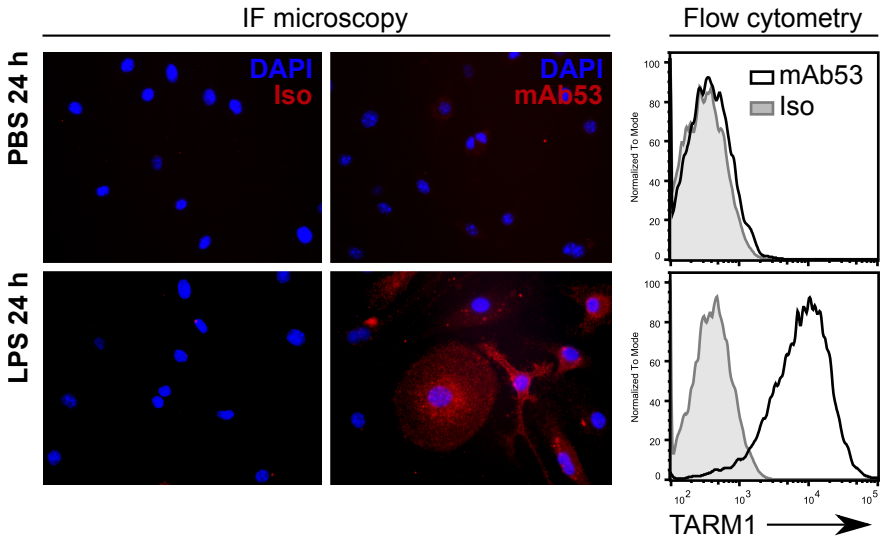

FIGURE 4.7: Anti-mouse TARM1 monoclonal antibody detects endogenous expression of TARM1 in LPS-stimulated BMM by immunofluorescent microscopy. Representative image from a screening panel of anti-mouse TARM1-specific antibodies. BMM were differentiated as described in *Materials and Methods*, stimulated with 100 ng/ml ultra-pure LPS for 24 h or left untreated. Cells were fixed with 2% PFA and stained with a panel of anti-mouse TARM1-specific antibodies or isotype control.

To screen anti-mouse TARM1-specific antibodies for suitability in immunofluorescent (IF) microscopy I used *in vitro* differentiated BMM that were treated with LPS (100 ng/ml) or left untreated for 24 h. Cells were differentiated for 6 days as described in *Materials and Methods*, detached from culture dishes and transferred into wells with sterile microscopy glass cover slips, allowed to attach for 6 h and stimulated with 100 ng/ml ultra-pure LPS for 24 h or left untreated. Cells were fixed with 2% PFA and stained with a panel of anti-mouse TARM1 specific antibodies or isotype control. Representative staining of mAb53 is shown in Figure 4.7. TARM1-specific antibody clones 2, 13, 20, 28, 29, 30 and 53 performed equally well in this assay. The IF microscopy staining of BMM showed that only LPS-treated cells expressed TARM1 protein. This was also confirmed by flow cytometric staining of BMM using mAb53 (Fig. 4.7 histogram overlays) and other clones.

4.3 Summary

To characterise the endogenous TARM1 protein expression specific antibodies were developed. I created soluble human and mouse TARM1 fusion proteins consisting of the TARM1 ectodomain fused to the human IgG_1 Fc domain to serve as immunogens. Two panels of monoclonal anti-mouse and -human TARM1 antibodies were raised and characterised for use in flow cytometry, Western blot and IF microscopy.

Many antibody clones performed well in the assays tested. I selected the following clones for further use in this work. Antibody clones mAb13, mAb53 (both rat anti-mouse TARM1) and mAb4 (mouse anti-human TARM1) stained TARM1-transfected and primary cells, as determined by flow cytometry. Clones mAb2 (rat anti-mouse TARM1) and mAb74 (mouse anti-human TARM1) detected Flag-tagged TARM1 in transfected cell lysates by Western blot. mAb53 performed well both in IF microscopy and in flow cytometry of primary cells.

The above clones were used in all the further experiments described in the following chapters.

Chapter 5

TARM1 protein characterisation

The vast majority of transmembrane proteins undergo post-translational modifications (PTM) that can have an impact on protein structure, stability and biological function. Glycosylation is amongst the most widespread modifications, affecting an estimated 70% of all eukaryotic proteins (Apweiler, Hermjakob, and Sharon 1999). Disruption of the normal glycosylation pattern has been implicated in a number of autoimmune conditions (Doyle and Mamula 2001). Thus, prediction of the glycosylation sites with a subsequent experimental validation is an important part of the characterisation of novel proteins as well as protein engineering.

Four main categories of glycosylation are defined according to the type of the bond formed between the sugar and the amino-acid. These are N-linked, O-linked, C-mannosylation and glyco-phosphatidylinositol (GPI) anchor attachments.

• **N-glycosylation** is achieved through the addition of oligosaccharides to the amino group of an asparagine. This process occurs co-translationally within the endoplasmic reticulum and affects protein folding.

• **O-linked glycosylation**, on the other hand, is not restricted to a single subcellular compartment and involves the modification of the hydroxyl group of a serine or a threonine (Reviewed in (Blom et al. 2004)).

• In **C-mannosylation**, a single α-mannopyranose is attached to the tryptophan residue via a C-C linkage (Hofsteenge et al. 1994).

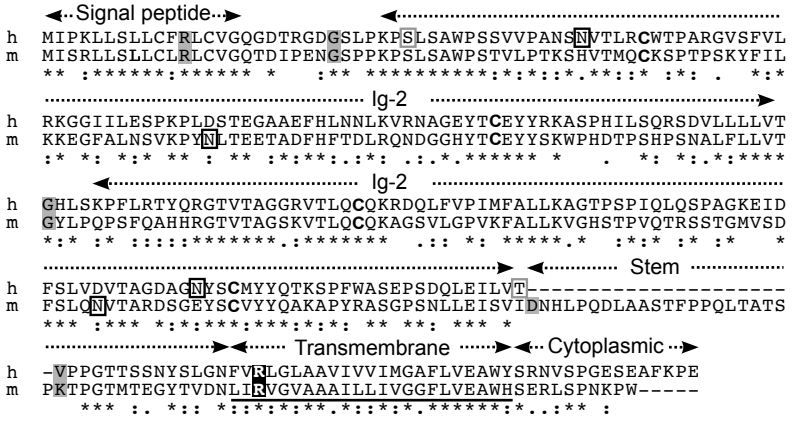

FIGURE 5.1: Amino-acid sequence alignment of human and mouse TARM1 orthologs showing predicted structural elements and post-translational modification sites. Structural protein domains are labeled above the alignment. Grey-shaded amino-acids are encoded at exonic splice junctions. Conserved cysteines that form the Ig-fold intrachain disulfide bridge are in bold font. The transmembrane region is underscored. Asparagines predicted to be glycosylated are enclosed in black rectangles. O-glycosylated sites are marked by grey rectangles

Some eukaryotic cell-surface proteins undergo **GPI-modification** at their carboxyl terminus which anchors them to the cell membrane. This modification requires a prior proteolytic cleavage of a C-terminal propeptide.

PTM sites can be predicted with various degrees of confidence, and recent advances in the development of computational protein analysis tools as well as the growing body of experimentally validated protein structures and post-translational modifications allowed refinement of such predictions. The sequon Asn-Xaa-Ser/Thr (where Xaa is any amino acid except Pro) was identified as a prerequisite sequence for the N-glycosylation. Such consensus was however more difficult to infer for GPI-anchors and O-glycosylation (Blom et al. 2004). Instead, the analysis of validated modification sites revealed the importance of sequence composition and the amino acid properties surrounding the sites of these types of glycosylation (B. Eisenhaber, Bork, and F. Eisenhaber 2001).

This chapter describes computational and experimental approaches used to characterise TARM1 protein PTMs.

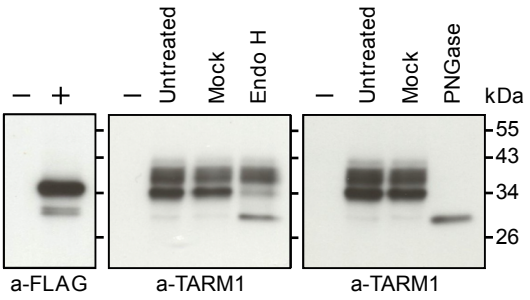

FIGURE 5.2: Western blot analysis of TARM1 glycosylation. *Left panel*: detection of FLAG-tagged full-length human TARM1 protein in total lysate of transfected Hek293T (+) and untransfected cells (-) with anti-FLAG antibody. *Center and Right panels*: total cell lysates of TARM1 transfected Hek293T cells were either left untreated (Untreated), mock treated (Mock) or treated with EndoH (center panel) or PNGase (right panel). The membrane was probed with anti-TARM1 mAb.

5.1 TARM1 is glycosylated

Several freely available prediction tools were used to analyse the protein sequences of human and mouse TARM1. Computational analysis identified two putative N-glycosylation sites (Fig. 5.1) in each sequence (NetNglyc v1.0 software (Gupta, Jung, and Brunak 2004)). In addition to the predicted N-glycosylation sites, human TARM1 is also predicted to have two O-glycosylation sites (NetOglyc v4.0 (Steentoft et al. 2013)). No C-mannosylation (NetCglyc v1.0 (Julenius 2007)) or GPI-anchor sites were found (big-PI predictor v.3 (B. Eisenhaber, Bork, and F. Eisenhaber 2001)) for either protein.

Experimental validation of the glycosylation state of proteins relies on the fact that variations in the composition of the oligosaccharides and the saturation of the predicted attachment sites affects the total protein mass and its mobility through the SDS-polyacrylamide gel. Thus, the analysis of the mobility shift following protein treatment with specific glycosidases allows such characterisation.

Peptide-N-glycosidase F (PNGaseF) is widely used to assess the N-glycosylation state. PNGaseF treatment results in the cleavage of the glycosidic bond between the asparagine and high mannose, hybrid or complex N-glycans. In contrast to PNGase, endoglycosidase H (Endo H) is unable to cleave off N-linked complex glycans synthesised during the transit through Golgi. This feature is useful when distinguishing between early and late protein trafficking.

I performed a deglycosylation study to validate the occupancy of the predicted glycan attachment sites in the human TARM1 and to establish the dominant protein form recognised by the anti-TARM1 monoclonal antibody used for Western blot assays.

To that end, Hek293T cells were transiently transfected with a FLAG-tagged full-length human TARM1 and total cell lysates were treated with either PNGaseF, EndoH or mock treated as described in the *Materials and Methods* section. Following the treatment, the protein mobility shift was examined by SDS-PAGE (Fig. 5.2).

Immunobloting using the anti-FLAG antibody or the monoclonal anti-TARM1 antibody showed a band of ∼34 kDa which was ∼4 kDa larger than the predicted 29.5 kDa for the unglycosylated TARM1 form. The anti-TARM1 mAb, but not the anti-FLAG mAb, also bound to a higher molecular mass (Mr) product that migrated as a broad band of ∼37-40 kDa. Conversely, the anti-FLAG mAb, but not the anti-TARM1 mAb recognised a low Mr band of ∼30 kDa, which could represent a degradation product.

The treatment with Endo H resulted in a conversion of the 34 kDa band, but not the high Mr band, to ∼30 kDa product (Fig. 5.2, centre panel). This suggests that the main protein species recognised by both the anti-FLAG and the anti-TARM1 mAb is the early, Endo H sensitive form. The treatment with PNGase F resulted in all TARM1 migrating at ∼30 kDa, which represents the fully deglycosylated form (Fig. 5.2, right panel).

These observations show that TARM1 protein is N-glycosylated and is recognised by the monoclonal anti-TARM1 antibody irrespective of its glycosylation state. The product migrating at an apparent Mr of ∼30 kDa represents the fully deglycosylated protein as predicted by theoretical mass calculation. The early TARM1 polypeptide residing within the ER as indicated by the EndoH sensitivity and running at an apparent Mr of ∼34 kDa was the predominant protein species recognised by the anti-TARM1 antibody. The fully glycosylated, EndoH resistant protein, exhibiting a broad molecular weight range, most likely represents different extents or branching of sugar moieties with differential effect on the total glycoprotein mass. The discrepancy between the staining of the predominant product and its fully deglycosylated form suggests that the anti-TARM1 mAb may have a lower affinity for the deglycosylated polypeptide. However, I can not rule out that the discrepancy could also be due to a partial degradation of TARM1 protein during the deglycosylation reaction.

The results suggest that ∼10 kDa oligosaccharide is added to TARM1 protein when it is expressed in Hek293T cells. The oligosaccharide size and composition is often cell-specific and can differ in primary cells from that observed here.

Since the treatment with PNGaseF resulted in the band running at an apparent Mr of a fully deglycosylated TARM1, it is likely that the predicted O-glycosylation sites are not occupied. I therefore did not proceed with the O-glycosidase treatment.

5.2 TARM1 associates with ITAM adapter FcRγ chain

As mentioned previously, a conserved arginine residue is embedded at position 3 within the TM of mouse and human TARM1. The transmembrane arginine is also present in TARM1 homolog OSCAR where it mediates the association with the FcRγ resulting in an increased receptor cell surface expression and transduction of activating signals (Merck, Gaillard, Gorman, et al. 2004). Signalling adapters have been shown to associate preferentially with either arginine or lysine embedded within the TM of the associating receptor. For instance, the majority of receptors known to associate with DAP12 bear a transmembrane lysine. However, a transmembrane arginine is a hallmark of an FcRγ and CD3ζ associating receptor. Mutagenesis experiments that substitute arginine for lysine or vice versa cause a dramatic reduction in the association efficiency (Feng, Call, and Wucherpfennig 2006). Such preferential assembly is dictated by several structural features of both the adapters and the associating receptors. Among these is the relative position of the pairing acidic and basic residues within the membrane-spanning domains of the assembling partners. All FcRγ associating receptors bear an arginine at position 3 in the N-terminal portion of the membrane-spanning segment which is well aligned with the aspartic acid of the FcRγ dimer. On the contrary, the aspartic acid in DAP10 and DAP12 are positioned towards the centre of the transmembrane segment aligning with the basic residue of the interacting receptor (Feng, Call, and Wucherpfennig 2006; Feng, Garrity, et al. 2005). Nevertheless, a cell-specific adapter association promiscuity was demonstrated for some immune receptors with implications for their biological functions (Nakahashi et al. 2007; Gilfillan et al. 2002; Diefenbach et al. 2002).

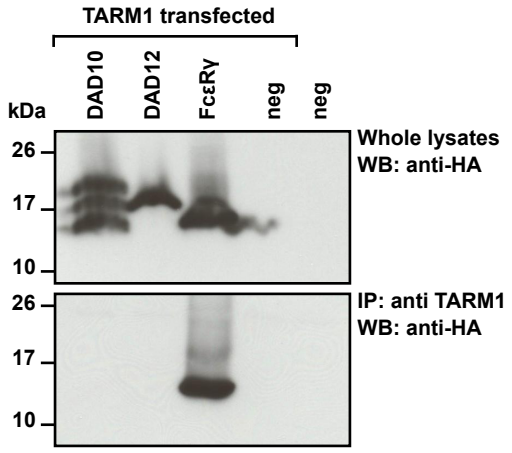

FIGURE 5.3: TARM1 co-immunoprecipitates with ITAM-containing adapter FcRγ. Hek293 cells stably expressing HA-tagged adapters DAP10, DAP12, FcRγ and parental adapter-negative cells (neg) were transiently transfected with full-length TARM1. Aliquots of whole lysates were analysed by Western blot with anti-HA antibody (top panel). TARM1 was then immunoprecipitated with monoclonal anti-TARM1 antibody and the complex was analysed by Western blot (bottom panel) with anti-HA antibody to detect the co-precipitated adapter.

To establish whether TARM1 associates with an ITAM-containing adapter, I used Hek293 cell-lines stably expressing haemagglutinin (HA) epitope-tagged FcRγ (HA-FcRγ) chain, DAP12 (HA-DAP12) and CD3ζ (HA-CD3ζ) adapters. Each cell-line was transiently transfected with a full-length N-terminally FLAG-tagged human TARM1. I used the monoclonal anti-TARM1 antibody to co-immunoprecipitate the TARM1-adapter complex from cell lysates.

Immunoblotting of the complexes with an anti-HA antibody, recognising the associated ITAM-adapter, revealed that only FcRγ co-immunoprecipitated with TARM1 (Fig. 5.3). These data demonstrate that TARM1 can stably associate with the ITAM adapter FcRγ consistent with activating function (Nakajima et al. 1999; A. Barrow, N. Raynal, et al. 2011; Lewis L Lanier et al. 1998; Merck, Gaillard, Gorman, et al. 2004).

5.3 Summary

In this chapter I provided evidence that human TARM1 is post-translationally modified by N-glycosylation as demonstrated by changes in the protein mobility shift through SDS-polyacrylamide gel following treatment with N-glycosidases. The monoclonal anti-TARM1 antibody clone chosen for use in immunoblotting applications recognises predominantly the fully glycosylated protein but is also capable of reacting with a deglycosylated form, albeit with lower affinity.

The cytoplasmic tails of human and mouse TARM1 are short and devoid of signalling motifs, a common feature of many immunoreceptors that associate with an ITAM-containing adaptor for signal transduction. In a co-immunoprecipitation experiment, where human TARM1 was transiently expressed in Hek293 cells stably expressing adapters DAP10, DAP12 and FcRγ, TARM1 associated with the FcRγ adapter.

Classically, ITAM-bearing adapters were thought to trigger activating signalling cascades initiated by the phosphorylation of tyrosine residues within the ITAM by the Src family protein tyrosine kinases (Iwashima et al. 1994) resulting in the activation of a number of well-characterised effector pathways. However, a growing number of studies have challenged this paradigm in the recent decade. For instance, signalling through DAP12 has been shown to inhibit TLR-mediated responses in macrophages (J. A. Hamerman, Tchao, et al. 2005). Similarly, the pairing of the FcRγ with FcαRI results in the inhibition of IgG-mediated activation of myeloid cells (Pasquier et al. 2005). It was therefore important to perform functional characterisation of TARM1 in order to determine the effects of its ligation on the responses of TARM1$^+$ cells. The antagonistic action of ITAM-bearing adaptors on TLR signalling is particularly relevant in this case as TARM1 expression is upregulated following TLR4 ligation.

In the following chapter I describe the expression profile of TARM1 in primary cells, the impact of TLR ligation on the TARM1 expression and identify the main TARM1-expressing cell subset *in vivo*.

Chapter 6

TARM1 expression profiling

6.1 TARM1 mRNA is expressed at similar sites in human and mouse

In order to gain insight into the transcriptional activity of human and mouse TARM1 genes in primary tissues, I performed a PCR-based screen of a commercially available human total RNA tissue panel and a total murine RNA tissue panel I prepared in-house using a C57BL/6 mouse. For screening, cDNA was synthesised by reverse transcription and examined for the presence of TARM1 transcript using specific primers amplifying a full-length coding region of TARM1 (Fig. 6.1).

Human and mouse tissues showed an overlapping pattern of TARM1 expression, with the transcript detectable in the lung, spleen, testis and thymus of both species. In mouse, TARM1 transcript was highly enriched within the bone marrow and, although, human bone marrow was not present on the panel, human fetal liver had a high TARM1 expression. Numerous studies investigating fetal hepatic cell composition report the presence of a large number of stem and progenitor cells similar to those found within the bone marrow. Human adult liver also contained TARM1 transcript, albeit at a lower level; this is in contrast to murine adult liver which lacked TARM1 expression. Interestingly, both human and murine lung showed a strong expression of TARM1 mRNA, which could be due to the presence of a large number of resident myeloid cells. Lymph node, present on the mouse tissue panel, but absent from the human panel, had a low level of TARM1 mRNA.

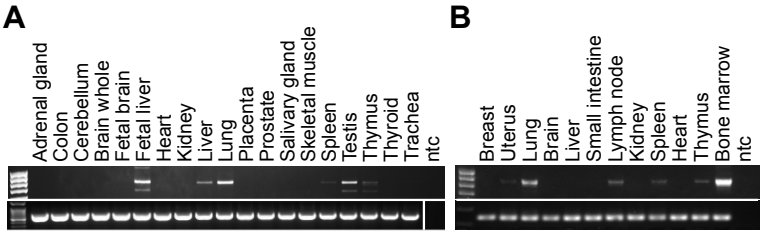

FIGURE 6.1: RT-PCR analysis of the expression of full-length TARM1 mRNA in human and mouse tissues. PCR was performed on cDNA synthesised from total tissue RNA obtained from (A) Human Total RNA Master Panel II, CloneTech, (B) Mouse tissue RNA panel produced in-house. TARM1 specific primers amplified full-length coding region transcript (*top panel*). Gapdh was used as a reference gene (*bottom panel*). ntc, no template control

All visible bands were excised from the gel and the PCR products were sequenced to validate amplicon identity. A secondary, lower-weight band visible in some tissues was a PCR artefact.

6.2 TLR signalling induces TARM1 expression on bone-marrow derived DC and Macrophages

Since treatment of BMDCs with the TLR4 agonist LPS induced upregulation of cell surface TARM1 expression, I screened a panel of TLR agonists for their ability to stimulate TARM1 expression. To this end, C57BL/6 bone-marrow was differentiated as described in *Materials and Methods* into BMDCs and macrophages (BMM) and treated with TLR agonists for 24 h. TARM1 cell-surface expression was then analysed by flow cytometry. As shown in Figure 6.2, signalling through several TLRs induced an increase in cell-surface expression of TARM1 to varying degrees. The maximal TARM1 induction in both BMM and BMDC was achieved following stimulation with LPS, a TLR4 agonist. LPS-induced cell-surface expression of TARM1 was confirmed in BMM by immunofluorescence microscopy (Fig. 6.3**A**). PCR analysis of LPS-stimulated BMM and BMDC (Fig. 6.3**B**) also showed a strong upregulation of TARM1 mRNA expression, indicating that the increase in TARM1 cell-surface expression could be due to an increase in the de novo mRNA synthesis.

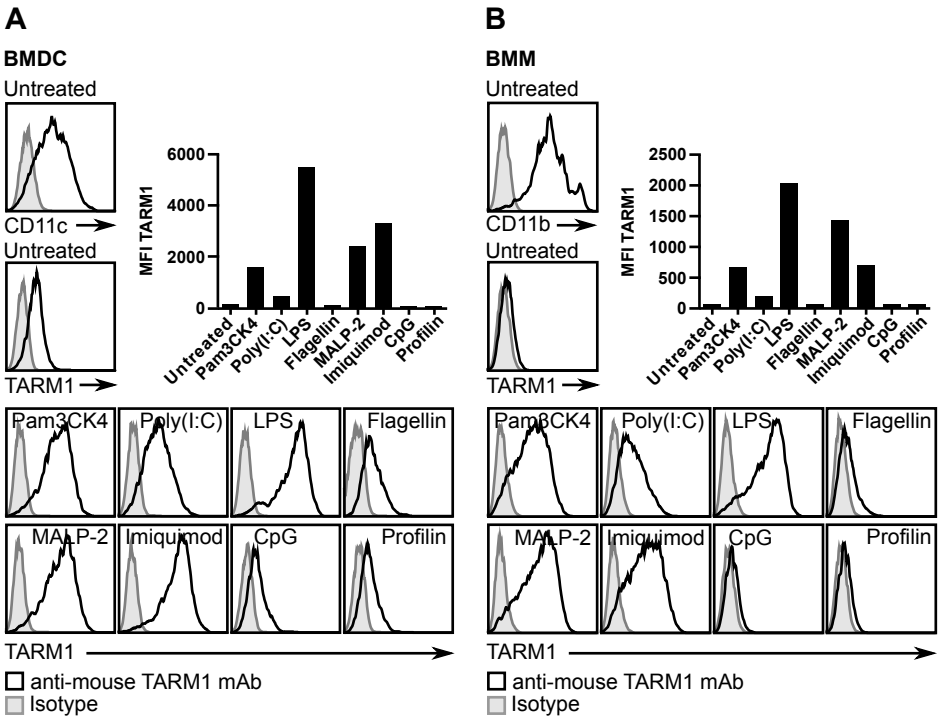

FIGURE 6.2: Flow cytometric analysis of TARM1 expression on BMDC (panel A) and BMM (panel B) following TLR stimulation. C57BL/6 bone marrow was differentiated into BMM and BMDC as described in Materials and Methods. Cells were stimulated with a panel of TLR agonists for 24 h and stained with anti-TARM1 monoclonal antibody or isotype control. Anti-CD11c (BMDC) and anti-CD11b (BMM) were used to assess the differentiation efficiency. MFI (median) of TARM1 staining was plotted for each TLR agonist. Dead cells, defined as 7-AAD$^+$ were excluded. The data is representative of at least 4 experiments showing comparable results.

6.3 TARM1 expression *in vivo* is restricted to the granulocytic cell lineage.

RT-PCR analysis of mouse tissues showed that the *Tarm1* mRNA was enriched in the bone marrow. Weaker bands were also visible in other tissues including lung, spleen, lymph nodes and thymus. In order to determine whether the presence of *Tarm1* transcript correlated with cell-surface protein expression in *ex vivo* samples, I analysed several tissues from healthy C57BL/6 mice by flow cytometry (Fig. 6.4**A**).

Cell-surface Tarm1 was expressed only in the bone marrow, and not in other tissues, which correlated with the high level of *Tarm1* transcript detected at this site. Closer inspection of Tarm1 cell-surface expression in the bone marrow revealed that only the Fsc^{hi}Ssc^{hi} cell population, consistent with granulocyte/monocyte precursors, was positive for TARM1 (Fig. 6.4**B**).

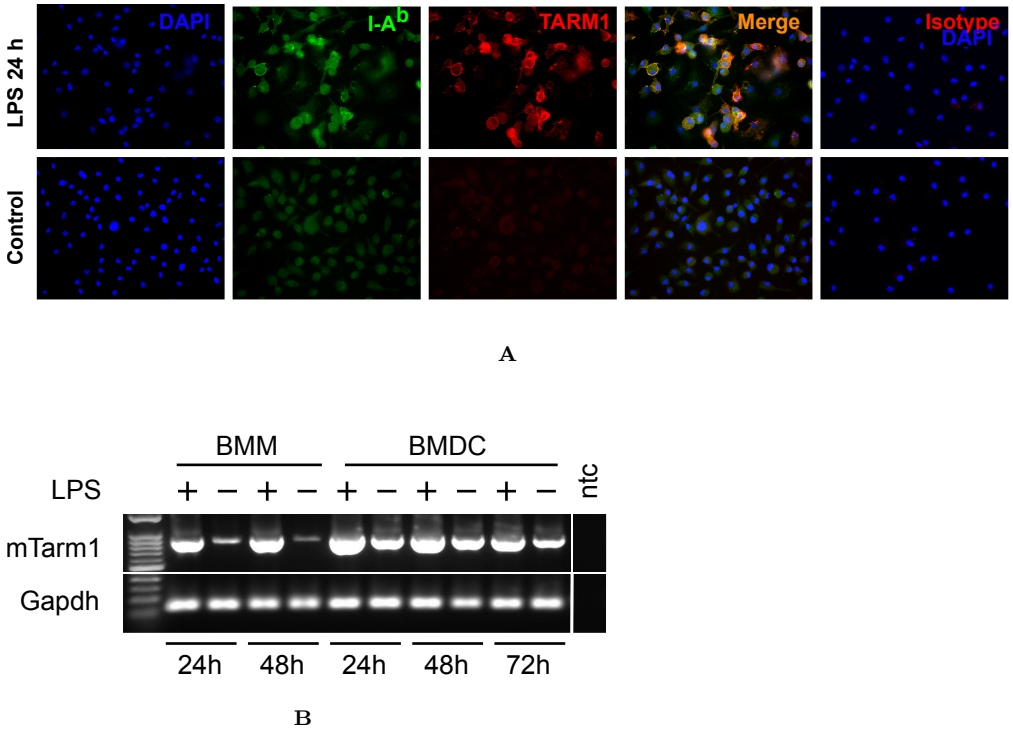

FIGURE 6.3: (A) Immunofluorescence microscopy of TARM1 expression on LPS-treated BMM. Following stimulation (24 h, LPS 100 ng/ml), cells were fixed with 2% PFA and co-stained with anti-TARM1 monoclonal antibody (red) and I-A^b (green). (B) PCR analysis of TARM1 mRNA expression in BMDC and BMM. Following stimulation, total RNA was extracted and reverse transcribed. Primers amplifying full-length TARM1 transcript were used. Gapdh served as a reference gene.

I also assessed TARM1 protein expression in key human lymphoid tissues (kindly provided by Dr. Kourosh Saeb-Parsy) including bone marrow, spleen and lymph nodes. Only spleen was present on the human total RNA panel. RT-PCR analysis showed a weak *TARM1* band in this tissue. As shown in Figure 6.5 TARM1 protein could be detected on the cell surface of granulocytes, identified by characteristic Fsc^{hi}Ssc^{hi} parameters and positive staining for CD16. Both BM and splenic CD16$^+$ granulocytes expressed TARM1, although the BM population had a higher density of TARM1 receptor as indicated by the higher MFI of positive staining. Granulocytes were present at a very low frequency in the lymph node sample. TARM1 expression was not detected on CD3$^+$ T cells or CD19$^+$ B cells. Some CD14$^+$ monocytes in the BM and spleen expressed a low level of cell-surface TARM1.

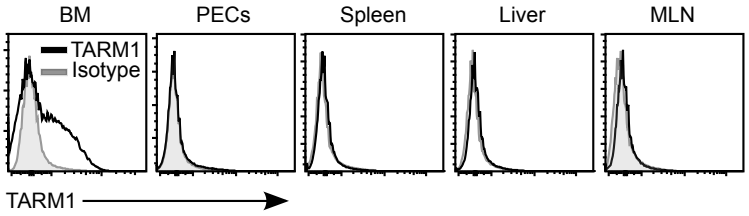

A

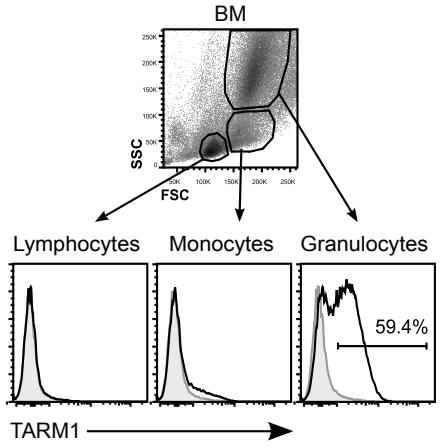

B

FIGURE 6.4: Flow cytometric analysis of TARM1 cell-surface expression in murine tissues. C57BL/6 mice were sacrificed at 8-10 weeks and total cell populations of bone marrow (BM), peritoneal exudate (PEC), spleen and mesenteric lymph nodes (MLN) were stained with anti-TARM1 mAb13 or rat IgG_{2b} isotype control for analysis by flow cytometry. (A) In healthy animals TARM1 expression is restricted to the bone marrow. The data is reprisentative of at least 3 independent experiments. (B) Within the bone marrow TARM1 expression is restricted to the high FSC:SSC cell population characteristic of granulo/monocytic lineage cells.

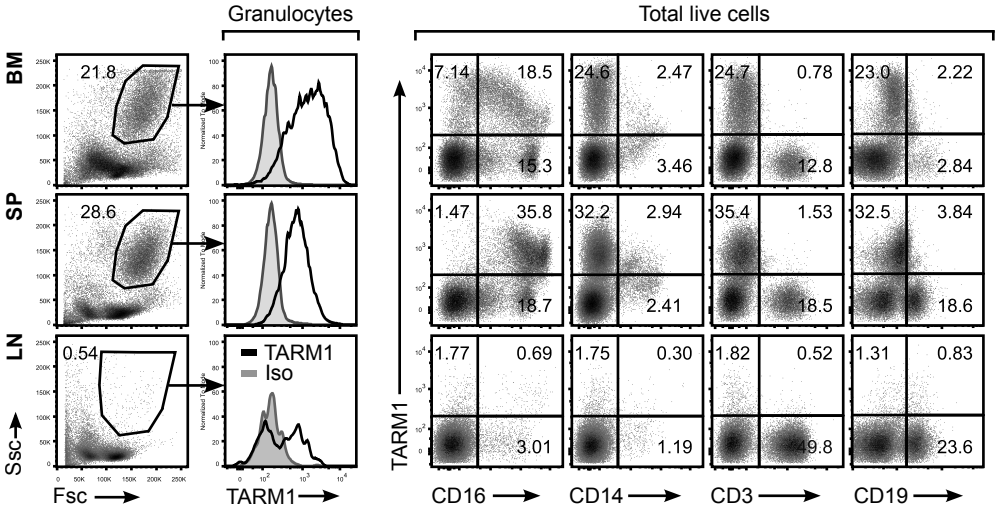

FIGURE 6.5: TARM1 is expressed on the cell surface of human granulocytes. Human bone marrow (BM), spleen (SP) and lymph nodes (LN) were stained with anti-TARM1 mAb4 or mouse IgG_1 isotype control and cell lineage markers for analysis by flow cytometry. For data analysis dead cells were excluded using Zombie Aqua (Biolegend) viability dye. Numbers on plots indicate percentages of cells within gates.

6.4 Summary

RT-PCR analysis of a panel of human and murine tissues showed an overlapping pattern of TARM1 expression in both species. The transcript was detected in human and mouse lung, spleen, testis and thymus. In mouse, *Tarm1* mRNA was also abundant within the bone marrow and, although human bone marrow was not present on the panel, flow cytometric analysis of this tissue showed a high expression of TARM1 protein. TARM1 was predominantly expressed within the granulocytic compartment defined by the characteristic $Fsc^{hi}Ssc^{hi}$ phenotype and positive staining for CD16. Some CD14 monocytes expressed a low level of TARM1 protein while $CD3^+$ T cells and $CD19^+$ B cells were $TARM1^-$. Bone marrow cells with a $CD16^{-/lo}$ phenotype were also $TARM1^+$ and most likely represent a myeloid precursor population that has not yet acquired CD16 expression associated with maturation.

A similar expression pattern was seen in mouse tissues by flow cytometry. TARM1 cell-surface expression was restricted to the bone marrow, where $TARM1^+$ cells made up 20% to 30% of the total bone marrow population. This number was as high as 59% within the $Fsc^{hi}Ssc^{hi}$ cell population, characteristic of granulocytes and granulomonocytic precursors.

The expression of TARM1 predominantly in lymphoid tissue suggested that it could be closely associated with immune cell function. Although TARM1 transcript was found in tissues of non-lymphoid origin such as lung and liver, these sites harbour large resident populations of specialised immune cells.

Bearing the above in mind, I examined TARM1 cell-surface expression on mouse BMDC and BMM stimulated with a panel of TLR agonists. This revealed that TARM1 is expressed on the surface of *in vitro*-derived resting BMDC (but not resting BMM) and that TARM1 expression was sensitive to TLR ligation (Fig. 6.2). While the majority of TLR agonists were able to induce TARM1 cell-surface expression, TLR4 (LPS, 100 ng/ml) was most effective. This observation pointed to a potential role of TARM1 in the innate immune responses to gram-negative bacteria.

Consequently, it was of interest to investigate TARM1 protein expression in the context of *in vivo* immune responses triggered following LPS treatment or bacterial infection, as described in the next chapter.

Chapter 7

TARM1 expression during inflammatory responses

7.1 Intraperitoneal administration of LPS induces TARM1 expression in bone-marrow and homing of TARM1$^+$ cells to the site of injection

As described in chapter 6, in healthy animals, constitutive expression of TARM1 was found within the bone marrow but not in the periphery. TARM1 expression was restricted to the bone marrow cell population identified by the $Fsc^{int/hi}Ssc^{hi}$ profile, characteristic of the granulo-monocytic lineage. Further, *in vitro* differentiated BMM and BMDC could be induced to express high levels of TARM1 following the treatment with TLR agonists, among which LPS produced the highest response. This observation prompted me to investigate whether a localised LPS administration *in vivo* would result in a similar upregulation of TARM1 and whether the response would be confined to the site of injection or induce a systemic TARM1 expression.

To that end, C57BL/6 mice were injected intraperitoneally (ip) with a low dose (3μg per mouse) of ultra-pure LPS. TARM1 expression was analysed by flow cytometry in the bone marrow and at the peripheral immune sites 24 h post-treatment. As previously observed, PBS control animals showed a constitutive TARM1 expression on granulo-monocytic population within the bone marrow but not at the peripheral sites (Fig. 7.1**A**).

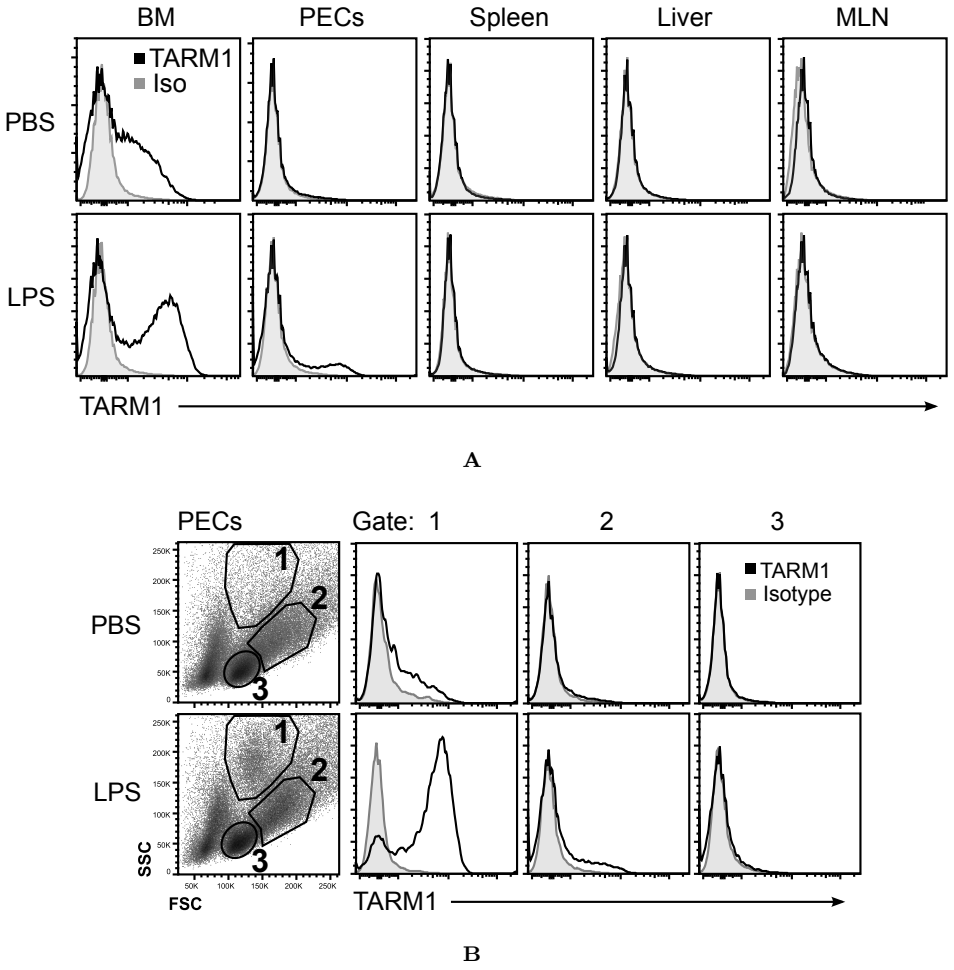

FIGURE 7.1: Flow cytometric analysis of TARM1 cell-surface expression in mouse tissues following intraperitoneal LPS administration. C57BL/6 mice were injected ip with either PBS or ultra-pure LPS (3 μg per mouse, Invivogen) and analysed 24 h later. (A) Total cell populations of bone marrow (BM), peritoneal exudate cells (PEC), spleen and mesenteric lymph nodes (MLN) were stained with anti-TARM1 mAb13 or isotype control for analysis by flow cytometry. Histograms represent total live cells. (B) Flow cytometric analysis of TARM1 cell-surface expression on peritoneal exudate cells (PECs). Histograms represent live cells within individual SSC:Fsc gates as indicated.

Conversely, LPS administration resulted in a strong upregulation of TARM1 cell surface expression in the bone marrow, and the appearance of a small TARM1$^+$ population in the peritoneal exudate cells (PECs). Other sites (spleen, liver and MLN) remained TARM1$^-$ 24 h post-treatment (Fig. 7.1**A**).

Closer examination of the PECs of control animals showed that they did not contain a clearly defined Fsc$^{int/hi}$Ssc^{hi} granulocyte population and consequently had ~1% TARM1$^+$ cells. Following LPS administration, a clear Fsc$^{int/hi}$Ssc^{hi} population representing ~16% of the total PECs could be observed and was comprised of predominantly TARM1$^+$ cells (Fig. 7.1**B**). The accumulation of the Fsc$^{int/hi}$Ssc^{hi} population at the

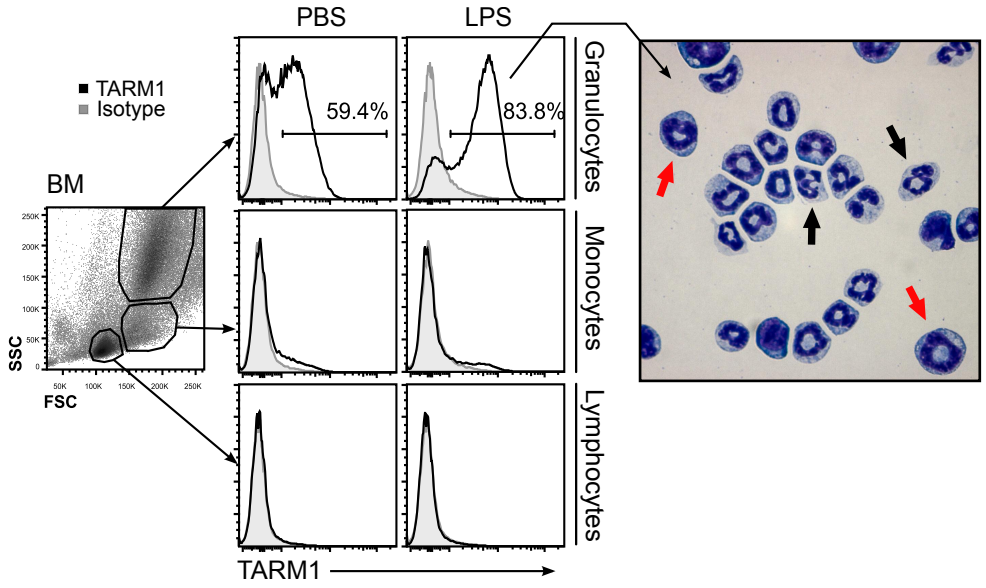

FIGURE 7.2: Flow cytometric analysis of TARM1 cell-surface expression in mouse bone marrow following intraperitoneal LPS administration. C57BL/6 mice were injected ip with either PBS or ultra-pure LPS (3 μg/mouse, Invivogen) and sacrificed 24 h later. BM cells were stained with anti-TARM1 mAb13 or isotype control. Histograms represent live cells within individual Fsc:Ssc gates as indicated. Inset: cytospin preparation of FACS-sorted and differentially stained TARM1$^+$ cells from the BM of LPS treated animals. BM - bone marrow. Promyelocytes (red arrows), mature neutrophils (black arrows).

site of injection was most likely the result of cell mobilisation from the bone marrow in response to the LPS-induced pro-inflammatory signals.

To examine the cellular morphology of TARM1$^+$ cells, the bone marrow of LPS treated animals was FACS sorted gating on the TARM1 marker. Sorted cells were spun onto microscope slides and differentially stained with Diff-Qiuck (inset Fig. 7.2). Cytospins revealed that TARM1 is expressed on a heterogeneous mixture of cells showing ring-shaped and hypersegmented nuclei characteristic of promyelocytes (red arrows) and mature neutrophils (black arrows), respectively (Cuenca et al. 2011).

The role of neutrophils as first responders, capable of rapid homing to the sites of immune challenge, is well established. Moreover, numerous studies describe the expansion of immature CD11b$^+$Gr-1$^+$ cells with ring-shaped nuclei in the bone marrow and their homing to the lymphoid tissues during inflammatory processes (Brudecki et al. 2012; Delano et al. 2007). Pathological conditions where such expansion was documented range from cancer to tissue damage and sepsis where these cells acquire immunoregulatory properties and function as a part of the heterogeneous myeloid-derived suppressor cell

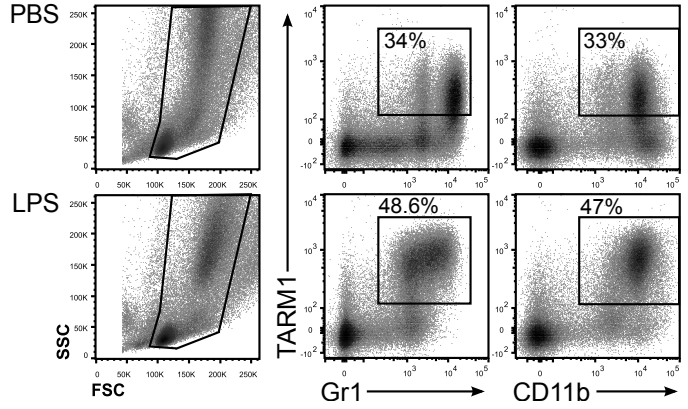

FIGURE 7.3: TARM1 cell-surface expression is upregulated on CD11b$^+$Gr1$^+$ cells in the BM following intraperitoneal LPS administration. C57BL/6 mice were injected ip with either PBS or ultra-pure LPS (3 μg/mouse, Invivogen) and the expression of TARM1, Gr1 and CD11b was examined by flow cytometry 24 h later.

(MDSC) population. Hestdal et al. demonstrated that Gr-1 is not restricted to a single cell lineage and that the level of Gr-1 expression correlates with the maturation stage of the myeloid cells ranging from Gr-1$^{neg/lo}$ immature progenitors and myelocytes, to Gr-1^{hi} differentiated neutrophils (Hestdal et al. 1991). The anti-Gr-1 antibody RB6-8C5, which was extensively used to identify neutrophils and perform cell depletion *in vivo*, was later shown to bind epitopes present on Ly6G and Ly6C cell-surface proteins (T. Fleming, M. Fleming, and Malek 1993). Characterisation of the cell surface expression pattern of these antigens showed that Ly6G is expressed predominantly on mature neutrophils and correlates with granulocyte maturation stage, whereas Ly6C expression is not restricted to neutrophils but has a wider cellular distribution including dendritic cells, subpopulations of lymphocytes and monocytes (T. Fleming, M. Fleming, and Malek 1993). Bone marrow monocytes as well as extravasated monocytes have been shown to express high levels of Ly6C (Sunderkötter et al. 2004) and, along with other cell-surface markers, this antigen is now widely used to identify the monocytic lineage. I initially used the Gr-1 antibody in combination with CD11b to determine whether the phenotype of the LPS-expanded TARM1$^+$ cells in the bone marrow and the peritoneum was in line with the phenotype of CD11b$^+$Gr-1$^+$ cell population with regulatory properties described by earlier studies.

Indeed, all TARM1$^+$ cells were also positive for CD11b and Gr-1 (Fig. 7.3). The bone marrow of healthy animals also contained a population of CD11b$^+$Gr1$^+$ cells that expressed a lower level of TARM1. Several studies demonstrated that the CD11b$^+$Gr1$^+$

cells in healthy animals lack the immunoregulatory capacity of $CD11b^{+}Gr1^{+}$ expanded during inflammatory responses suggesting that the presence of inflammatory mediators and growth factors accompanying inflammation are required by this cell population for the functional transition to MDSCs (Delano et al. 2007; Sander et al. 2010).

The dramatic upregulation of TARM1 on $CD11b^{+}Gr1^{+}$ in response to inflammatory signals is intriguing. To gain a greater insight into the identity of $TARM1^{+}$ cells and to compare their phenotype under steady-state condition of health to that during an inflammatory response, I performed a flow cytometric characterisation of tissues using Ly6G and Ly6C specific antibodies and prototypical cell-surface markers of myeloid and lymphoid lineages. C57BL/6 mice were administered LPS or PBS ip, as previously, and the bone marrow cells and PECs were analysed by flow cytometry 24 h later.

The results confirmed that the $TARM1^{+}$ population within the bone marrow belonged to the granulo-monocytic subset with $CD11b^{+}Ly6G^{+}Ly6C^{+}$ phenotype and was negative for classical T cell, B cell and DC markers CD3, CD19 and CD11c, respectively (Fig. 7.4**A**). $TARM1^{+}$ cells in the bone marrow of control animals were predominantly $CD11b^{+}Ly6G^{hi}Ly6C^{int}$ with a ∼17% also expressing MHC class II (MHC-II). LPS administration induced an upregulation of TARM1 expression and expansion of the $TARM1^{+}$ population size, as was observed in previous experiments (Fig. 7.4**A**).

The high expression of the CD11b and Ly6G antigens on $TARM1^{+}$ cells in the bone marrow of healthy controls suggested they most likely represented mature neutrophils. On the contrary, under the conditions of inflammatory response following LPS administration, an expansion of the $TARM1^{+}$ population was accompanied by a markedly reduced expression of the Ly6G antigen, indicating a shift towards a more immature myeloid phenotype.

This shift was even more apparent in the peritoneal exudate cells of LPS treated mice. Two distinct $TARM1^{+}$ populations that differed in their Fsc profile, the expression of Ly6G, Ly6C and MHC-II were observed. These populations were gated separately based on their Fsc characteristics during flow cytometric analysis. Gate 1 - $TARM1^{+}Fsc^{int}$, and gate 2 - $TARM1^{+}Fsc^{hi}$ (Fig. 7.4**B**). Lineage marker analysis of these two subgroups revealed that only the Fsc^{hi} population (gate 2) was MHC-II^{+}, co-expressed CD11b, high levels of Ly6C and low Ly6G ($CD11b^{+}Ly6C^{hi}Ly6G^{lo}$MHC-$II^{+}$). The $TARM1^{+}Fsc^{int}$

subpopulation (gate 1) did not express MHC-II and was CD11b^{+}Ly6C^{int}Ly6G^{hi}MHC-II^{-}. These phenotypic characteristics are consistent with the granulocytic origin of the population in gate 1, and monocytic origin of the population in gate 2. Since the total TARM1^{+} population did not express CD11c in either the bone marrow or the peritoneum, MHC-II expression is unlikely to be due to the presence of DCs and macrophages. The MHC-II^{+} cells resembled what has been termed "inflammatory monocytes". These cells are rapidly recruited to the sites of inflammation where they give rise to pro-inflammatory DCs and macrophages (Geissmann et al. 2010; Serbina and Pamer 2006).

In the experiments described here I used a model of a mild peritonitis where the endotoxicosis was induced with a low dose of LPS (0.15 mg/kg, whereas LD50 dose is 1–25 mg/kg (Fink 2014)). Even at this dose profound changes in TARM1 expression and TARM1^{+} cells were observed 24 h following the injection. Since this response was mediated through TLR4 ligation and did not recapitulate the complexity of the immune response mediated by live infection, it was of interest to investigate the fate of TARM1^{+} cells during systemic bacterial challenge.

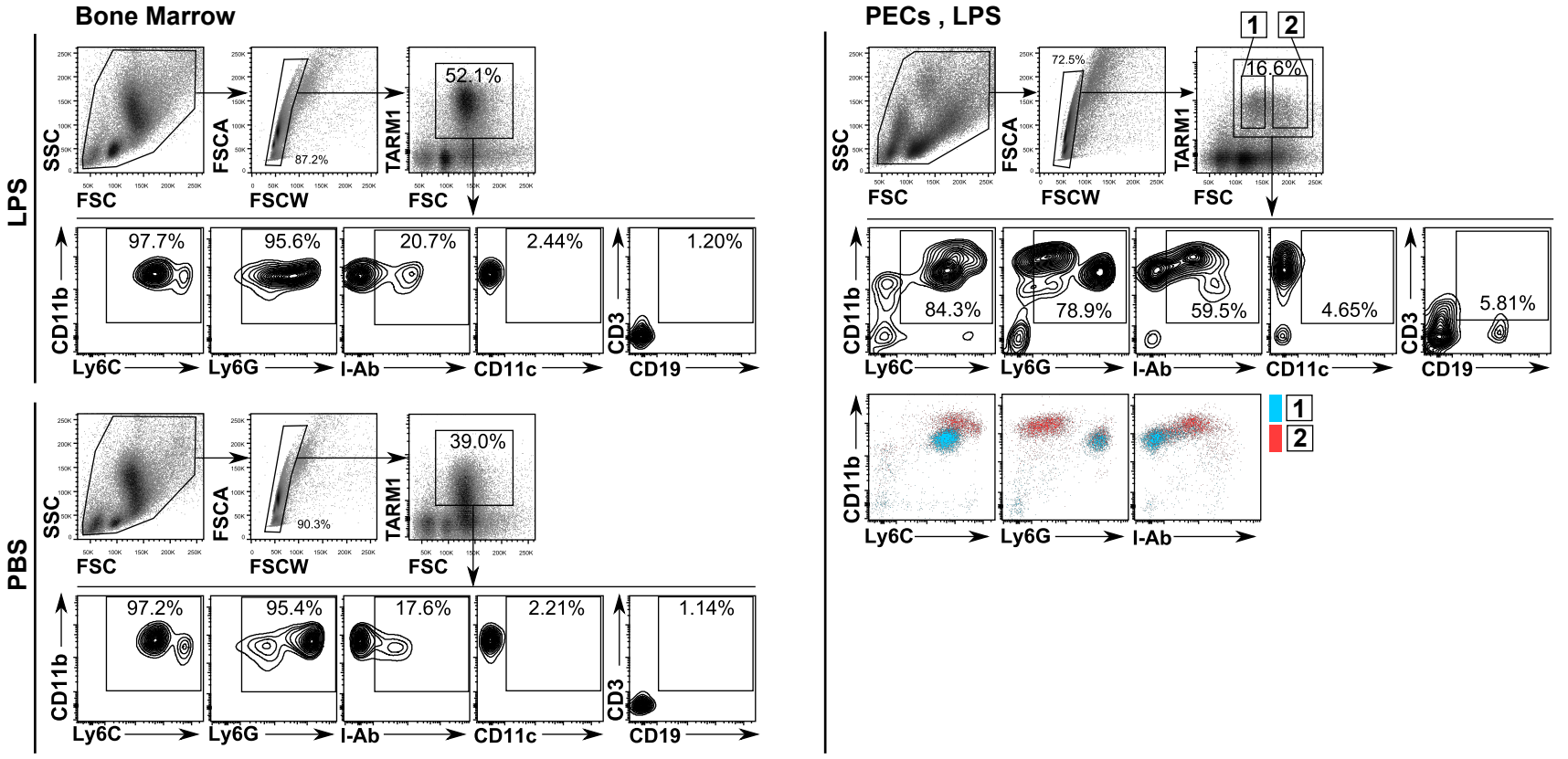

FIGURE 7.4: Flow cytometric characterisation of TARM1$^+$ population in mouse bone marrow and peritoneal exudate cells following intraperitoneal administration of LPS. C57BL/6 mice were injected ip with either PBS or ultra-pure LPS (3 μg/mouse, Invivogen) and sacrificed 24 h later. (A) BM and (B) PECs were isolated and stained with anti TARM1 mAb13 and cell lineage markers. BM - bone marrow, PECs - peritoneal exudate cells

7.2 Systemic challenge of C57BL/6 mice with Salmonella typhimurium results in accumulation of TARM1$^+$ in multiple organs

It is well established that neutrophils are instrumental in the control of murine salmonellosis. I used a live-attenuated vaccine strain of Salmonella enterica serovar Typhimurium (*S.* Typhimurium) SL3261 in a systemic challenge of C57BL/6 mice. High inoculum of this strain was well-tolerated by C57BL/6 as was previously established by Dr. P Mastroeni (private communication). Four groups of three mice were injected with 1×10^6 CFU or PBS directly into the tail vein and euthanised at 1, 2, 3 and 4 weeks post infection.

Flow cytometric analysis of the spleen revealed an accumulation of TARM1$^+$ cells up to week 3 and a decline at week 4 (Fig. 7.5). This pattern followed closely the dynamics of the infection progression and resolution. The accumulation of TARM1$^+$ cells in the spleens of mice at 2 wpi was confirmed by confocal microscopy of tissue sections (Fig. 7.6). A clear TARM1 staining was observed in the tissues of infected mice at this time point, whereas the tissue of vehicle (PBS) treated animals displayed virtually no positive staining. This is consistent with the FACS data showing approximately 10% increase in TARM1$^+$ cells in the spleens of infected mice at 2 wpi. Although TARM1$^+$ cells were observed in clusters, severe splenomegaly with disruption of tissue architecture precluded reliable identification of the cluster location such as red/white pulp or germinal centers.

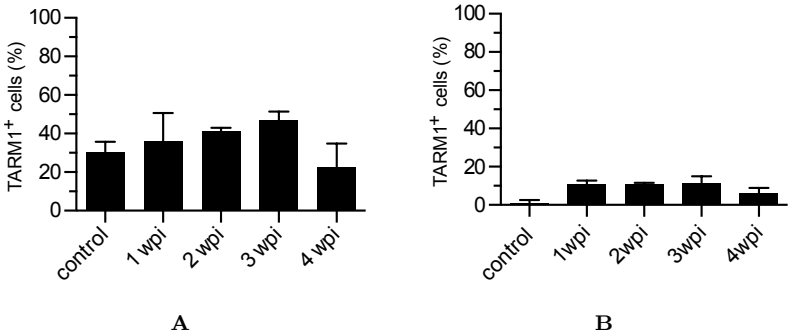

FIGURE 7.5: Percentage of TARM1$^+$ cells in the total (A) bone marrow and (B) spleen of *S. typhimurium* infected mice at indicated time points following infection. Each time point is representative of 3 mice. The experiment was repeated twice with similar outcomes.

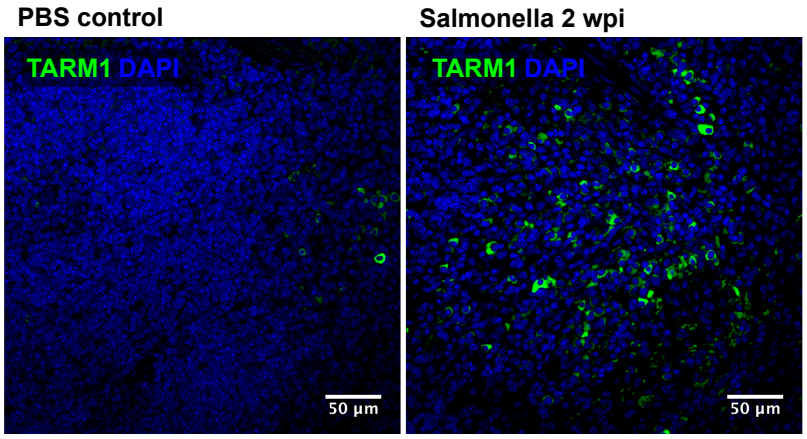

FIGURE 7.6: Confocal microscopy of TARM1 expression in the mouse spleen 2 weeks following Salmonella infection. Spleen fragments were harvested into 4% paraformaldehyde and fixed for 24 h, paraffin-embedded and stored until analysis. Microscopy sections were deparaffinised, and heat-induced epitope retrieval was perfomed in citrate buffer pH 5.5. Sections were stained with anti-TARM1 mAb53 (Green) and DAPI.

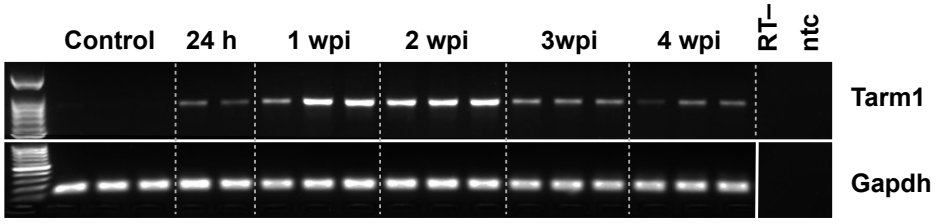

FIGURE 7.7: RT-PCR analysis of *Tarm1* mRNA expression in total splenocytes of *S. typhimurium* infected and control animals. Spleens were harvested at the indicated time points following infection and 30 mg fragments were stored at -80 ℃ in RNA-later (Qiagen). For analysis cDNA was generated from total RNA using oligo-d(T) primers. Full-length TARM1 transcript was amplified using primers specific to exon 1 and 6. Gapdh served as a reference gene. RT-, reverse transcriptase negative control; ntc, no template control

PCR analysis performed on the total RNA obtained from the same tissue showed a clear pattern of *Tarm1* gene upregulation with a peak at 1-2 wpi, which mirrored the accumulation and subsequent decline of TARM1$^+$ cells over the course of infection (Fig. 7.7). PCR analysis was also performed on samples obtained at 8 wpi, when the infection was fully resolved, and showed a return to the pre-infection level of *Tarm1* expression (data not shown). The RT-PCR data was corroborated by a quantitative analysis of *Tarm1* gene expression in the spleen using quantitative PCR (qPCR). For this purpose, I designed and validated *Tarm1* specific qPCR primers. The amplification efficiency and the dynamic range were determined over a range of 2-fold template dilutions and compared to those obtained for the reference gene *Gapdh* (Fig. 7.8**A**). *Tarm1* primer specificity was determined by the melting curve analysis of the amplification product.

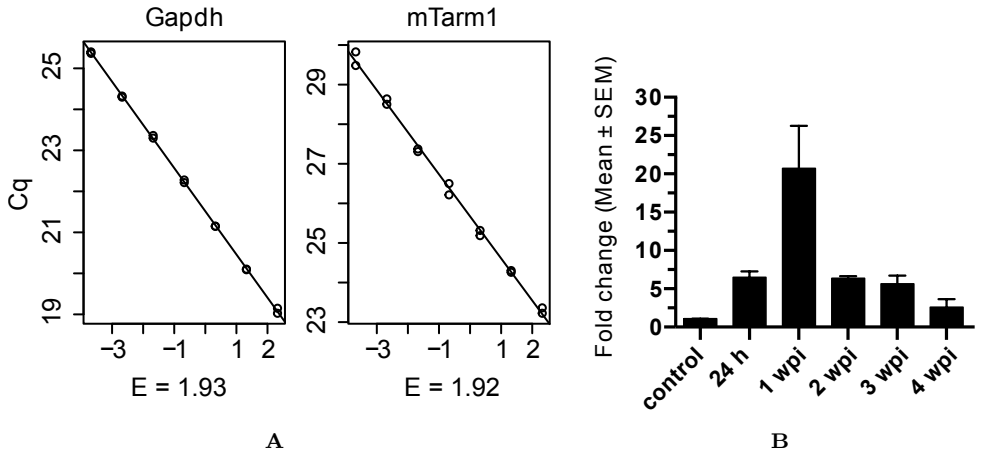

FIGURE 7.8: (A)Validation of *Tarm1* primer pair amplifications efficiency and qPCR analysis of the *Tarm1* gene expression in mouse spleens following *S. typhimurium* infection. (B) qPCR was performed on cDNA generated from total spleen RNA as described for RT-PCR. *Tarm1* primers spanning the splice junction of exons 5 and 6 were used.

The results showed a peak of *Tarm1* gene expression at 1 wpi reaching ∼22 fold increase over uninfected control (Fig. 7.8**B**).

The phenotype of TARM1$^+$ cells under the inflammatory conditions of intraperitoneal *in vivo* LPS administration distinguished two populations differing in their expression of Ly6C and Ly6G antigens, namely, CD11b$^+$Ly6C^{int}Ly6G^{hi} and CD11b$^+$Ly6C^{hi} Ly6G^{lo}. Therefore, I studied the differences in TARM1 cell-surface expression within the CD11b$^+$Ly6C$^+$ and CD11b$^+$Ly6G$^+$ cell subsets in the bone marrow and spleen throughout the infection time-course. The TARM1 expression was analysed on subpopulations expressing varying levels of Ly6C and Ly6G antigens.

In the bone marrow, two CD11b$^+$Ly6C$^+$ subsets could be discerned based on the expression level of these markers (Fig. 7.9, left panel). In control mice, the CD11b$^+$Ly6C^{hi} population was underrepresented (gate 2, left panel) and expressed little TARM1, whereas CD11b$^+$Ly6C^{int} cells comprised the predominant TARM1$^+$ population. At 1 wpi, as the infection became established, an accumulation of the CD11b$^+$Ly6C^{hi} population with a concomitant increase in the cell-surface expression of TARM1 was observed. TARM1 expression peaked between week 1 and 2 post-infection on both CD11b$^+$Ly6C^{hi} and CD11b$^+$Ly6C^{int} cell subsets and declined at 4 wpi.

Similarly, CD11b$^+$Ly6G$^+$ cells could be divided into distinct subpopulations based on their expression level of the Ly6G antigen (Fig. 7.9, right panel). TARM1 expression in control animals was observed predominantly on the Ly6G^{hi} population that represented

the majority of all $CD11b^{+}Ly6G^{+}$ cells (gate 4, right panel). However, a reduction in the abundance of this population and the accumulation of $Ly6G^{-/lo/int}$ cells was observed following the infection. This shift is most likely indicative of the altered granulopoiesis leading to the accumulation of $Ly6G^{-/lo}$ myeloid precursors to replace the rapidly depleted pool of mature $Ly6G^{hi}$ granulocytes. At 1 wpi, high TARM1 expression was evident on all $CD11b^{+}Ly6G^{+}$ cells irrespective of their maturation stage. This trend reversed noticeably by 3 wpi when the $CD11b^{+}Ly6G^{neg}$ cells decreased in abundance and lost the expression of TARM1. $CD11b^{+}Ly6G^{hi}$ mature granulocytes maintained high TARM1 expression throughout weeks 1-3, whereafter the expression returned to a near base-line level at week 4.

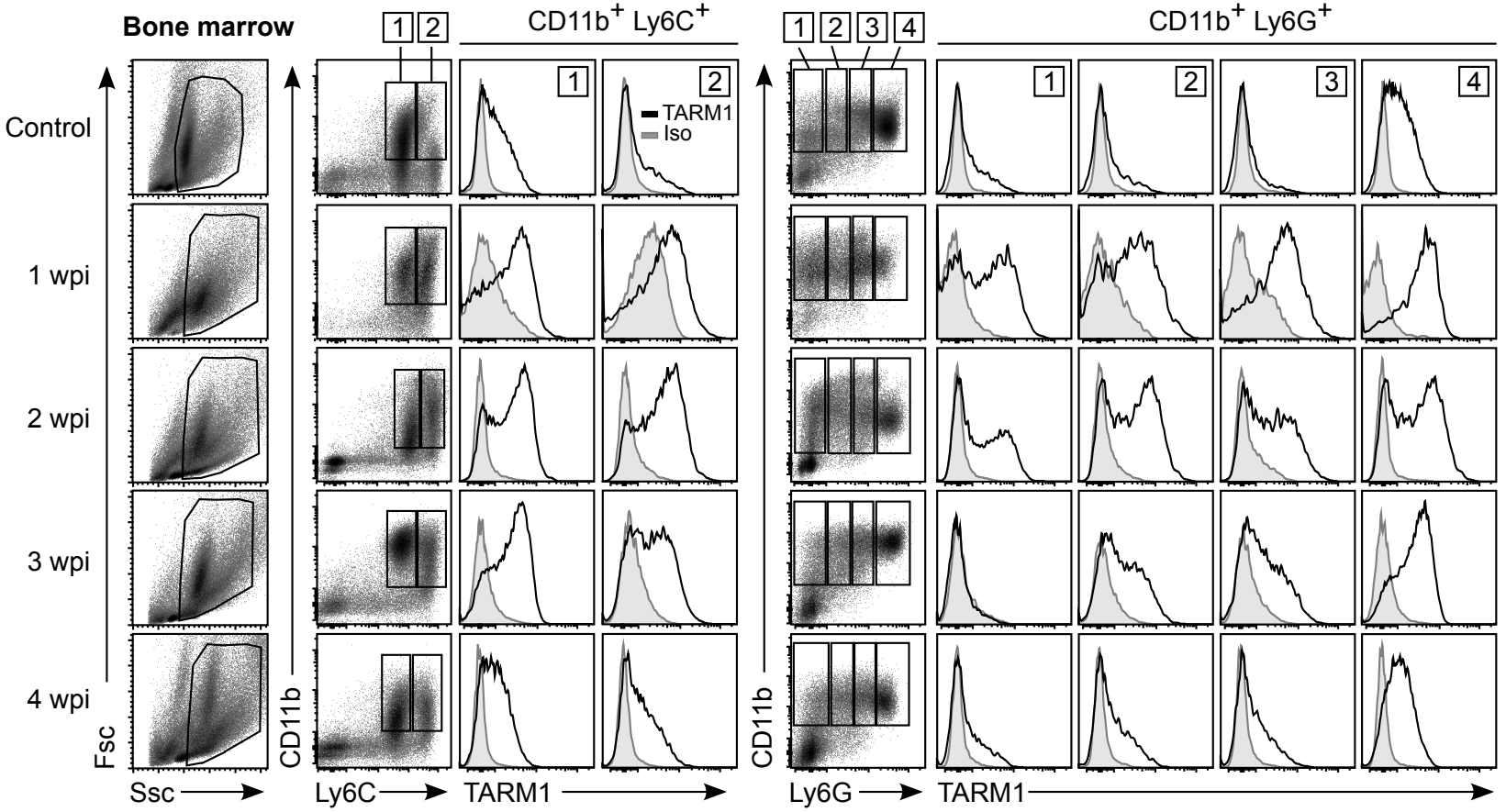

FIGURE 7.9: Flow cytometric characterisation of TARM1 expression in mouse bone marrow cells following iv administration of *S. typhimurium*. C57BL/6 mice were injected iv with either PBS or *S. typhimurium* strain SL3261 and sacrificed at the indicated time points. Cells were isolated and stained with anti TARM1 mAb13 and cell lineage markers.

A very similar trend was observed in the spleen (Fig. 7.10). As was mentioned earlier, TARM1$^+$ cells represent ∼1% of the total splenocytes in healthy animals. This is well-correlated with a similarly low abundance of CD11b$^+$Ly6C$^+$Ly6G$^+$ cells outside of the bone marrow under steady-state conditions. As the infection progressed, an accumulation of CD11b$^+$Ly6C$^+$ granulocytes in the spleen was observed following similar dynamics to that in the bone marrow, both in the relative cell abundance and the expression of TARM1 (Fig. 7.10, left panel). The influx of granulocytes into the spleen over the course of infection could be seen by flow cytometry as the increase in the frequency of larger, more granular cells characterised as Ssc$^{\text{int/hi}}$Fsc$^{\text{hi}}$.

At the peak of infection, between weeks 1-2, the predominant cell subset was CD11b$^+$Ly6G$^{\text{int}}$ (Fig. 7.10, gate 3), whereafter cells with higher Ly6G expression (gate 4) began to accumulate. It appears that in the spleen, TARM1 expression correlated with the level of Ly6G expression with a peak at 1-2 wpi.

Although the lineage markers I used to study TARM1$^+$ cells identified them as mature (CD11b$^+$Ly6G$^{\text{hi}}$) and immature (CD11b$^+$Ly6G$^{\text{lo/int}}$) neutrophils, a more detailed characterisation is required to gain insight into their potential function during inflammatory responses.

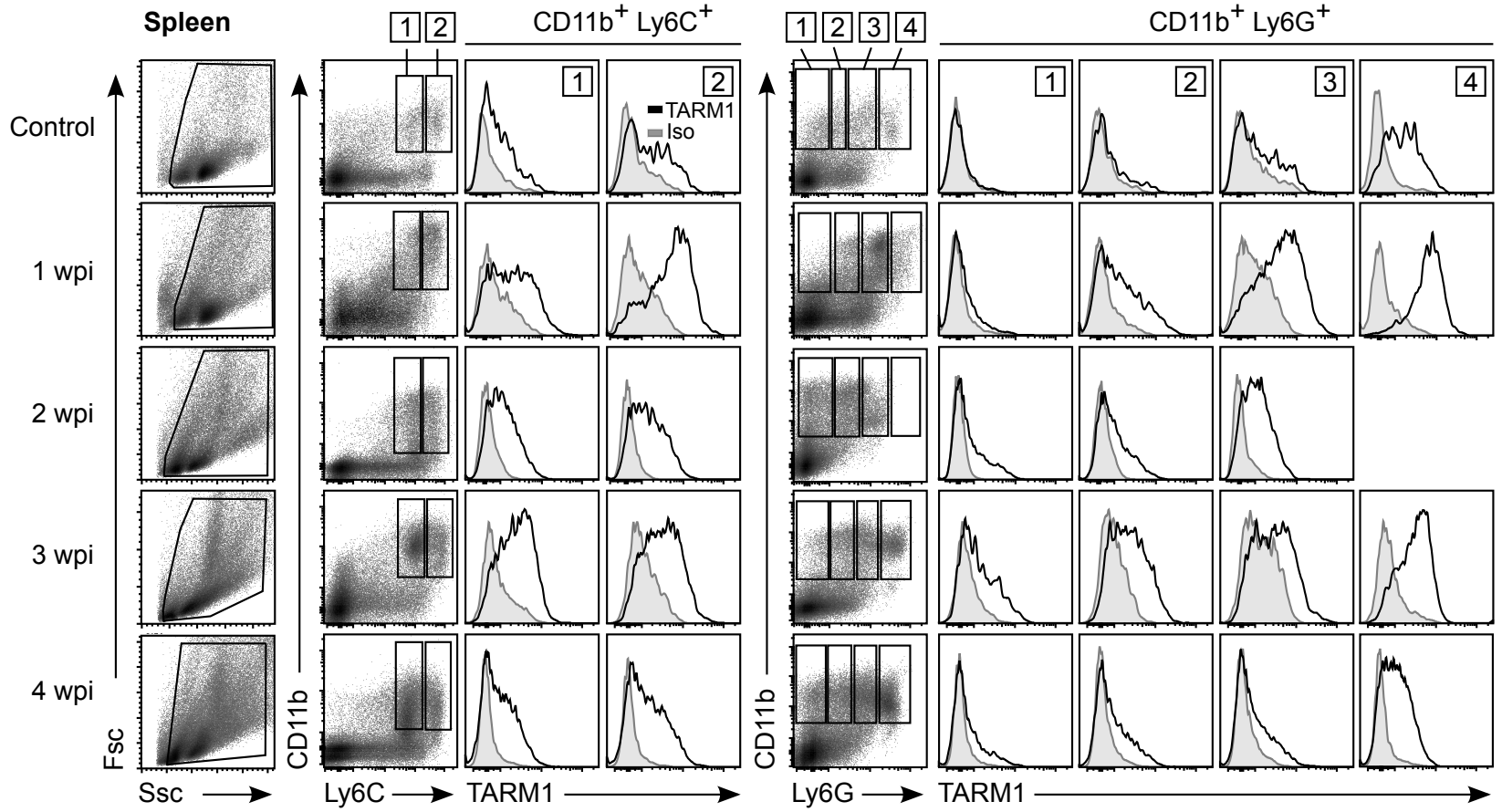

FIGURE 7.10: Flow cytometric characterisation of TARM1 expression in mouse splenocytes following iv administration of *S. typhimurium*. C57BL/6 mice were injected iv with either PBS or *S. typhimurium* strain SL3261 and sacrificed at the indicated time points. Cells were isolated and stained with anti-TARM1 mAb13 and cell lineage markers.

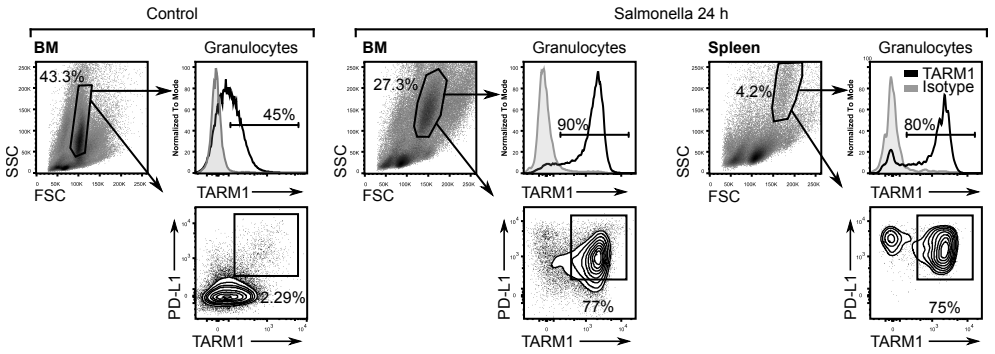

FIGURE 7.11: TARM1$^+$ cells upregulate PD-L1 expression 24 h following Salmonella infection. C57BL/6 mice were injected iv with either PBS or *S. typhimurium* strain SL3261 and sacrificed 24 h later. TARM1 and PD-L1 expression were examined by flow cytometry on splenocytes and BM.

A number of studies emerged over the past decade uncovering neutrophil functions previously not associated with cells of the innate immune system. For instance, IFN-γ stimulated neutrophils acquire the ability to suppress T cell proliferation through upregulation of PD-L1 (Kleijn et al. 2013). Neutrophils were shown to suppress Th1 responses during intracellular Brucella infection (Barquero-Calvo et al. 2013). High levels of PD-L1 were also found on the peripheral blood neutrophils in patients with an active tuberculosis (McNab et al. 2011). With this in mind, I characterised PD-L1 expression on TARM1$^+$ cells in the BM and spleen of mice following Salmonella infection. Majority of the TARM1$^+$ cells in the bone marrow and spleen expressed PD-L1 24 h following infection (Fig. 7.11). The finding that TARM1$^+$ cells upregulate the expression of PD-L1 suggested they may exert a suppressive immune effect.

7.2.1 Human circulating neutrophils express TARM1

I also examined TARM1 cell-surface expression in human peripheral blood. Similarly to mice, human TARM1 was detected on circulating granulocytes, but the expression varied greatly among donors (Fig. 7.12**A**). To confirm TARM1 expression on granulocytes, I prepared a neutrophil-enriched cell fraction by Ficoll density centrifugation of peripheral blood obtained from a donor with high TARM1 expression ($\sim$ 93% purity) and analysed the lysate by Western blot. The neutrophil-depleted fraction was used as a control. A clear TARM1-specific band was detected in the lysate of neutrophil-enriched fraction but not in the neutrophil-depleted mononuclear cell lysate (Fig. 7.12**B**). These results are inline with the results of flow cytometric analysis of TARM1 expression in human

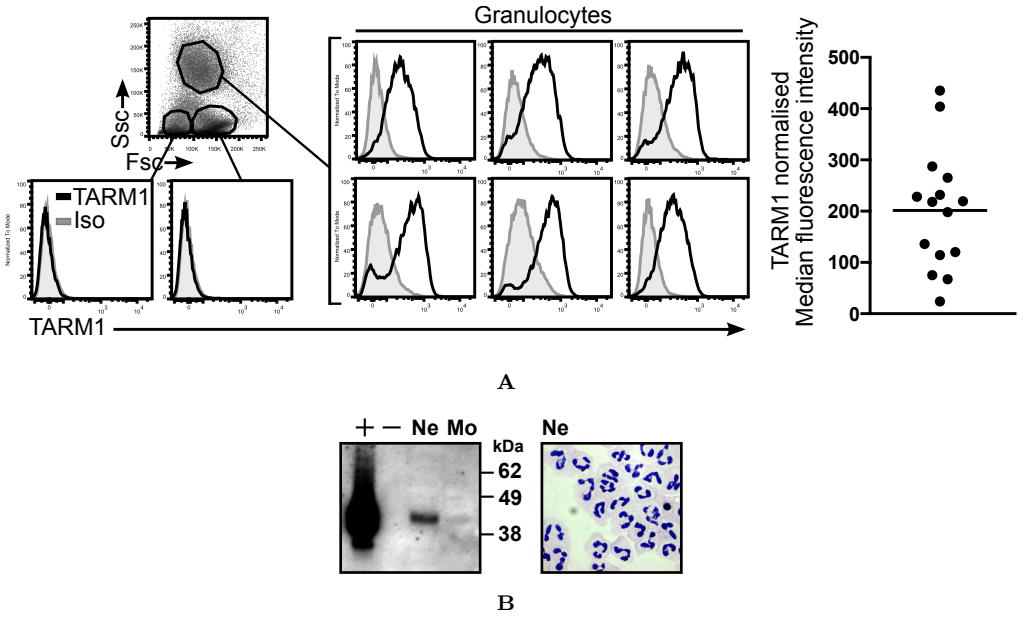

FIGURE 7.12: TARM1 is expressed on the surface of human peripheral blood granulocytes. (A) Flow cytometry of whole human blood. Human peripheral blood was collected from healthy donors (n=15) and red blood cells were removed by sedimentation using HetaSep (Stemcell Technologies). TARM1 expression was analysed by flow cytometry. Only granulocytes were positive for TARM1. Representative plots from several donors are shown. The values for median fluorescence intensity staining of TARM1 were normalised to isotype control value for each donor. (B) Western blot. TARM1 protein is detected in purified neutrophils but not in neutrophil-depleted mononuclear cell fraction. Neutrophils were isolated by Ficoll density centrifugation. Purity was assessed by microscopy of neutrophil cytospins (right panel) and was routinely above 90%. +, hTARM1 transfected Hek293T cells; −, Hek293T transfected with a control construct; Ne, neutrophils; Mo, neutrophil-depleted mononuclear cell fraction. (left panel) Cytospin preparation of purified neutrophils.

tissues shown in Chapter 6, Figure 6.5, page 80, where cell-surface TARM1 was detected in $CD16^{+}$ neutrophils in the bone marrow and spleen and $CD16^{lo/-}$ immature myelocytes in the bone marrow.

These results show that under conditions of health, TARM1 expression is found predominantly in the bone marrow $CD11b^{+}Ly6C^{+}Ly6G^{+}$ mature neutrophils and myelocytes. Increased TARM1 expression and homing of $TARM1^{+}$ cells to peripheral sites is strongly associated with inflammation. Similarly to mice, human TARM1 appears to be restricted to the granulocytic population suggesting conservation of function.

7.3 Summary

The data, showing that high levels of cell-surface expression of TARM1 could be induced *in vitro* on BMM and BMDC by treatment with TLR agonists, prompted me to investigate whether an *in vivo*, localised administration of TLR4 agonist LPS or a systemic bacterial challenge would elicit similar effects on TARM1 expression and shed light on its cell distribution in the context of acute or sustained inflammatory responses. To address these questions, I used a mouse model of sterile peritonitis induced with a low dose of LPS administered ip and a systemic challenge with an attenuated vaccine strain of *S. typhimurium* SL3261.

Sterile peritonitis was induced with ip administration of LPS (3 μg) and a BM, spleen, liver, lymph nodes and PECs were analysed by flow cytometry 24 h later. The data showed that LPS treatment induced a rapid and robust upregulation of TARM1 cell-surface expression in the BM, expansion of the TARM1$^+$ population size and its migration to the peritoneum. Morphological examination of cytospins prepared from TARM1$^+$ cells sorted from the BM of LPS treated animals showed that they comprised a heterogeneous mixture of myeloid precursors with ring-shaped nuclei and mature neutrophils.

Flow cytometric characterisation of TARM1$^+$ cells using prototypical markers of granulocytes, DCs and lymphocytes showed that in control animals TARM1 expression was low and restricted to the BM cells with a phenotype of mature neutrophils CD11b$^+$Ly6G^{hi}Ly6C$^+$. Whereas the inflammatory response 24 h following LPS administration was accompanied by a decrease in the expression of Ly6G antigen, indicating a shift towards a more immature myeloid phenotype among TARM1$^+$ cells.

An increased frequency of myeloid precursors in the bone marrow and peripheral sites is sometimes observed during inflammation as a consequence of its modulatory effect on the myelopoiesis (Terashima et al. 1996). Acute infection or other inflammatory processes where the reserves of mature granulocytes are rapidly mobilised from the bone marrow and the circulation to the sites of inflammation trigger an accelerated proliferation of bone marrow granulocytic precursors to replenish the rapidly consumed mature cells in a process referred to as demand-adapted or emergency granulopoiesis (Manz and Boettcher 2014; Takizawa, Boettcher, and Manz 2012; Boettcher et al. 2012).The extent of the myelopoietic proliferation is governed by the nature and the severity of the pathology

and the combination of hematopoietic growth factors. Of particular interest for this work is the association of an increase in TARM1 expression on neutrophil precursors and mature neutrophils during inflammation. Boettcher et al. demonstrated that ip administration LPS (two doses of 35 μg) mimics the acute conditions necessary to initiate emergency granulopoiesis (Boettcher et al. 2012). Although the dose of LPS I used was twenty times lower than in the study by Boettcher et al, the induction of a modest shift towards an increased frequency of $Ly6G^{lo}$ neutrophil precursors could be observed.

The $TARM1^+$ cells infiltrating the peritoneum of LPS treated animals were composed of two distinct populations that differed in their expression of Ly6G, Ly6C and MHC-II markers and were $CD11b^+Ly6C^{hi}Ly6G^{lo}$MHC-$II^+$ monocytic and $CD11b^+Ly6C^{int}Ly6G^{hi}$MHC-$II^-$ granulocytic phenotypes. Since both populations lacked CD11c, the expression of MHC-II was unlikely due to the presence of DCs or macrophages. Instead, low or absent Ly6G with high levels of Ly6C and MHC-II is a hallmark of inflammatory monocytes that have been implicated in both pro-inflammatory and suppressive processes (Geissmann et al. 2010; Serbina and Pamer 2006). These cells were described to rapidly migrate to sites of inflammation where they gave rise to DCs and macrophages (Geissmann et al. 2010; Serbina and Pamer 2006)

Since LPS-induced sterile peritonitis did not recapitulate the complexity and duration of the immune response mediated by live infection, it was of interest to determine the fate of $TARM1^+$ cells during systemic bacterial challenge.

Mice were challenged with an attenuated vaccine strain of Salmonella typhimurium via tail vein. Flow cytometric analysis showed that TARM1 expression followed the infection dynamics peaking at the height of infection between weeks 1 and 2. In the bone marrow TARM1 expression was strongly upregulated on mature granulocytes and immature myeloid cells. An influx of $TARM1^+$ cells expressing different levels of Ly6C and Ly6G antigens was observed in the spleens of infected mice. These cells persisted in the spleen for the duration of the infection and maintained elevated expression of cell-surface TARM1.

A growing number of studies show that perturbations in myelopoiesis seen during inflammation and cancer lead to the emergence of so called myeloid-derived suppressor cells (MDSC), a heterogeneous population of myeloid precursors with a potent T cell

suppressive function (Cuenca et al. 2011; Delano et al. 2007). Historically, this population in mice was identified by the co-expression of CD11b and Gr-1 antigens. However, as discussed earlier, anti Gr-1 antibody recognises epitopes on both Ly6C and Ly6G antigens with a wide cell distribution. High expression of Ly6C with low or absent Ly6G is a hallmark of inflammatory monocytes which have been shown to exert either pro-inflammatory or immunosuppressive effects (Geissmann et al. 2010; Serbina and Pamer 2006). High expression of Ly6G with low or no expression of Ly6C identifies granulocytic cells such as mature neutrophils and granulocyte precursors.

Although terminally differentiated neutrophils are only a small fraction of MDSCs, a large body of work suggests that both human and mouse neutrophils can be induced to acquire APC-like phenotype *in vitro* or under pathological conditions *in vivo* where they exert immunoregulatory effects on T cells often resulting in the suppression of Th1 responses (Rodriguez et al. 2009; Gosselin et al. 1993; Alemán et al. 2005; Ostanin et al. 2012; Abdallah et al. 2011). In patients with acute infectious disease or cancer granulocytic MDSCs have been shown to release arginase-I into the circulation resulting in the depletion of L-arginine and the impairment of T cell function (Darcy et al. 2014; Rodriguez et al. 2009). Secretion of IL-10 (X. Zhang et al. 2009) and PD-L1 (McNab et al. 2011) expression during bacterial infections were also proposed as regulatory mechanisms employed by neutrophils. Interestingly, TARM1$^+$ cells expressed PD-L1 (Fig. 7.11) 24 h following infection. This points to a potential role of TARM1$^+$ cells in the control of inflammation in the models used here.

MDSCs were first characterised in tumour-bearing mice and their prominent role in tumour immune evasion has since been well-established. A growing body of evidence suggests that MDSCs are also induced in a broad range of pathological conditions including tissue damage (Noel et al. 2011) and microbial sepsis (Delano et al. 2007) where their role may be to protect against severe hyperinflammatory response. Delano et al reported that polymicrobial sepsis induced an expansion of immature Gr-1$^+$CD11b$^+$ cells and their accumulation in the spleens of infected mice. The authors suggested that this population had an important host-protective anti-inflammatory function (Delano et al. 2007). Indeed, Brudecki et al. also observed a progressive expansion of Gr-1$^+$CD11b$^+$ population and accumulation of immature myeloid cells with ring-shaped nuclei in mice with CLP-induced polymicrobial sepsis (Brudecki et al. 2012). Using adoptive MDSC transfers the authors demonstrated that the function of this population

during severe sepsis depended on the context in which it expanded. MDSCs derived from day 3 early septic mice were proinflammatory, whereas MDSCs isolated from day 12 late septic mice were immunosuppressive, and, when transferred to recipient animals, improved survival during early septic hyperinflammation (Brudecki et al. 2012). Derive et al, confirmed that during polymicrobial sepsis mainly the granulocytic MDSC subset ($CD11b^{+}Ly6G^{hi}Ly6C^{lo}$) accumulated progressively in the spleens of septic mice and had differential responses to TLR4 and IL6 stimulation depending on the time following the onset of sepsis Derive et al. 2012.

Much of the earlier work performed on murine neutrophils and MDSCs defined them as $CD11b^{+}Gr1^{+}$ which does not accurately reflect the true identity of these cell subsets.Therefore, studies using the Gr-1 antibody should be interpreted with caution. Unique markers are needed to facilitate a more sensitive and reliable means of discrimination between different components of the regulatory cell subsets. The identification of TARM1 offers an intriguing possibility of being a marker of activated regulatory cells. However, a more detailed phenotyping strategy and functional analysis must be employed for a reliable characterisation of the nature of $TARM1^{+}$ cells.

It was of great interest to explore whether TARM1 protein itself had a regulatory potential. Next chapter describes the characterisation of TARM1 functional effects on T cell responses *in vitro*.

Chapter 8

TARM1 costimulates proinflammatory cytokine secretion by macrophages and neutrophils and inhibits T cell proliferation

An outstanding question that remains to be answered is whether the TARM1 transmembrane protein can function as a bona fide 'receptor' either by binding to an as yet unidentified extracellular ligand or by transducing intracellular signals that modulate the function of TARM1-expressing cells.

To gain insight into whether TARM1 can communicate with the extracellular environment, I generated TARM1-2B4-NFAT-GFP reporter cells which were used to search for TARM1 ligand. To evaluate whether TARM1 can bind to a cellular ligand, I examined the effects of the recombinant TARM1 extracellular domain on T cell activation and proliferation *in vitro* by generating soluble mouse and human fusion proteins comprised of the extracellular portion of TARM1 fused to the human IgG_1 Fc. Finally, to evaluate whether TARM1 protein could transduce intracellular signals, I stimulated BMM and neutrophils with an anti-TARM1 mAb in the presence or absence of various

TLR ligands, to determine whether TARM1 stimulation could modulate the function of TARM1-expressing cells.

8.1 Generation and validation of TARM1-2B4 reporter lines

I used a widely adopted 2B4-NFAT-GFP reporter system to screen for a physiological ligand for TARM1. The murine T cell hybridoma 2B4 carries a stably transduced GFP gene under the control of a nuclear factor of activated T cells (NFAT) transcriptional response element and was therefore chosen to generate TARM1 reporter cells. Thus, cross-linking of an ITAM receptor in 2B4-NFAT-GFP reporter cell-line will result in NFAT activation and translocation to the nucleus and induction of GFP expression.

This system provides a sensitive and convenient flow cytometry-based assay for a high-throughput screening of cells to identify candidates expressing physiological ligands for the assayed receptor (H. Arase et al. 2002).

TARM1 requires association with the FcRγ adaptor in order to signal. This adaptor is not expressed in the mouse 2B4-NFAT-GFP reporter cells. It was therefore necessary to circumvent the requirement of TARM1 for FcRγ association in this reporter system. Signalling through the T cell receptor complex culminates in NFAT activation and the 2B4 T cell hybridoma contains all the necessary Src-family kinases and downstream signalling molecules required for this purpose. CD3ζ contains three ITAM motifs and can thus serve as a strong trigger for the downstream signalling cascade culminating in NFAT activation. Therefore, in order to eliminate the need for a signalling adaptor molecule and to improve the sensitivity of the system for TARM1 cross-linking, the extracellular portion of the TARM1 receptor was fused to the intracellular portion of the human CD3ζ, as shown in Fig. 8.1.

Cloning strategy and generation of a stable TARM1 reporter cell line. The ectodomains of mouse and human TARM1 were first cloned into pDisplay vector (mouse TARM1 BamHI-GQTDIP...EGYTVD-SalI; human TARM1 BamHI-GDTRGD... TSSNYSLG-SalI). Next, the region of pDisplay containing the TARM1 sequence flanked by the Igκ signal peptide and HA-tag at the 5' end and Myc-tag and platelet-derived

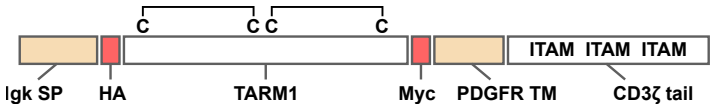

FIGURE 8.1: Schematic respresentation of TARM1-CD3ζ chimeric construct. Igκ SP - murine Igκ-chain signal peptide, HA - hemagglutinin A epitope tag, Myc - myc epitope tag, PDGFR TM - platelet-derived growth factor receptor transmembrane domain, CD3ζ - the ITAM-containing intracellular portion of CD3ζ.

growth factor receptor transmembrane domain (PDGFR-TM) at the 3' end was sub-cloned into pMXs-puro retroviral vector containing human CD3ζ tail (using EcoRV-XhoI restriction sites). The resulting construct encoded, in the 5' to 3' orientation, Igκ signal peptide, HA-tag, TARM1 ectodomain, Myc-tag, PDGFR TM and human CD3ζ tail (Fig. 8.1). 2B4-NFAT-GFP cells were transduced with TARM1 retroviral constructs and grown under pyromycin selection until stable lines (TARM1-2B4) were established ($\sim$ 3 weeks). To determine whether TARM1-2B4 cells could respond to TARM1 ligation, cells were cultured in the presence of plate-bound anti-HA antibody and were analysed by flow cytometry 24 h later. Using this method of TARM1 stimulation, over 70% of human and mouse TARM1-2B4 reporter cells, but not parental cells, became GFP^+ indicating that TARM1 NFAT-GFP reporter cells were suitable for screening different cell-lines for the presence of TARM1 ligands.

8.1.1 Screen for human TARM1 ligands

To search for a physiological ligand for human TARM1, I used the human TARM1 2B4 GFP reporter cells to screen common human cell lines representing different lineages such as fibroblasts, neuronal cells, myeloid and lymphoid cells. During the initial screen of cell lines, TARM1 reporter cells, but not control RAET1L reporter cell line or parental 2B4 cells, responded with a moderate GFP induction (39% GFP^+ cells) only to primary human dermal fibroblast (HDF) (representative plots are shown in Figure 8.2A).

In order to minimise the heterogeneity in TARM1 2B4 reporter cell responses, the top 10% of responding cells were single-cell sorted and cultured until clonal TARM1 GFP reporter cell lines were established. Next, I tested the response strength of the individual TARM1 2B4 reporter cell clones to HDF (representative clones are shown in Figure 8.2B) and identified clone B4 as the best responder showing over 90% GFP^+ cells after over night coculture. Clone B4 was chosen for further coculture experiments.

I screened a panel of cell lines using TARM1 2B4 reporter cell clone B4 and confirmed that HDF cells were capable of stimulating a robust GFP response (Fig. 8.2C). In addition, both Jurkat and primary mouse $CD4^+$ T cells were able to induce GFP response in TARM1 2B4 reporter cells (Fig. 8.2D). Interestingly, both HDF and, to a lesser extent, chicken fibroblast cell line RSV-B4 triggered GFP production in TARM1 reporter cells suggesting that the putative ligand may be conserved across species.

TARM1 is encoded in close proximity to and is phylogenetically related to a collagen-binding receptor OSCAR (A. Barrow, N. Raynal, et al. 2011). Fibroblasts synthesise components of the extracellular matrix including collagen. Therefore I used a human TARM1-Fc fusion protein to assay for collagen-binding activity using a library of triple-helical collagens I-V described previously (A. Barrow, N. Raynal, et al. 2011). No specific binding of human TARM1-Fc fusion could be detected in ELISA assay. TARM1-Fc fusion protein also failed to show binding to HDF cells in flow cytometric assay suggesting that the interaction of TARM1 with its putative ligand may be of low affinity making it unsuitable for use in flow cytometric assays.

8.2 TARM1-Fc inhibits T cell activation and proliferation *in vitro*

Next I investigated the potential functional role of the interaction of TARM1 receptor with a putative ligand expressed on T cells. Our group and others (I. A. Smith et al. 2010) have previously used chimeric Fc fusion proteins to study immunomodulatory activity of several receptors in *in vitro* T cell proliferation assays. I used this system to examine the effects of TARM1 Fc fusion protein on anti-CD3 anti-CD28 induced T cell activation and proliferation *in vitro*.

Purified primary mouse $CD4^+$ T cells were labelled with CFSE and activated for 72 h with plate-bound anti-CD3 (clone 145-2C11) and anti-CD28 (clone 37.51) antibodies in the presence of plate-bound mouse TARM1-Fc fusion protein or control Fc fusion proteins. No proliferation was observed as measured by CFSE dilution when TARM1-Fc was present in the wells (Fig. 8.3).

Although the CFSE dilution assay provided information about the effect of TARM1-Fc on T cell proliferation, this technique does not allow to assess T cell activation. T

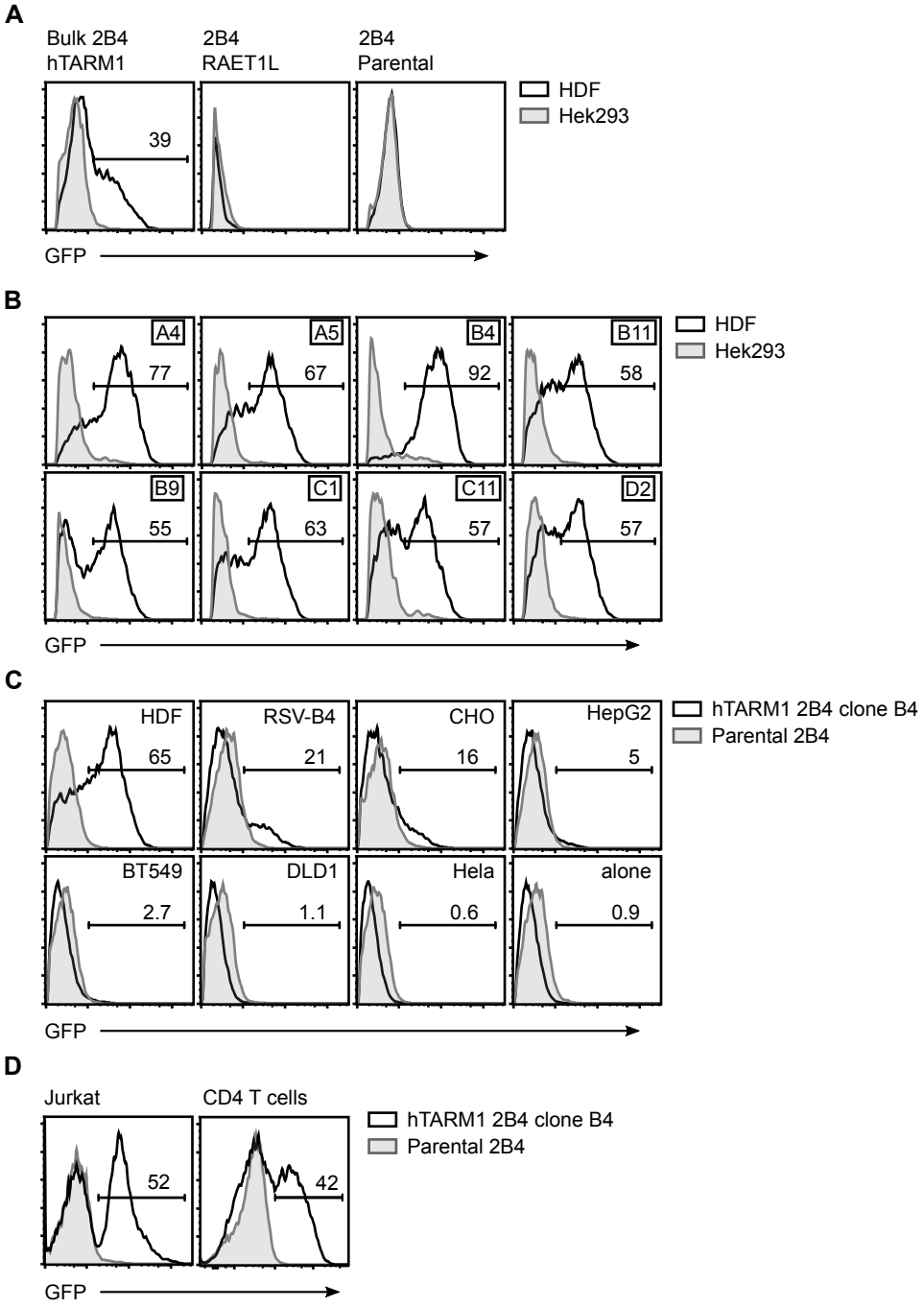

FIGURE 8.2: TARM1-2B4-NFAT-GFP reporter cells detect a putative TARM1 ligand expressed on fibroblasts and T cells. The reporter cells expressed chimeric receptor composed of the ectodomain of human TARM1 and the CD3ζ cytoplasmic region. (A) Bulk human TARM1 2B4 reporter cells or control RAET1L 2B4 reporter cell line and parental (untransduced) 2B4 cells were cocultured overnight with human dermal fibroblasts (HDF) and GFP induction in reporter cells was assayed by flow cytometry. (B) Representative plots showing differences in GFP induction by TARM1 2B4 reporter single cell clones following over night coculture with HDF. Hek293 was used as a control target cell line. Inset in the top right corner indicates clone number. Clone B4 showed the highest GFP response. (C) Coculture of TARM1 2B4 clone B4 and control parental 2B4 with a panel of target cell lines. (D) Coculture of TARM1 2B4 clone B4 and control parental 2B4 with Jurkat cell line and primary mouse $CD4^+$ T cells. The % of GFP^+ cells is shown above the gate.

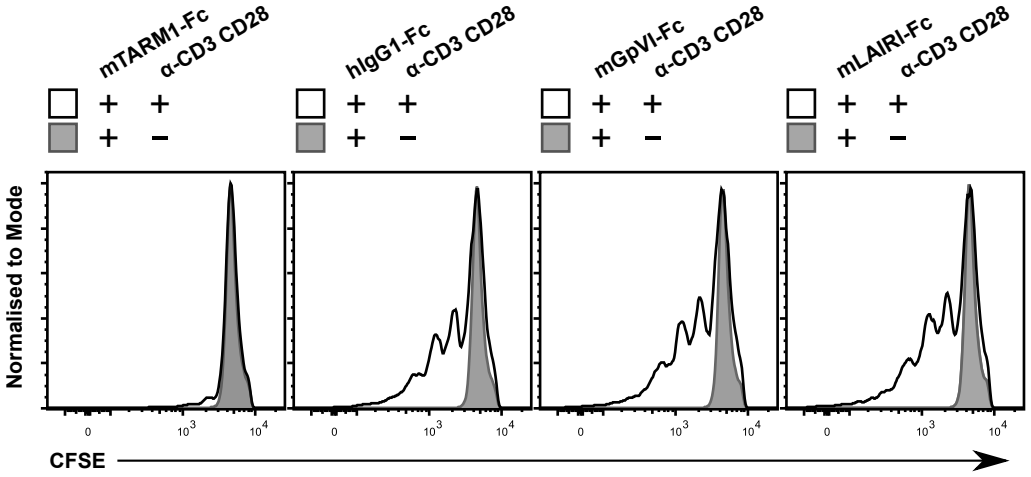

FIGURE 8.3: TARM1-Fc inhibits T cell proliferation. Primary mouse $CD4^+$ T cells were isolated immunomagnetically by positive selection. Cells were labelled with CFSE and activated with plate-bound anti-CD3 (clone 145-2C11) and anti-CD28 (clone 37.51) antibodies in the presence of either plate-bound mouse TARM1-Fc fusion protein or control human IgG_1 or control fusion proteins mouse GpVI-Fc and mouse LairI-Fc. CFSE dilution was analysed by flow cytometry after 72 h of culture. FIlled histograms indicate non-activated cells. Open histograms are T cells activated in the presence of Fc fusion proteins as indicated.

cells that do not enter S-phase following CD3 and CD28 cross-linking may still become activated and ready to participate in the immune response.

I wished to establish whether in addition to the inhibition of T cell proliferation TARM1 also suppressed T cell activation. Since cell activation and proliferation is accompanied by an increase in cellular metabolism, I used a tetrazolium dye MTT as a redox indicator in a metabolic proliferation assay. MTT assay allows multiple measurements to be made throughout the course of cell stimulation and enables the study of T cell activation dynamics. Another hallmark of lymphocyte activation is the secretion of IL-2 and the upregulation of IL-2 receptor alpha chain (CD25) and a C-type lectin CD69. CD69 in particular is rapidly induced by TCR/CD3 engagement, and can be detected on the cell surface of activated T cells within 2-3 hours following stimulation (Testi, Phillips, and LEWIS L Lanier 1989). Therefore the use of a metabolic MTT assay, analysis of IL-2 secretion in combination with flow cytometric analysis of cell surface expression of CD25 and CD69 allow for an accurate determination of T cell activation independent of the proliferative status (Caruso et al. 1997).

I repeated the experiment in which purified primary mouse $CD4^+$ T cells were activated as described above in the presence of plate-bound TARM1-Fc fusion protein or $hIgG_1$

for 90 h and analysed CFSE dilution by flow cytometry. No proliferation was observed in the presence of TARM1-Fc fusion protein (Fig. 8.4**A**). MTT assay performed at 0 h, 20 h, 40 h and 80 h time points showed a stark inhibition of T cell metabolic activity (Fig. 8.4**B**) in the presence of TARM1-Fc. ELISA assay of IL-2 secretion performed 20 h following activation showed a significant inhibition of secretion in the presence of TARM1-Fc fusion protein (Fig. 8.4**D**). No inhibition was observed where human IgG_1 was used instead of TARM1-Fc.

The inhibition of T cell response by TARM1- Fc fusion protein could not be attributed to cytotoxicity as TARM1-Fc had no impact on T cell viability (Fig. 8.4**C**) as determined by staining with AnnexinV and PI at 90 h of culture. Viable cells were defined as $AnnexinV^{-}PI^{-}$. The decrease in live cell number in the presence of TARM1-Fc fusion protein was most likely due to the inhibition of T cell activation.

To analyse the effects of TARM1 on the activation of T cells using CD69 and CD25 expression as markers of activation I wished to minimise the impact of cell isolation procedure. Therefore I used a negative immunomagnetic selection method to obtain a total splenic T cell population comprised of both $CD4^{+}$ and $CD8^{+}$ cells. Cells were activated with plate-bound α-CD3 antibody, as described above, in the presence of plate-bound TARM1-Fc or $hIgG_1$ for 3 days. T cell stimulation in the presence of TARM1 resulted in a marked reduction in the frequency of $CD69^{+}CD25^{+}$ double-positive cells (Fig. 8.5, left panel) and the total cell-surface expression of CD69 and CD25 (Fig. 8.5, right panel). The suppression of T cell activation was observed across wide anti-CD3 antibody concentrations (Fig 8.6)

These data indicate that, at least *in vitro*, TARM1 exerts a suppressive effect on both T cell activation and proliferative T cell responses.

8.3 TARM1 costimulates proinflammatory cytokine secretion in BMMs and primary neutrophils

In Chapter 6 I showed that TARM1 expression is upregulated on BMM, BMDC and neutrophils in response to TLR stimulation. ITAM adaptor-associated receptors such as OSCAR and TREM-1 have been shown to synergise with TLR signalling. Ligation of either OSCAR (Merck, Gaillard, Scuiller, et al. 2006) or TREM1 (Bouchon, Dietrich, and

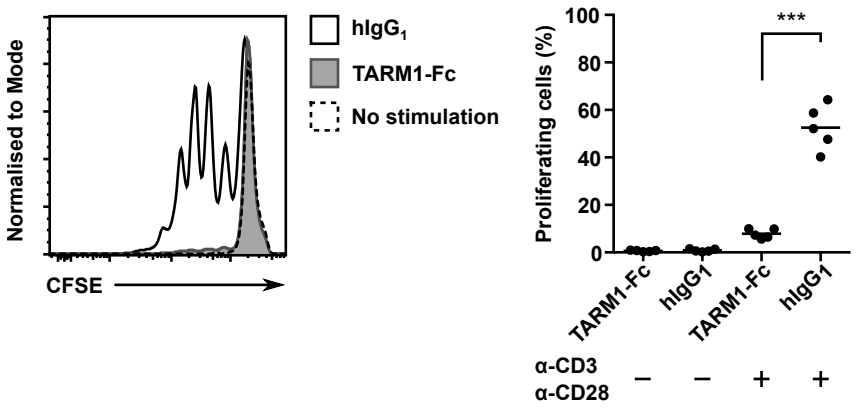

A

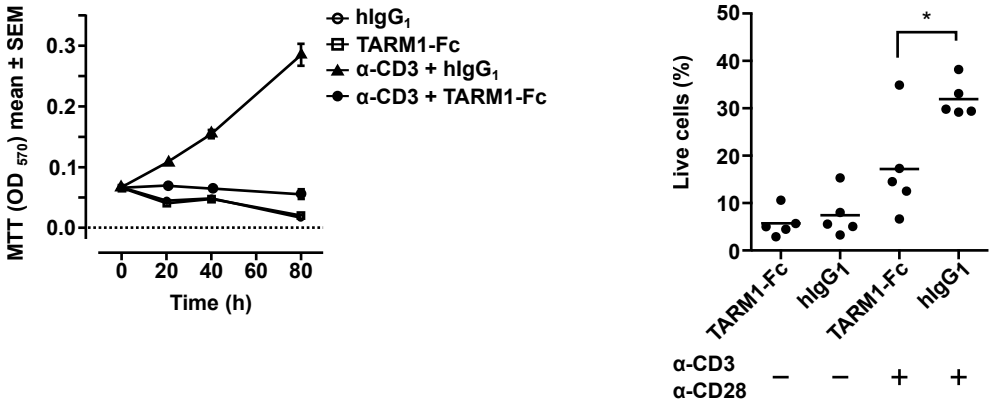

B C

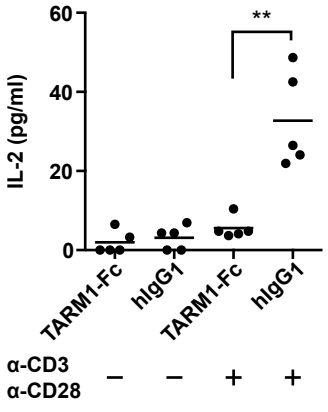

D

FIGURE 8.4: TARM1 inhibits CD4$^+$ T cell activation and proliferation *in vitro*. (A) CFSE dilution assay. CD4$^+$ T cells isolated by positive selection from the spleens and lymph nodes of NOD mice (n=5) were labelled with CFSE and stimulated with plate bound anti-CD3 (1 μg/ml) and anti-CD28 (0.25 μg/ml) antibodies in the presence of either plate bound TARM1-Fc (10 μg/ml) or control human IgG$_1$ (10 μg/ml). Proliferation was determined by CFSE dilution after 90 h of culture. Percent of proliferating cells was determined by gating on cells that divided at least once. Statistical analysis was performed using two-tailed t test, where $***$ corresponds to $p<0.0001$. (B) Metabolic MTT assay. CD4$^+$ T cells were isolated by negative selection from spleens of NOD mice (n=4) and activated with plate bound anti-CD3 (1 μg/ml) in the presence of either plate bound TARM1-Fc (10 μg/ml) or control human IgG$_1$ (10 μg/ml). T cell activation and proliferation was determined at 0 h, 20 h, 40 h and 80 h of culture. (C) TARM1-Fc does not affect T cell viability. T cell viability was determined by flow cytometry using AnnexinV and PI at 90 h of culture. AnnexinV$^-$PI$^-$ cells were considered viable. (D) TARM1-Fc suppresses IL-2 secretion by activated CD4$^+$ T cells

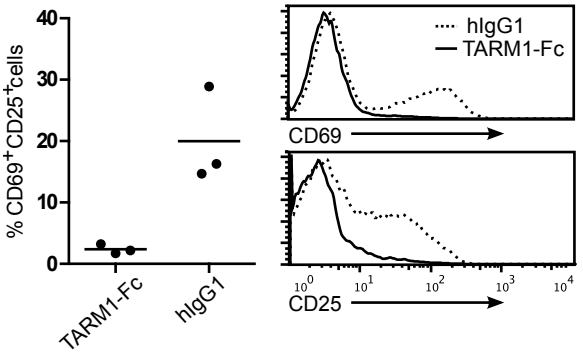

FIGURE 8.5: TARM1 inhibits upregulation of activation markers CD25 and CD69 by stimulated T cells *in vitro*. T cells were isolated by negative selection from spleens of C57BL/6 mice (n=3) and activated with plate-bound anti-CD3 antibody (1 μg/ml) in the presence of either plate bound TARM1-Fc (10 μg/ml) or control human IgG_1 (10 μg/ml). The plots show percentage of $CD25^+CD69^+$ double-positive T cells (left) and representative histograms of CD69 (top) and CD25 (bottom) expression in the presence of TARM1 or human IgG_1 as determined by flow cytometry after 3 days of culture.

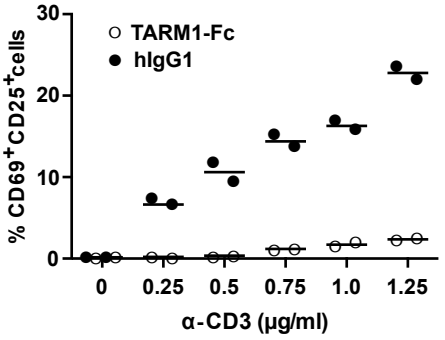

FIGURE 8.6: TARM1 inhibits upregulation of activation markers CD25 and CD69 by stimulated T cells *in vitro* across wide anti-CD3 antibody concentrations. Pan-T cells were isolated immunomagnetically by negative selection from spleens of C57BL/6 mice (n=2) and activated for 3 days with the indicated concentrations of anti-CD3 antibody in the presence of plate-bound TARM1-Fc (10 μg/ml) or human IgG_1 control. Expression of activation markers was analysed by flow cytometry. The plot shows percentages of $CD25^+CD69^+$ double-positive T cells.

Marco Colonna 2000; Bouchon, Facchetti, et al. 2001) on monocytes and neutrophils was shown to mediate the secretion of proinflammatory cytokines. Co-ligation of these receptors in the presence of TLR agonists, particularly LPS, was demonstrated to enhance TLR-dependent cytokine secretion and the downstream proinflammatory responses of myeloid cells (A. D. Barrow et al. 2015; Merck, Gaillard, Scuiller, et al. 2006; Bouchon, Facchetti, et al. 2001). Neutrophils and monocytes that infiltrate human tissues during bacterial infections as well as peritoneal neutrophils of patients with bacterial sepsis and mice with experimental LPS-induced shock express high levels of TREM1 (Bouchon,

Facchetti, et al. 2001). Therefore, the synergistic action of TREM1 and TLRs was implicated in the morbidity of bacterial sepsis (Bouchon, Facchetti, et al. 2001). This was supported by the finding that the blockade of TREM1 in mice reduced the mortality from LPS-induced shock (Bouchon, Facchetti, et al. 2001). Because TARM1 expression was also upregulated by TLR ligands, particularly LPS, I examined whether TARM1 ligation in the presence or absence of TLR agonists *in vitro* could modulate the secretion of proinflammatory cytokines by BMMs and neutrophils. For this experiment, neutrophils were isolated from mouse BM by FACS. It was shown that mouse BM contains large quantities of mature, functionally competent neutrophils that respond to stimulation in a comparable manner to the peripheral blood neutrophils (Boxio et al. 2004). To assess the effects of TARM1 cross-linking, BMMs and primary mouse BM neutrophils were cultured in tissue culture plates coated with either TARM1-specific antibody or isotype control (Fig. 8.7). Cross-linking of TARM1 in the absence of TLR agonists did not stimulate cytokine secretion by either BMMs or neutrophils. However, the concomitant stimulation of TARM1 and TLR-1/2, -3, -4, and -7 enhanced secretion of the proinflammatory cytokines TNF-α and IL-6 by BMMs (Fig. 8.7A). Similarly, stimulation of TARM1 together with TLR4 enhanced the secretion of TNF-α and IL-6 by neutrophils (Fig. 8.7B). These results show that TARM1 stimulation cooperates with TLR signalling to enhance the secretion of proinflammatory cytokines by macrophages and neutrophils and may play a role in the modulation of cellular responses to pro-inflammatory stimuli.

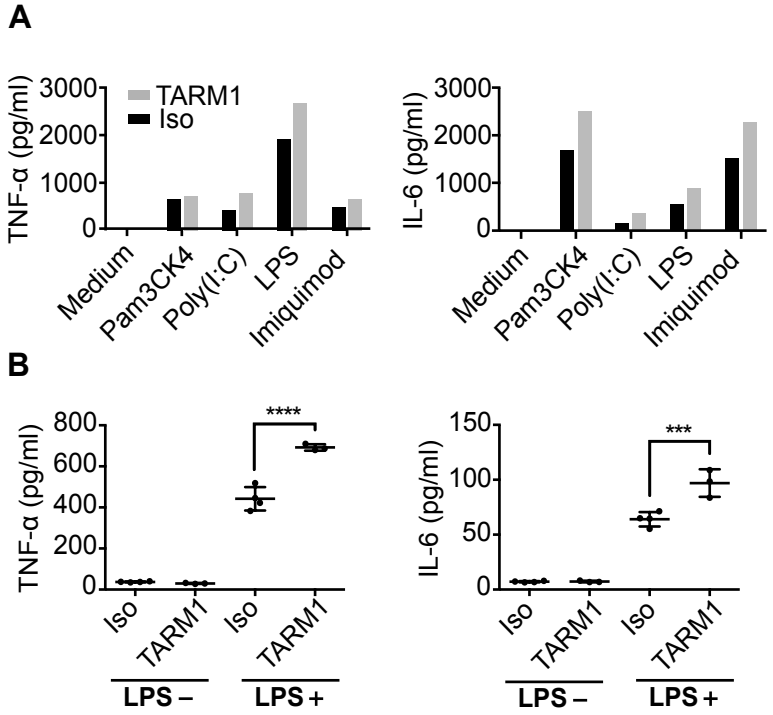

FIGURE 8.7: TARM1 costimulates the secretion of proinflammatory cytokines by macrophages and neutrophils in a TLR-dependent manner. Concentrations of TNF-a or IL-6 in supernatants derived from (A) BMMs or (B) primary neutrophil cultures stimulated with either immobilised anti-TARM1 (TARM1) specific antibody or rat IgG2a isotype control (Iso), with or without agonists for TLR-1/2, -3, -4, and -7. ***p $\leq$ 0.001, ****p $\leq$ 0.0001.

8.4 Summary

In this chapter I described the generation, validation and use of the TARM1-2B4-NFAT-GFP reporter system to identify cells expressing a putative extracellular ligand for TARM1. A screen of a panel of cell lines showed that T cells and fibroblasts induced a robust GFP response in the TARM1 2B4 reporter cells suggesting that T cells and fibroblasts may express the ligand for TARM1 receptor.

Next I examined the effects of TARM1 binding to its putative ligand on T cells. I used an immobilised recombinant TARM1 Fc fusion protein in combination with anti-CD3/anti-CD28 stimulation to evaluate the activation and proliferation of T cells. The expression of activation markers CD25 and CD69, IL-2 secretion as well as the metabolic activity of stimulated T cells were markedly reduced in the presence of TARM1-Fc fusion protein. In addition, T cell proliferation was also significantly suppressed by TARM1 Fc fusion protein.

Finally, I evaluated whether TARM1 protein could act as a receptor by transducing intracellular signals to modulate the function of TARM1-expressing cells such as neutrophils and BMM. Cross-linking of TARM1 in the presence of TLR-1/2, -3, -4, and -7 agonists resulted in enhanced pro-inflammatory response of BMM and neutrophils evidenced by an increased secretion of TNF-α and IL-6. Interestingly, these cytokines are critical for the induction and expansion of $CD11b^{+}Gr1^{+}$ MDSCs in the BM and their subsequent migration to the periphery (Marigo et al. 2010; Bunt et al. 2007; Sade-Feldman et al. 2013). In humans, the role of IL-6 in the context of multiple pathologies, particularly cancer, has attracted a lot of interest in recent years. Chronic inflammation is now widely accepted as one of the factors facilitating tumour development (Atsumi et al. 2014; Park et al. 2010) and elevated levels of IL-6 have been found in patients with a variety of tumours such as prostate, ovarian (Berek et al. 1991) and breast cancer (Sansone et al. 2007) and is a prognostic factor for poor outcome (Scambia et al. 1995; Nakashima et al. 2000; Michalaki et al. 2004).

The direct role of IL-6 in tumour progression is complex due to its pleiotropic effects on both tumour cells and the immune compartment where it can signal in both paracrine and autocrine manner. In mouse model of obesity-induced hepatocellular carcinoma,

enhanced production of IL-6 and TNF was shown to lead to the activation of the oncogenic transcription factor STAT3, whereas ablation of the IL-6 gene prevented tumour development (Park et al. 2010). In a different model tumour-derived exosomes were demonstrated to induce STAT3-dependent immunosuppressive function in mouse and human MDSCs in a TLR2-dependent manner through an autocrine production of IL-6 (Chalmin et al. 2010).

Collectively, these results show that TARM1 functions as a bona fide receptor by binding to an as yet unidentified extracellular ligand expressed on fibroblasts and T cells and signalling bidirectionally to inhibit T cell responses while transducing an activating intracellular signal to TARM1-expressing myeloid cells enhancing their responses following stimulation with TLR agonists.

These data also provide tentative support to the hypothesis proposed in chapter 7 suggesting that mature neutrophils and immature myeloid cells, that could be part of the MDSC population, upregulate TARM1 following a pro-inflammatory stimulus, migrate to the peripheral sites where TARM1 may act as a co-regulatory receptor controlling T cell activation while potentiating the production of IL-6 and TNF-α by myeloid cells.

Extensive functional analysis of TARM1$^+$ cells will be required to establish whether its expression is indeed associated with regulatory cells such as MDSCs and to determine the role of TARM1 in their function.

Chapter 9

Discussion

In this work I describe the characterisation of a novel receptor TARM1 encoded within the leukocyte receptor complex (LRC). My investigation into TARM1 pursued a number of aims starting with the verification of *TARM1* status as a *bona fide* gene and placing it within the current phylogenetic and evolutionary context. A further line of research examined TARM1 protein structure, biochemistry and function including TARM1 post-translational modifications, association with signalling adaptor proteins, gene expression profile *in vivo* and establishing whether TARM1 is a functional receptor capable of modulating cellular immune responses.

I used computational methods and analyses to examine the genomic organisation and sequence of the human and mouse *TARM1* orthologs; I showed that in both species *TARM1* is extensively conserved in sequence and exon structure and encodes two Ig-like folds identifying it as a member of the broader IgSF. Similarly to the activating members of the LRC, TARM1 has a short cytoplasmic tail and encodes a conserved arginine in its TM, where it may serve as an association site for ITAM-bearing signalling adaptors such as FcRγ.

Phylogenetic analysis of translated amino acid sequence of the extracellular portion of TARM1 showed that it is related to other members of the LRC, particularly OSCAR and SIRL-1. In human, TARM1 shares the highest sequence similarity with the inhibitory receptor SIRL-1 (Steevels, Lebbink, et al. 2010) (*VSTM-1* gene) encoded adjacent to TARM1. In mouse and rat, *Sirl-1* is a pseudogene with no evidence of transcriptional activity.

Gene duplication and exon shuffling are among the mechanisms that may have contributed to the evolution of the LRC (A. Barrow and J. Trowsdale 2008). Phylogenetic analysis of individual Ig-like domains of human and mouse LRC members showed that the first Ig-like domain of TARM1 in both species clusters with high confidence with the single Ig-like domain of human SIRL-1 suggesting a common evolutionary origin. A prominent theme among the LRC-encoded gene families is the clustering of closely related genes encoding receptors with opposing functions, as exemplified by the activating and inhibitory KIR and LILR genes. It is possible that SIRL-1 and TARM1 have a common ancestral relationship and have evolved to function antagonistically in primates.

The genomic location of *TARM1* on the centromeric boundary of the LRC in human and mouse as well as its extensive conservation in mice and humans warranted further analysis of TARM1 phylogenetics and evolution. I identified and analysed the genomic region of TARM1 in several mammalian orders (Primates, Carnivora, Rodentia, Lagomorpha, Proboscida and Monotrema) using conserved framework genes. The data indicated that TARM1 appeared early in mammalian evolution, as evidenced by its presence in the platypus, and has undergone rounds of expansion and contraction resulting in the birth and death of the members of the *Tarm1* family in different mammalian orders. In early primates (represented here by the bushbaby) and in the genomes of Carnivora (cat and dog), *Tarm1* has undergone rounds of duplication events, including an inverse duplication, giving rise to two additional *Tarm1* genes.

To enable further characterisation of TARM1 protein, I developed secreted human and mouse TARM1-Fc fusion proteins to serve as immunogens for the generation of monoclonal anti-TARM1 antibodies and to facilitate the study of TARM1 function. I characterised two panels of mAbs against human and mouse TARM1 receptors and selected several clones optimised for use in flow cytometry and Western blot.

I used the newly characterised monoclonal antibodies to show that TARM1 could be immunoprecipitated with an ITAM-bearing adaptor FcRγ suggesting it may function as an activating receptor on TARM1-bearing cells.

RT-PCR screening of mouse and human tissues showed that TARM1 transcript was highly enriched in the BM. Flow cytometric analysis of mouse BM and other tissues including spleen, PECs, liver and lymph nodes showed that in healthy animals

TARM1 cell-surface expression was indeed restricted to the BM. Detailed analysis of the TARM1$^+$ cells showed that they had a prototypical phenotype of granulocytes CD11b$^+$Ly6G$^+$Ly6C$^+$. Of the total BM granulocytes, over 59% were TARM1$^+$. In healthy animals, no TARM1 expression was found in the spleen, PECs, liver or lymph nodes, which could be explained by a low frequency of granulocytes ($\leq$ 1%) in these tissues in the steady state.

I examined TARM1 cell-surface expression in human BM, spleen, mesenteric lymph nodes and peripheral blood. The pattern of human TARM1 expression resembled closely that observed in mouse suggesting evolutionary conservation of TARM1 function. As in mice, cell-surface TARM1 expression in human tissues was detected predominnatly in the cell population having the characteristic granulomonocytic phenotype of FSC^{hi}SSC$^{int\text{-}hi}$ and CD16$^+$CD3$^-$CD19$^-$. In the BM TARM1 expression was also observed on myeloid precursor cells that were CD16$^-$CD3$^-$CD19$^-$. A proportion of CD14$^+$ monocytes in the BM and spleen also had a low-level TARM1 expression.

TARM1 expression could also be detected on mouse BM-derived DCs but not macrophages. The expression could be strongly upregulated in BMDC and induced in BMM by treatment with TLR agonists. The TLR4 ligand LPS was particularly effective at inducing high levels of TARM1 transcript and sell-surface receptor expression. Such robust induction points to a potential role for TARM1 in modulating the innate immune response to gram-negative bacteria.

I explored this hypothesis by studying TARM1 induction in the context of a localised endotoxin-induced inflammatory response. Intraperitoneal administration of a low-dose LPS induced a strong upregulation of cell surface TARM1 expression by BM CD11b$^+$Ly6G$^+$Ly6C$^+$ cells and their migration to the peritoneum. I examined the morphology of FACS sorted, differentially stained TARM1$^+$ BM cells. This population consisted of cells showing ring-shaped or hypersegmented nuclei characteristic of promyelocytes and mature neutrophils, respectively (Cuenca et al. 2011).

Interestingly, more than 50% of TARM1$^+$ cells that migrated to the peritoneum expressed MHC II and had a CD11b$^+$Ly6C^{hi}Ly6G^{lo} phenotype but lacked the DC/-macrophage marker CD11c. Given the rapid recruitment to the peritoneum following

LPS injection, the CD11b^{+}Ly6C^{hi}Ly6G^{lo}MHC II^{+}TARM1^{+} cells likely represented inflammatory monocytes. These cells were shown to rapidly migrate to sites of inflammation, where they could give rise to proinflammatory DCs and macrophages (Henderson et al. 2003) or exert immunosuppressive effects (Geissmann et al. 2010; Serbina and Pamer 2006; Ribechini et al. 2017; Gallina et al. 2006). It is still poorly understood what factors govern whether monocytes develop to augment inflammatory responses or become monocytic suppressor cells. Several studies demonstrated that the progression towards the immunosuppressive function, often observed during cancer development or chronic infection, takes place in several stages. Ribechini et al. described a two-stage process that "licenses" murine Ly6C^{hi} and human CD14^{+} monocytes to acquire suppressor functions. This process is initiated by the release of GM-CSF in the absence of strong activating signals such as IFNγ resulting in structural changes in the IFNγR pathway. Subsequent exposure of licensed monocytes to IFNγ alone or in combination with LPS stabilises the expression of inducible nitric oxide synthase (iNOS) in mouse and indoleamine 2,3-dioxygenase (IDO) in human monocytes leading to their conversion into suppressor cells (Ribechini et al. 2017). Conversely, in the context of acute inflammation such as sepsis, the presence of pathogen-derived strong activating signals such as TLR agonists results in classic activation of myeloid cells (Ribechini et al. 2017).

In the model of LPS-induced sterile inflammation, the immune response is mediated through TLR4 ligation and does not recapitulate all of the complex features of a live bacterial infection. It was therefore of interest to study the induction of TARM1 expression and the distribution pattern of TARM1^{+} cells during systemic bacterial challenge. I used a live-attenuated vaccine strain of Salmonella in a systemic challenge of C57BL/6 mice. Flow cytometric analysis showed that TARM1 expression followed the infection dynamics peaking at the height of infection between weeks 1 and 2. In the bone marrow TARM1 expression was strongly upregulated on mature granulocytes and immature myeloid cells. An influx of TARM1^{+} neutrophils and monocytes was observed in the spleens of infected mice, where they persisted for the duration of the infection and maintained an elevated expression of cell-surface TARM1.

Further studies are required to determine whether proinflammatory signalling induced by TLR ligands other than LPS can regulate human TARM1 cell-surface expression to the same extent and to determine TARM1 cell and tissue distribution in the context of human pathologies such as sepsis. The proinflammatory environment has been shown

to increase neutrophil lifespan (Brach, Gruss, Herrmann, et al. 1992; Colotta et al. 1992), and since TARM1 expression is upregulated by neutrophils in the context of inflammatory responses, it would be of interest to investigate whether an increased TARM1 expression ($TARM^{hi}$) could be the hallmark of neutrophils with enhanced *in vivo* lifespans.

Interestingly, the expression of a closely related SIRL-1 receptor in human is also restricted to neutrophils and monocytes, where it plays a role in the negative regulation of the oxidative burst (Steevels, Avondt, et al. 2013) and can prevent the pathogenic release of neutrophil extracellular traps in cells from systemic lupus erythematosus patients (Van Avondt et al. 2013).

The amino acid sequence of the single IgV domain of SIRL-1 is ∼48% identical to the first Ig-like domain of TARM1. However, owing to its two ITIMs, SIRL-1 exerts inhibitory effects on neutrophil function (Steevels, Avondt, et al. 2013; Van Avondt et al. 2013), whereas TARM1 associates with ITAM-bearing adaptor FcRγ, suggesting an activating function (Daëron et al. 2008). To test the TARM1 signalling potential, I assessed the outcome of TARM1 crosslinking on FACS sorted mouse BM neutrophils and BMM. Indeed, TARM1 engagement enhanced the secretion of proinflammatory cytokines by BMMs and BM neutrophils stimulated with TLR ligands, such as LPS. This supports the hypothesis that TARM1 functions as a co-stimulatory receptor on immune cells and is a paired receptor of the inhibitory SIRL-1 receptor. The integration of opposing signals delivered by TARM1-SIRL1 axis may be essential for balancing of the innate and adaptive immune cell responses.

A large body of work suggests that both human and mouse neutrophils can be activated by, and may exert immunoregulatory effects on, T cells (Gosselin et al. 1993; Abdallah et al. 2011; Alemán et al. 2005; Iking-Konert et al. 2005; Ostanin et al. 2012). Notably, T cells from the synovial fluid of rheumatoid arthritis patients were shown to activate neutrophils at the site of inflammation (Iking-Konert et al. 2005). In patients with renal cell carcinoma, neutrophils were shown to suppress T cell responses through the release of L-arginine metabolising enzyme arginase I (Rodriguez et al. 2009). Pillay et al. described a population of human neutrophils that suppress T-cell proliferation during acute systemic inflammation induced by endotoxin challenge. The inhibition required cell-contact established via the neutrophil-expressed integrin Mac-1 and was

mediated by the release of hydrogen peroxide into the immunological synapse formed with T cells (Pillay et al. 2012). In murine models, the secretion of IL-10 (X. Zhang et al. 2009; Boari et al. 2012; Doz et al. 2013; Ocuin et al. 2011) and the expression of programmed death ligand 1 (McNab et al. 2011; Kleijn et al. 2013) have been proposed as the major components of the immunosuppressive mechanisms employed by neutrophils during bacterial, fungal and parasitic infections. These suppressive neutrophils have been shown to attenuate inflammatory monocytes during septic peritonitis (Ocuin et al. 2011), control the inflammatory response of dendritic cells, macrophages, and T cells (Pillay et al. 2012). In contrast to murine neutrophils, there is no consensus on whether human neutrophils are capable of IL-10 production and the literature abounds with conflicting reports (De Santo et al. 2010; Davey et al. 2011). The contradictions could be related to differences in neutrophil purification methods and experimental conditions. A recent study showed that a monocyte contamination of less than 1% in preparations of human neutrophils could be responsible for the bulk of IL-10 secretion (Calzetti et al. 2017). It was proposed that human neutrophils are incapable of IL-10 production due to an inactive chromatin configuration at the IL-10 locus (Tamassia et al. 2013). However, recently it was shown that IL-10 secretion by human neutrophils could be induced following their direct cell-contact with LPS-treated Treg cells or exposure to exogenous IL-10. These conditions contributed to chromatin reorganisation at the IL-10 locus enabling gene expression (Lewkowicz et al. 2016).

TARM1 is expressed at high levels on neutrophils during inflammation. Therefore, I explored whether it could be involved in the neutrophil-mediated T cell regulation. I used a recombinant TARM1-Fc fusion protein to study T cell responses *in vitro*. I demonstrated that the TARM1 receptor ectodomain was capable, at least *in vitro*, of potently inhibiting CD3/CD28-induced $CD4^+$ and $CD8^+$ T cell activation and proliferation. I also demonstrated that TARM1 protein could function as a *bona fide* receptor by transducing intracellular signals to modulate the function of TARM1-expressing cells such as neutrophils and BMM. Cross-linking of TARM1 in the presence of TLR-1/2, -3, -4, and -7 agonists resulted in enhanced proinflammatory response of BMM and neutrophils as evidenced by an increased secretion of TNF-α and IL-6. Although these results are encouraging, great caution should be exercised in making any inferences about the function of TARM1 *in vivo*. The high avidity of recombinant TARM1 Fc fusion protein may not be physiological and the use of monoclonal antibody as a surrogate ligand to cross-link

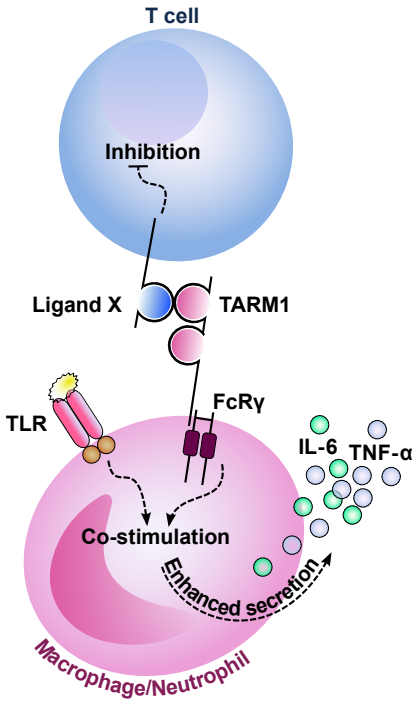

FIGURE 9.1: Model for TARM1-mediated bi-directional signalling in the immune system. TARM1 receptor signalling synergises with specific inflammatory stimuli, e.g. TLR agonists, such as Pam3CK4 (TLR1/2), Poly I:C (TLR3), LPS (TLR4) or Imiquimod (TLR7), to enhance the secretion of proinflammatory cytokines, such as TNF-α and IL-6, by TARM1-expressing cells. Conversely, engagement of the TARM1 ectodomain with an as yet unidentified ligand (Ligand X) expressed on T cells results in the inhibition of T cell activation and proliferation.

TARM1 may lead to artificial cellular responses. Further experiments to determine the TARM1 ligand will be required to confirm these data.

Bearing in mind that TARM1 cell surface expression was rapidly upregulated by neutrophils and inflammatory monocytes *in vivo* during immune challenge, and TARM1$^+$ cells homed to the sites of inflammation, TARM1 may represent a previously uncharacterised negative regulator of T cell activation expressed by neutrophils and inflammatory monocytes, macrophages, and DCs to modulate the early stages of T cell responses while transducing an activating intracellular signal to TARM1-expressing myeloid cells enhancing their responses following stimulation with TLR agonists. A schematic depiction of this model is shown in Figure 9.1. Bidirectional signalling has been previously demonstrated between myeloid cells and innate lymphocytes, such as NK cells, as exemplified by the interaction between AICL and NKp80 (Welte et al. 2006). Similarly to TARM1, the cell surface expression of AICL is also regulated by TLR ligands. The AICL/NKp80 bidirectional signalling interaction resulted in the activation of both NK cells and monocytes, respectively. A TARM1 knock-out mouse or *in vivo* TARM1 blocking experiments will be required to truly determine the validity of this model.

In mouse model of S. Typhimurium infection used in this work, TARM1 expression was also observed on cells showing a classical phenotype of MDSCs (ring-shaped nuclei,

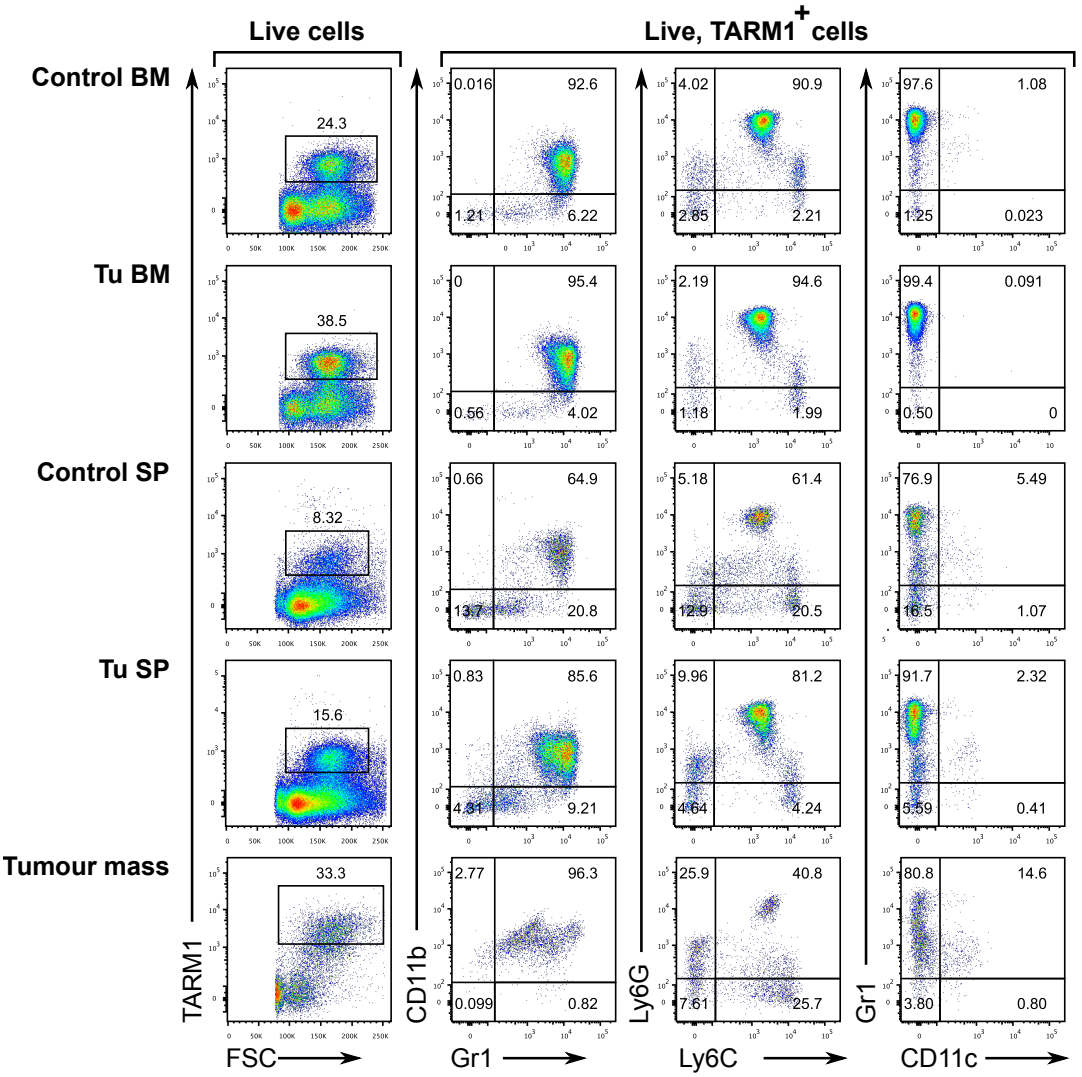

FIGURE 9.2: TARM1 is expressed on MDSC-like cells that infiltrate spleen and tumour mass. Flow cytometric analysis of the expression of TARM1, CD11b, Ly6G, Ly6C and CD11c on cells from OT1 tumour-bearing and control mice. TARM1 gate was set relative to isotype control. BM - bone marrow, SP - spleen, Tu - tumour

$CD11b^{+}Gr1^{+}$). I wanted to explore whether TARM1 expression was indeed associated with suppressive myeloid cells. The accumulation of MDSCs in tumour-bearing mice and cancer patients is well-documented in the literature (Youn et al. 2008; Ostrand-Rosenberg and Sinha 2009).

Therefore, I conducted a preliminary flow cytometric analysis of TARM1 expression in OT1 mice carrying a T cell-lineage restricted oncogenic gene fusion nucleophosmin - anaplastic lymphoma kinase (Malcolm et al. 2016) (*ex vivo* samples were kindly provided by Dr. CJ Fairbairn). These animals develop spontaneous lymphomas histopathologically mimicking human anaplastic large cell lymphoma (ALCL) (Malcolm et al. 2016).

Flow cytometric staining of BM, spleen and the tumour mass showed an expansion of cells bearing G-MDSC phenotype ($CD11b^{+}Ly6G^{hi}Ly6C^{int}$) in the BM and their infiltration into the spleen and the tumour mass in line with earlier studies. Interestingly, the majority of $TARM1^{+}$ cells expressed the G-MDSC phenotype and were present in the tumour mass Fig. 9.2.

The extent of neutrophilic infiltration in human tumours as well as high neutrophil-lymphocyte ratio in the blood were identified as the most powerful immunologic predictors of poor prognostic outcome in human oncology (Jensen et al. 2009; Y.-W. Li et al. 2011; Donskov and Maase 2006; Shen et al. 2014). As I described in the Introduction (page 19), the role of neutrophils in tumourigenesis is complex and multifaceted and their function changes as tumours evolve (Mishalian et al. 2013). Evidence that emerged from mouse models suggests that tumour associated neutrophils (TANs) undergo a switch from a cytotoxic to an immunosuppressive phenotype as the tumour transitions from early to late stages (Fridlender et al. 2009; Eruslanov et al. 2014; Mishalian et al. 2013). It is still unclear whether the paradigm of N1 cytotoxic neutrophils and N2 immunosuppressive pro-tumourigenic neutrophils applies to human pathologies (Fridlender et al. 2009). Eruslanov et al. found that early-stage human lung tumours were infiltrated with APC-like hybrid TANs that could augment or directly stimulate antigen-dependent and independent memory and effector T cell responses, and capture and cross-present tumour antigens (Eruslanov et al. 2014; Eruslanov 2017). The authors observed that TANs present in larger tumours had a diminished ability to stimulate T cells suggesting that neutrophils undergo a phenotypic and functional switch as the tumour progresses.

The majority of data on human cancers was obtained from late-stage tumours and describes pro-tumourigenic functions of TANs. For example, neutrophils have been implicated in promoting tumour angiogenesis and invasiveness by induction of VEGF expression and the release of matrix metalloproteinases (Ardi et al. 2007; Kuang, Zhao, Wu, et al. 2011; Shamamian et al. 2001).

These findings warrant further research into the role of TARM1 on neutrophils and present the exciting possibility of using TARM1 (or its ligand) as a pharmaceutical target to regulate or selectively deplete TARM1-expressing cells such as MDSCs and activated neutrophils or to control T cell responses by targeting TARM1 ligand. This approach would be highly relevant in numerous pathologies caused by excessive or aberrant T cell

activation such as in autoimmune and inflammatory conditions or pathological MDSC-mediated T cell suppression as observed in cancer patients.

The identification of the inhibitory TARM1 ligand expressed on T cells will be a crucial next step that could help shed light on as yet uncharacterised mechanisms of T cell regulation.

Bibliography

Abadie, Valérie et al. (2005). "Neutrophils rapidly migrate via lymphatics after Mycobacterium bovis BCG intradermal vaccination and shuttle live bacilli to the draining lymph nodes". In: *Blood* 106.5, pp. 1843–1850.

Abdallah, Delbert S Abi et al. (2011). "Mouse neutrophils are professional antigen-presenting cells programmed to instruct Th1 and Th17 T-cell differentiation". In: *International immunology* 23.5, pp. 317–326.

Agrawal, A., Q.M. Eastman, and D.G. Schatz (1998). "Transposition mediated by RAG1 and RAG2 and its implications for the evolution of the immune system". In: *Nature* 394.6695, pp. 744–751.

Aicher, Alexandra et al. (2000). "Characterization of human inducible costimulator ligand expression and function". In: *The Journal of Immunology* 164.9, pp. 4689–4696.

Alemán, Mercedes et al. (2005). "In Tuberculous Pleural Effusions, Activated Neutrophils Undergo Apoptosis and Acquire a Dendritic Cell–Like Phenotype". In: *Journal of Infectious Diseases* 192.3, pp. 399–409.

Allan, David SJ et al. (1999). "Tetrameric complexes of human histocompatibility leukocyte antigen (HLA)-G bind to peripheral blood myelomonocytic cells". In: *The Journal of experimental medicine* 189.7, pp. 1149–1156.

Allen, Rachel L, Chris A O'Callaghan, et al. (1999). "Cutting edge: HLA-B27 can form a novel β2-microglobulin-free heavy chain homodimer structure". In: *The Journal of Immunology* 162.9, pp. 5045–5048.

Allen, Rachel L, Tim Raine, et al. (2001). "Cutting edge: Leukocyte receptor complex-encoded immunomodulatory receptors show differing specificity for alternative HLA-B27 structures". In: *The Journal of Immunology* 167.10, pp. 5543–5547.

Altschul, Stephen F et al. (1997). "Gapped BLAST and PSI-BLAST: a new generation of protein database search programs". In: *Nucleic acids research* 25.17, pp. 3389–3402.

Apweiler, Rolf, Henning Hermjakob, and Nathan Sharon (1999). "On the frequency of protein glycosylation, as deduced from analysis of the SWISS-PROT database". In: *Biochimica et Biophysica Acta (BBA)-General Subjects* 1473.1, pp. 4–8.

Arase, Hisashi et al. (2002). "Direct recognition of cytomegalovirus by activating and inhibitory NK cell receptors". In: *Science* 296.5571, pp. 1323–1326.

Ardi, Veronica C et al. (2007). "Human neutrophils uniquely release TIMP-free MMP-9 to provide a potent catalytic stimulator of angiogenesis". In: *Proceedings of the National Academy of Sciences* 104.51, pp. 20262–20267.

Arnon, Tal I et al. (2001). "Recognition of viral hemagglutinins by NKp44 but not by NKp30". In: *European journal of immunology* 31.9, pp. 2680–2689.

Atsumi, Toru et al. (2014). "Inflammation amplifier, a new paradigm in cancer biology". In: *Cancer research* 74.1, pp. 8–14.

Barquero-Calvo, Elıas et al. (2013). "Neutrophils exert a suppressive effect on Th1 responses to intracellular pathogen Brucella abortus". In: *PLoS pathogens* 9.2, e1003167.

Barrow, A.D., N. Raynal, et al. (2011). "OSCAR is a collagen receptor that costimulates osteoclastogenesis in DAP12-deficient humans and mice". In: *The Journal of Clinical Investigation* 121.9, p. 3505.

Barrow, A.D. and J. Trowsdale (2008). "The extended human leukocyte receptor complex: diverse ways of modulating immune responses". In: *Immunological reviews* 224.1, pp. 98–123.

Barrow, Alexander D et al. (2015). "OSCAR Is a Receptor for Surfactant Protein D That Activates TNF-α Release from Human CCR2+ Inflammatory Monocytes". In: *The Journal of Immunology* 194.7, pp. 3317–3326.

Bashirova, Arman A et al. (2014). "LILRB2 Interaction with HLA Class I Correlates with Control of HIV-1 Infection". In: *PLoS genetics* 10.3, e1004196.

Beauvillain, Céline et al. (2007). "Neutrophils efficiently cross-prime naive T cells in vivo". In: *Blood* 110.8, pp. 2965–2973.

Bennett, Frann et al. (2003). "Program death-1 engagement upon TCR activation has distinct effects on costimulation and cytokine-driven proliferation: attenuation of ICOS, IL-4, and IL-21, but not CD28, IL-7, and IL-15 responses". In: *The Journal of Immunology* 170.2, pp. 711–718.

Berek, Jonathan S et al. (1991). "Serum interleukin-6 levels correlate with disease status in patients with epithelial ovarian cancer". In: *American journal of obstetrics and gynecology* 164.4, pp. 1038–1043.

Blasius, Amanda L et al. (2006). "Siglec-H is an IPC-specific receptor that modulates type I IFN secretion through DAP12". In: *Blood* 107.6, pp. 2474–2476.

Blom, Nikolaj et al. (2004). "Prediction of post-translational glycosylation and phosphorylation of proteins from the amino acid sequence". In: *Proteomics* 4.6, pp. 1633–1649.

Boari, Jimena Tosello et al. (2012). "IL-17RA signaling reduces inflammation and mortality during Trypanosoma cruzi infection by recruiting suppressive IL-10-producing neutrophils". In: *PLoS pathogens* 8.4, e1002658.

Boettcher, Steffen et al. (2012). "Cutting edge: LPS-induced emergency myelopoiesis depends on TLR4-expressing nonhematopoietic cells". In: *The Journal of Immunology* 188.12, pp. 5824–5828.

Bonaccorsi, Irene et al. (2010). "The immune inhibitory receptor LAIR-1 is highly expressed by plasmacytoid dendritic cells and acts complementary with NKp44 to control IFNα production". In: *PLoS One* 5.11, e15080.

Bouchon, Axel, Jes Dietrich, and Marco Colonna (2000). "Cutting edge: inflammatory responses can be triggered by TREM-1, a novel receptor expressed on neutrophils and monocytes". In: *The Journal of Immunology* 164.10, pp. 4991–4995.

Bouchon, Axel, Fabio Facchetti, et al. (2001). "TREM-1 amplifies inflammation and is a crucial mediator of septic shock". In: *nature* 410.6832, pp. 1103–1107.

Boxio, Rachel et al. (2004). "Mouse bone marrow contains large numbers of functionally competent neutrophils". In: *Journal of leukocyte biology* 75.4, pp. 604–611.

Brach, Marion A, HJ Gruss, F Herrmann, et al. (1992). "Prolongation of survival of human polymorphonuclear neutrophils by granulocyte-macrophage colony-stimulating factor is caused by inhibition of programmed cell death". In: *Blood* 80.11, pp. 2920–2924.

Brendel, Volker, Liqun Xing, and Wei Zhu (2004). "Gene structure prediction from consensus spliced alignment of multiple ESTs matching the same genomic locus". In: *Bioinformatics* 20.7, pp. 1157–1169.

Brudecki, Laura et al. (2012). "Myeloid-derived suppressor cells evolve during sepsis and can enhance or attenuate the systemic inflammatory response". In: *Infection and immunity* 80.6, pp. 2026–2034.

Bunt, Stephanie K et al. (2007). "Reduced inflammation in the tumor microenvironment delays the accumulation of myeloid-derived suppressor cells and limits tumor progression". In: *Cancer research* 67.20, pp. 10019–10026.

Burge, Chris and Samuel Karlin (1997). "Prediction of complete gene structures in human genomic DNA". In: *Journal of molecular biology* 268.1, pp. 78–94.

Burshtyn, Deborah N et al. (1996). "Recruitment of tyrosine phosphatase HCP by the killer cell inhibitory receptor". In: *Immunity* 4.1, pp. 77–85.

Butte, Manish J et al. (2007). "Programmed death-1 ligand 1 interacts specifically with the B7-1 costimulatory molecule to inhibit T cell responses". In: *Immunity* 27.1, pp. 111–122.

Calzetti, Federica et al. (2017). "The importance of being "pure" neutrophils". In: *Journal of Allergy and Clinical Immunology* 139.1, pp. 352–355.

Cannons, Jennifer L, Stuart G Tangye, and Pamela L Schwartzberg (2011). "SLAM family receptors and SAP adaptors in immunity". In: *Annual review of immunology* 29, pp. 665–705.

Cao, Wei et al. (2006). "Plasmacytoid dendritic cell–specific receptor ILT7–FcεRIγ inhibits Toll-like receptor–induced interferon production". In: *Journal of Experimental Medicine* 203.6, pp. 1399–1405.

Caruso, Arnoldo et al. (1997). "Flow cytometric analysis of activation markers on stimulated T cells and their correlation with cell proliferation". In: *Cytometry* 27.1, pp. 71–76.

Casbon, Amy-Jo et al. (2015). "Invasive breast cancer reprograms early myeloid differentiation in the bone marrow to generate immunosuppressive neutrophils". In: *Proceedings of the National Academy of Sciences* 112.6, E566–E575.

Chalmin, Fanny et al. (2010). "Membrane-associated Hsp72 from tumor-derived exosomes mediates STAT3-dependent immunosuppressive function of mouse and human myeloid-derived suppressor cells". In: *The Journal of clinical investigation* 120.2, p. 457.

Chang, Chih-Chao et al. (2002). "Tolerization of dendritic cells by TS cells: the crucial role of inhibitory receptors ILT3 and ILT4". In: *Nature immunology* 3.3, p. 237.

Chemnitz, Jens M et al. (2004). "SHP-1 and SHP-2 associate with immunoreceptor tyrosine-based switch motif of programmed death 1 upon primary human T cell stimulation, but only receptor ligation prevents T cell activation". In: *The Journal of Immunology* 173.2, pp. 945–954.

Chtanova, Tatyana et al. (2008). "Dynamics of neutrophil migration in lymph nodes during infection". In: *Immunity* 29.3, pp. 487–496.

Colonna, Marco, Francisco Navarro, et al. (1997). "A common inhibitory receptor for major histocompatibility complex class I molecules on human lymphoid and myelomonocytic cells". In: *The Journal of experimental medicine* 186.11, pp. 1809–1818.

Colonna, Marco, Jacqueline Samaridis, et al. (1998). "Cutting edge: human myelomonocytic cells express an inhibitory receptor for classical and nonclassical MHC class I molecules". In: *The Journal of Immunology* 160.7, pp. 3096–3100.

Colotta, Francesco et al. (1992). "Modulation of granulocyte survival and programmed cell death by cytokines and bacterial products". In: *Blood* 80.8, pp. 2012–2020.

Cuenca, Alex G et al. (2011). "A paradoxical role for myeloid-derived suppressor cells in sepsis and trauma". In: *Molecular medicine* 17.3-4, p. 281.

Curiel, Tyler J et al. (2003). "Blockade of B7-H1 improves myeloid dendritic cell-mediated antitumor immunity". In: *Nature medicine* 9.5, p. 562.

Da Silva, Fabiano Pinheiro et al. (2007). "CD16 promotes Escherichia coli sepsis through an FcRγ inhibitory pathway that prevents phagocytosis and facilitates inflammation". In: *Nature medicine* 13.11, pp. 1368–1374.

Daëron, Marc et al. (2008). "Immunoreceptor tyrosine-based inhibition motifs: a quest in the past and future". In: *Immunological reviews* 224.1, pp. 11–43.

Darcy, Christabelle J et al. (2014). "Neutrophils with myeloid derived suppressor function deplete arginine and constrain T cell function in septic shock patients". In: *Critical Care* 18.4, R163.

Davey, M.S. et al. (2011). "Failure to detect production of IL-10 by activated human neutrophils." In: *Nature immunology* 12, pp. 1017–1020.

De Santo, Carmela et al. (2010). "Invariant NKT cells modulate the suppressive activity of IL-10-secreting neutrophils differentiated with serum amyloid A". In: *Nature immunology* 11.11, p. 1039.

Delano, Matthew J et al. (2007). "MyD88-dependent expansion of an immature GR-1+ CD11b+ population induces T cell suppression and Th2 polarization in sepsis". In: *The Journal of experimental medicine* 204.6, pp. 1463–1474.

Dennis, G., H. Kubagawa, and M.D. Cooper (2000). "Paired Ig-like receptor homologs in birds and mammals share a common ancestor with mammalian Fc receptors". In: *Proceedings of the National Academy of Sciences* 97.24, p. 13245.

Derive, Marc et al. (2012). "Myeloid-derived suppressor cells control microbial sepsis". In: *Intensive care medicine* 38.6, pp. 1040–1049.

Diana, Julien et al. (2013). "Crosstalk between neutrophils, B-1a cells and plasmacytoid dendritic cells initiates autoimmune diabetes". In: *Nature medicine* 19.1, pp. 65–73.

Diefenbach, Andreas et al. (2002). "Selective associations with signaling proteins determine stimulatory versus costimulatory activity of NKG2D". In: *Nature immunology* 3.12, pp. 1142–1149.

Donskov, Frede and Hans von der Maase (2006). "Impact of immune parameters on long-term survival in metastatic renal cell carcinoma". In: *Journal of clinical oncology* 24.13, pp. 1997–2005.

Doyle, Hester A and Mark J Mamula (2001). "Post-translational protein modifications in antigen recognition and autoimmunity". In: *Trends in immunology* 22.8, pp. 443–449.

Doz, Emilie et al. (2013). "Mycobacteria-Infected Dendritic Cells Attract Neutrophils That Produce IL-10 and Specifically Shut Down Th17 CD4 T Cells through Their IL-10 Receptor". In: *The Journal of Immunology* 191.7, pp. 3818–3826.

Eisenhaber, Birgit, Peer Bork, and Frank Eisenhaber (2001). "Post-translational GPI lipid anchor modification of proteins in kingdoms of life: analysis of protein sequence data from complete genomes". In: *Protein Engineering* 14.1, pp. 17–25.

Eissmann, Philipp et al. (2005). "Molecular basis for positive and negative signaling by the natural killer cell receptor 2B4 (CD244)". In: *Blood* 105.12, pp. 4722–4729.

Eruslanov, Evgeniy B (2017). "Phenotype and function of tumor-associated neutrophils and their subsets in early-stage human lung cancer". In: *Cancer Immunology, Immunotherapy*, pp. 1–10.

Eruslanov, Evgeniy B et al. (2014). "Tumor-associated neutrophils stimulate T cell responses in early-stage human lung cancer". In: *The Journal of clinical investigation* 124.12, pp. 5466–5480.

Fanger, Neil A et al. (1997). "Activation of human T cells by major histocompatability complex class II expressing neutrophils: proliferation in the presence of superantigen, but not tetanus toxoid". In: *Blood* 89.11, pp. 4128–4135.

Felsenstein, Joseph (1985). "Confidence limits on phylogenies: an approach using the bootstrap". In: *Evolution*, pp. 783–791.

Feng, Jianwen, Matthew E Call, and Kai W Wucherpfennig (2006). "The assembly of diverse immune receptors is focused on a polar membrane-embedded interaction site". In: *PLoS biology* 4.5, e142.

Feng, Jianwen, David Garrity, et al. (2005). "Convergence on a distinctive assembly mechanism by unrelated families of activating immune receptors". In: *Immunity* 22.4, pp. 427–438.

Fink, Mitchell P (2014). "Animal models of sepsis". In: *Virulence* 5.1, pp. 143–153.

Fleming, TJ, ML Fleming, and TR Malek (1993). "Selective expression of Ly-6G on myeloid lineage cells in mouse bone marrow. RB6-8C5 mAb to granulocyte-differentiation antigen (Gr-1) detects members of the Ly-6 family." In: *The Journal of Immunology* 151.5, pp. 2399–2408.

Fridlender, Zvi G et al. (2009). "Polarization of tumor-associated neutrophil phenotype by TGF-β:"N1" versus "N2" TAN". In: *Cancer cell* 16.3, pp. 183–194.

Fuchs, Anja et al. (2005). "Paradoxic inhibition of human natural interferon-producing cells by the activating receptor NKp44". In: *Blood* 106.6, pp. 2076–2082.

Gallina, Giovanna et al. (2006). "Tumors induce a subset of inflammatory monocytes with immunosuppressive activity on CD8+ T cells". In: *The Journal of clinical investigation* 116.10, pp. 2777–2790.

Ganesan, Latha P et al. (2003). "The protein-tyrosine phosphatase SHP-1 associates with the phosphorylated immunoreceptor tyrosine-based activation motif of FcγRIIa to modulate signaling events in myeloid cells". In: *Journal of Biological Chemistry* 278.37, pp. 35710–35717.

Geissmann, Frederic et al. (2010). "Development of monocytes, macrophages, and dendritic cells". In: *Science* 327.5966, pp. 656–661.

Ghebeh, Hazem et al. (2006). "The B7-H1 (PD-L1) T lymphocyte-inhibitory molecule is expressed in breast cancer patients with infiltrating ductal carcinoma: correlation with important high-risk prognostic factors". In: *Neoplasia* 8.3, pp. 190–198.

Gilfillan, Susan et al. (2002). "NKG2D recruits two distinct adapters to trigger NK cell activation and costimulation". In: *Nature immunology* 3.12, pp. 1150–1155.

Gisbergen, Klaas PJM van, Irene S Ludwig, et al. (2005). "Interactions of DC-SIGN with Mac-1 and CEACAM1 regulate contact between dendritic cells and neutrophils". In: *FEBS letters* 579.27, pp. 6159–6168.

Gisbergen, Klaas PJM van, Marta Sanchez-Hernandez, et al. (2005). "Neutrophils mediate immune modulation of dendritic cells through glycosylation-dependent interactions between Mac-1 and DC-SIGN". In: *Journal of Experimental Medicine* 201.8, pp. 1281–1292.

Gosselin, EJ et al. (1993). "Induction of MHC class II on human polymorphonuclear neutrophils by granulocyte/macrophage colony-stimulating factor, IFN-gamma, and IL-3." In: *The Journal of Immunology* 151.3, pp. 1482–1490.

Guo, Xiaohuan et al. (2012). "VSTM1-v2, a novel soluble glycoprotein, promotes the differentiation and activation of Th17 cells". In: *Cellular Immunology.*

Gupta, R, E Jung, and S Brunak (2004). "Prediction of N-glycosylation sites in human proteins". In: *pre paration.*

Guselnikov, S.V. et al. (2010). "The amphibians Xenopus laevis and Silurana tropicalis possess a family of activating KIR-related Immunoglobulin-like Receptors". In: *Developmental & Comparative Immunology* 34.3, pp. 308–315.

Hamerman, J.A. et al. (2006). "Cutting edge: inhibition of TLR and FcR responses in macrophages by triggering receptor expressed on myeloid cells (TREM)-2 and DAP12". In: *The Journal of Immunology* 177.4, p. 2051.

Hamerman, Jessica A and Lewis L Lanier (2006). "Inhibition of immune responses by ITAM-bearing receptors". In: *Science Signaling* 2006.320, re1.

Hamerman, Jessica A, Nadia K Tchao, et al. (2005). "Enhanced Toll-like receptor responses in the absence of signaling adaptor DAP12". In: *Nature immunology* 6.6, pp. 579–586.

Hamid, Omid et al. (2013). "Safety and tumor responses with lambrolizumab (anti–PD-1) in melanoma". In: *N Engl J Med* 2013.369, pp. 134–144.

Harding, Fiona A, Jane A Gross, et al. (1992). "CD28-mediated signalling co-stimulates murine T cells and prevents induction of anergy in T-cell clones". In: *Nature* 356.6370, p. 607.

Harpaz, Y., C. Chothia, et al. (1994). "Many of the immunoglobulin superfamily domains in cell adhesion molecules and surface receptors belong to a new structural set which is close to that containing variable domains." In: *Journal of molecular biology* 238.4, p. 528.

Haslett, Christopher et al. (1985). "Modulation of multiple neutrophil functions by preparative methods or trace concentrations of bacterial lipopolysaccharide." In: *The American journal of pathology* 119.1, p. 101.

Henderson, Robert B et al. (2003). "Rapid recruitment of inflammatory monocytes is independent of neutrophil migration". In: *Blood* 102.1, pp. 328–335.

Hestdal, K et al. (1991). "Characterization and regulation of RB6-8C5 antigen expression on murine bone marrow cells." In: *The Journal of Immunology* 147.1, pp. 22–28.

Hiby, Susan E et al. (2004). "Combinations of maternal KIR and fetal HLA-C genes influence the risk of preeclampsia and reproductive success". In: *Journal of Experimental Medicine* 200.8, pp. 957–965.

Hirayasu, Kouyuki et al. (2016). "Microbially cleaved immunoglobulins are sensed by the innate immune receptor LILRA2". In: *Nature microbiology* 1.6, p. 16054.

Hofsteenge, Jan et al. (1994). "New type of linkage between a carbohydrate and a protein: C-glycosylation of a specific tryptophan residue in human RNase Us". In: *Biochemistry* 33.46, pp. 13524–13530.

Hui, Enfu et al. (2017). "T cell costimulatory receptor CD28 is a primary target for PD-1–mediated inhibition". In: *Science* 355.6332, pp. 1428–1433.

Hutloff, Andreas et al. (1999). "ICOS is an inducible T-cell co-stimulator structurally and functionally related to CD28". In: *Nature* 402, pp. 21–24.

Iking-Konert, Christof et al. (2005). "Transdifferentiation of polymorphonuclear neutrophils to dendritic-like cells at the site of inflammation in rheumatoid arthritis: evidence for activation by T cells". In: *Annals of the rheumatic diseases* 64.10, pp. 1436–1442.

Iwashima, Makio et al. (1994). "Sequential interactions of the TCR with two distinct cytoplasmic tyrosine kinases". In: *Science* 263.5150, pp. 1136–1139.

Jensen, Hanne Krogh et al. (2009). "Presence of intratumoral neutrophils is an independent prognostic factor in localized renal cell carcinoma". In: *Journal of clinical oncology* 27.28, pp. 4709–4717.

Jones, Andrew et al. (2016). "Immunomodulatory functions of BTLA and HVEM govern induction of extrathymic regulatory T cells and tolerance by dendritic cells". In: *Immunity* 45.5, pp. 1066–1077.

Jones, Des C et al. (2011). "HLA class I allelic sequence and conformation regulate leukocyte Ig-like receptor binding". In: *The Journal of Immunology* 186.5, pp. 2990–2997.

Julenius, Karin (2007). "NetCGlyc 1.0: prediction of mammalian C-mannosylation sites". In: *Glycobiology* 17.8, pp. 868–876.

Kamphorst, Alice O et al. (2017). "Rescue of exhausted CD8 T cells by PD-1–targeted therapies is CD28-dependent". In: *Science* 355.6332, pp. 1423–1427.

Kanamaru, Yutaka et al. (2008). "Inhibitory ITAM signaling by FcαRI-FcRγ chain controls multiple activating responses and prevents renal inflammation". In: *The Journal of Immunology* 180.4, pp. 2669–2678.

Kaufmann, Daniel E and Bruce D Walker (2009). "PD-1 and CTLA-4 inhibitory cosignaling pathways in HIV infection and the potential for therapeutic intervention". In: *The Journal of Immunology* 182.10, pp. 5891–5897.

Kehrel, Beate et al. (1998). "Glycoprotein VI is a major collagen receptor for platelet activation: it recognizes the platelet-activating quaternary structure of collagen, whereas CD36, glycoprotein IIb/IIIa, and von Willebrand factor do not". In: *Blood* 91.2, pp. 491–499.

Keir, Mary E et al. (2008). "PD-1 and its ligands in tolerance and immunity". In: *Annu. Rev. Immunol.* 26, pp. 677–704.

Khandpur, Ritika et al. (2013). "NETs are a source of citrullinated autoantigens and stimulate inflammatory responses in rheumatoid arthritis". In: *Science translational medicine* 5.178, 178ra40–178ra40.

Khayyamian, Saman et al. (2002). "ICOS-ligand, expressed on human endothelial cells, costimulates Th1 and Th2 cytokine secretion by memory CD4+ T cells". In: *Proceedings of the National Academy of Sciences* 99.9, pp. 6198–6203.

Kleijn, Stan de et al. (2013). "IFN-γ-Stimulated Neutrophils Suppress Lymphocyte Proliferation through Expression of PD-L1". In: *PloS one* 8.8, e72249.

Kuang, Dong-Ming, Qiyi Zhao, Chen Peng, et al. (2009). "Activated monocytes in peritumoral stroma of hepatocellular carcinoma foster immune privilege and disease progression through PD-L1". In: *Journal of Experimental Medicine* 206.6, pp. 1327–1337.

Kuang, Dong-Ming, Qiyi Zhao, Yan Wu, et al. (2011). "Peritumoral neutrophils link inflammatory response to disease progression by fostering angiogenesis in hepatocellular carcinoma". In: *Journal of hepatology* 54.5, pp. 948–955.

Lafferty, Kevin John and AJ Cunningham (1975). "A new analysis of allogeneic interactions." In: *Australian Journal of Experimental Biology & Medical Science* 53.1.

Lande, Roberto et al. (2011). "Neutrophils activate plasmacytoid dendritic cells by releasing self-DNA–peptide complexes in systemic lupus erythematosus". In: *Science translational medicine* 3.73, 73ra19–73ra19.

Lanier, Lewis L et al. (1998). "Immunoreceptor DAP12 bearing a tyrosine-based activation motif is involved in activating NK cells". In: *Nature* 391.6668, pp. 703–707.

Latchman, Yvette, Paul F McKay, and Hans Reiser (1998). "Cutting edge: identification of the 2B4 molecule as a counter-receptor for CD48". In: *The Journal of Immunology* 161.11, pp. 5809–5812.

Latour, Sylvain et al. (2003). "Binding of SAP SH2 domain to FynT SH3 domain reveals a novel mechanism of receptor signalling in immune regulation". In: *Nature cell biology* 5.2, p. 149.

Leavenworth, Jianmei W et al. (2015). "A p85 [alpha]-osteopontin axis couples the receptor ICOS to sustained Bcl-6 expression by follicular helper and regulatory T cells". In: *Nature immunology* 16.1, pp. 96–106.

Lebbink, Robert Jan, Maaike CW van den Berg, et al. (2008). "The soluble leukocyte-associated Ig-like receptor (LAIR)-2 antagonizes the collagen/LAIR-1 inhibitory immune interaction". In: *The Journal of Immunology* 180.3, pp. 1662–1669.

Lebbink, Robert Jan, Nicolas Raynal, et al. (2009). "Identification of multiple potent binding sites for human leukocyte associated Ig-like receptor LAIR on collagens II and III". In: *Matrix biology* 28.4, pp. 202–210.

Lee, Delphine J et al. (2007). "LILRA2 activation inhibits dendritic cell differentiation and antigen presentation to T cells". In: *The Journal of Immunology* 179.12, pp. 8128–8136.

Lepin, Eric JM et al. (2000). "Functional characterization of HLA-F and binding of HLA-F tetramers to ILT2 and ILT4 receptors". In: *European journal of immunology* 30.12, pp. 3552–3561.

Lewkowicz, N et al. (2016). "Induction of human IL-10-producing neutrophils by LPS-stimulated Treg cells and IL-10". In: *Mucosal immunology* 9.2, p. 364.

Li, Yi-Wei et al. (2011). "Intratumoral neutrophils: a poor prognostic factor for hepatocellular carcinoma following resection". In: *Journal of hepatology* 54.3, pp. 497–505.

Liang, Bitao et al. (2008). "Regulatory T cells inhibit dendritic cells by lymphocyte activation gene-3 engagement of MHC class II". In: *The Journal of Immunology* 180.9, pp. 5916–5926.

Lichterfeld, Mathias and G Yu Xu (2012). "The emerging role of leukocyte immunoglobulin-like receptors (LILRs) in HIV-1 infection". In: *Journal of leukocyte biology* 91.1, pp. 27–33.

Maasho, Kerima et al. (2005). "The inhibitory leukocyte-associated Ig-like receptor-1 (LAIR-1) is expressed at high levels by human naive T cells and inhibits TCR mediated activation". In: *Molecular immunology* 42.12, pp. 1521–1530.

Madrigal, J Alejandro et al. (1991). "Molecular definition of a polymorphic antigen (LA45) of free HLA-A and-B heavy chains found on the surfaces of activated B and T cells." In: *The Journal of experimental medicine* 174.5, pp. 1085–1095.

Malcolm, Tim et al. (2016). *Assessing the origins of anaplastic large cell lymphoma in murine models via forced lineage specificity of NPM-ALK expression in T cells.*

Mantovani, Alberto et al. (2011). "Neutrophils in the activation and regulation of innate and adaptive immunity". In: *Nature Reviews Immunology* 11.8, pp. 519–531.

Manz, Markus G and Steffen Boettcher (2014). "Emergency granulopoiesis". In: *Nature Reviews Immunology* 14.5, pp. 302–314.

Marigo, Ilaria et al. (2010). "Tumor-induced tolerance and immune suppression depend on the C/EBPβ transcription factor". In: *Immunity* 32.6, pp. 790–802.

McNab, Finlay W et al. (2011). "Programmed death ligand 1 is over-expressed by neutrophils in the blood of patients with active tuberculosis". In: *European journal of immunology* 41.7, pp. 1941–1947.

Megiovanni, Anna Maria et al. (2006). "Polymorphonuclear neutrophils deliver activation signals and antigenic molecules to dendritic cells: a new link between leukocytes upstream of T lymphocytes". In: *Journal of leukocyte biology* 79.5, pp. 977–988.

Merck, Estelle, Claude Gaillard, Daniel M Gorman, et al. (2004). "OSCAR is an FcRgamma-associated receptor that is expressed by myeloid cells and is involved in antigen presentation and activation of human dendritic cells". In: *Blood* 104.5, pp. 1386–1395.

Merck, Estelle, Claude Gaillard, Mathieu Scuiller, et al. (2006). "Ligation of the FcRγ chain-associated human osteoclast-associated receptor enhances the proinflammatory responses of human monocytes and neutrophils". In: *The Journal of Immunology* 176.5, pp. 3149–3156.

Meyaard, L. (2008). "The inhibitory collagen receptor LAIR-1 (CD305)". In: *Journal of leukocyte biology* 83.4, pp. 799–803.

Meyaard, Linde, Gosse J Adema, et al. (1997). "LAIR-1, a novel inhibitory receptor expressed on human mononuclear leukocytes". In: *Immunity* 7.2, pp. 283–290.

Meyaard, Linde, Jolanda Hurenkamp, et al. (1999). "Leukocyte-associated Ig-like receptor-1 functions as an inhibitory receptor on cytotoxic T cells". In: *The Journal of Immunology* 162.10, pp. 5800–5804.

Michalaki, V et al. (2004). "Serum levels of IL-6 and TNF-α correlate with clinicopathological features and patient survival in patients with prostate cancer". In: *British journal of cancer* 90.12, pp. 2312–2316.

Mishalian, Inbal et al. (2013). "Tumor-associated neutrophils (TAN) develop pro-tumorigenic properties during tumor progression". In: *Cancer Immunology, Immunotherapy* 62.11, pp. 1745–1756.

Moretta, Lorenzo and Alessandro Moretta (2004). "Killer immunoglobulin-like receptors". In: *Current opinion in immunology* 16.5, pp. 626–633.

Nakahashi, Chigusa et al. (2007). "Dual assemblies of an activating immune receptor, MAIR-II, with ITAM-bearing adapters DAP12 and FcRγ chain on peritoneal macrophages". In: *The Journal of Immunology* 178.2, pp. 765–770.

Nakajima, Hideo et al. (1999). "Cutting edge: human myeloid cells express an activating ILT receptor (ILT1) that associates with Fc receptor γ-chain". In: *The Journal of Immunology* 162.1, pp. 5–8.

Nakashima, Jun et al. (2000). "Serum interleukin 6 as a prognostic factor in patients with prostate cancer". In: *Clinical cancer research* 6.7, pp. 2702–2706.

Navarro, Francisco et al. (1999). "The ILT2 (LIR1) and CD94/NKG2A NK cell receptors respectively recognize HLA-G1 and HLA-E molecules co-expressed on target cells". In: *European journal of immunology* 29.1, pp. 277–283.

Nei, M. and S. Kumar (2000). *Molecular evolution and phylogenetics*. Oxford University Press.

Nieswandt, Bernhard and Steve P Watson (2003). "Platelet-collagen interaction: is GPVI the central receptor?" In: *Blood* 102.2, pp. 449–461.

Nikolaidis, N., J. Klein, and M. Nei (2005). "Origin and evolution of the Ig-like domains present in mammalian leukocyte receptors: insights from chicken, frog, and fish homologues". In: *Immunogenetics* 57.1, pp. 151–157.

Nikolova, Elena B and Michael W Russell (1995). "Dual function of human IgA antibodies: inhibition of phagocytosis in circulating neutrophils and enhancement of responses in IL-8-stimulated cells." In: *Journal of leukocyte biology* 57.6, pp. 875–882.

Noel, Greg et al. (2011). "Neutrophils, not monocyte/macrophages, are the major splenic source of postburn IL-10". In: *Shock* 36.2, pp. 149–155.

Nordkamp, Marloes JM Olde et al. (2014). "Leukocyte-associated Ig-like receptor-1 is a novel inhibitory receptor for surfactant protein D". In: *Journal of leukocyte biology* 96.1, pp. 105–111.

Ocuin, Lee M et al. (2011). "Neutrophil IL-10 suppresses peritoneal inflammatory monocytes during polymicrobial sepsis". In: *Journal of leukocyte biology* 89.3, pp. 423–432.

Oehler, Leopold et al. (1998). "Neutrophil Granulocyte–committed Cells Can Be Driven to Acquire Dendritic Cell Characteristics". In: *The Journal of experimental medicine* 187.7, pp. 1019–1028.

Ostanin, Dmitry V et al. (2012). "Acquisition of antigen-presenting functions by neutrophils isolated from mice with chronic colitis". In: *The Journal of Immunology* 188.3, pp. 1491–1502.

Ostrand-Rosenberg, Suzanne and Pratima Sinha (2009). "Myeloid-derived suppressor cells: linking inflammation and cancer". In: *The Journal of Immunology* 182.8, pp. 4499–4506.

Parham, Peter and Ashley Moffett (2013). "Variable NK cell receptors and their MHC class I ligands in immunity, reproduction and human evolution". In: *Nature Reviews Immunology* 13.2, pp. 133–144.

Park, Eek Joong et al. (2010). "Dietary and genetic obesity promote liver inflammation and tumorigenesis by enhancing IL-6 and TNF expression". In: *Cell* 140.2, pp. 197–208.

Pasquier, Benoit et al. (2005). "Identification of FcαRI as an inhibitory receptor that controls inflammation: dual role of FcRγ ITAM". In: *Immunity* 22.1, pp. 31–42.

Pear, Warren S et al. (1993). "Production of high-titer helper-free retroviruses by transient transfection". In: *Proceedings of the National Academy of Sciences* 90.18, pp. 8392–8396.

Pelletier, Martin et al. (2010). "Evidence for a cross-talk between human neutrophils and Th17 cells". In: *Blood* 115.2, pp. 335–343.

Pentcheva-Hoang, Tsvetelina et al. (2007). "Programmed death-1 concentration at the immunological synapse is determined by ligand affinity and availability". In: *Proceedings of the National Academy of Sciences* 104.45, pp. 17765–17770.

Petersen, Thomas Nordahl et al. (2011). "SignalP 4.0: discriminating signal peptides from transmembrane regions". In: *Nature methods* 8.10, pp. 785–786.

Pfirsch-Maisonnas, Severine et al. (2011). "Inhibitory ITAM signaling traps activating receptors with the phosphatase SHP-1 to form polarized "inhibisome" clusters". In: *Science signaling* 4.169, ra24–ra24.

Pillay, Janesh et al. (2012). "A subset of neutrophils in human systemic inflammation inhibits T cell responses through Mac-1". In: *The Journal of clinical investigation* 122.1, p. 327.

Poggi, Alessandro et al. (1998). "p40/LAIR-1 regulates the differentiation of peripheral blood precursors to dendritic cells induced by granulocyte-monocyte colony-stimulating factor". In: *European journal of immunology* 28.7, pp. 2086–2091.

Powles, Thomas et al. (2014). "MPDL3280A (anti-PD-L1) treatment leads to clinical activity in metastatic bladder cancer". In: *Nature* 515.7528, pp. 558–562.

Purdy, Amanda K and Kerry S Campbell (2009). "Natural killer cells and cancer: regulation by the killer cell Ig-like receptors (KIR)". In: *Cancer biology & therapy* 8.23, pp. 2209–2218.

Radsak, M et al. (2000). "Polymorphonuclear neutrophils as accessory cells for T-cell activation: major histocompatibility complex class II restricted antigen-dependent induction of T-cell proliferation". In: *Immunology* 101.4, pp. 521–530.

Rajalingam, Raja, Peter Parham, and Laurent Abi-Rached (2004). "Domain shuffling has been the main mechanism forming new hominoid killer cell Ig-like receptors". In: *The Journal of Immunology* 172.1, pp. 356–369.

Raulet, David H (2006). "Missing self recognition and self tolerance of natural killer (NK) cells". In: *Seminars in immunology*. Vol. 18. 3. Elsevier, pp. 145–150.

Ravetch, Jeffrey V and Lewis L Lanier (2000). "Immune inhibitory receptors". In: *Science* 290.5489, pp. 84–89.

Reth, Michael (1989). "Antigen receptor tail clue." In: *Nature* 338.6214, p. 383.

Ribechini, Eliana et al. (2017). "Novel GM-CSF signals via IFN-γR/IRF-1 and AKT/mTOR license monocytes for suppressor function". In: *Blood advances* 1.14, pp. 947–960.

Rodriguez, Paulo C et al. (2009). "Arginase I–producing myeloid-derived suppressor cells in renal cell carcinoma are a subpopulation of activated granulocytes". In: *Cancer research* 69.4, pp. 1553–1560.

Sade-Feldman, Moshe et al. (2013). "Tumor necrosis factor-α blocks differentiation and enhances suppressive activity of immature myeloid cells during chronic inflammation". In: *Immunity* 38.3, pp. 541–554.

Saitou, Naruya and Masatoshi Nei (1987). "The neighbor-joining method: a new method for reconstructing phylogenetic trees." In: *Molecular biology and evolution* 4.4, pp. 406–425.

Sander, Leif E et al. (2010). "Hepatic acute-phase proteins control innate immune responses during infection by promoting myeloid-derived suppressor cell function". In: *Journal of Experimental Medicine* 207.7, pp. 1453–1464.

Sandstrom, Andrew et al. (2014). "The intracellular B30. 2 domain of butyrophilin 3A1 binds phosphoantigens to mediate activation of human Vγ9Vδ2 T cells". In: *Immunity* 40.4, pp. 490–500.

Sansone, Pasquale et al. (2007). "IL-6 triggers malignant features in mammospheres from human ductal breast carcinoma and normal mammary gland". In: *The Journal of clinical investigation* 117.12, p. 3988.

Scambia, G et al. (1995). "Prognostic significance of interleukin 6 serum levels in patients with ovarian cancer". In: *British journal of cancer* 71.2, pp. 354–356.

Schnabl, E et al. (1990). "Activated human T lymphocytes express MHC class I heavy chains not associated with beta 2-microglobulin." In: *The Journal of experimental medicine* 171.5, pp. 1431–1442.

Schultz, Heidi S, Li Guo, et al. (2016). "OSCAR-collagen signaling in monocytes plays a proinflammatory role and may contribute to the pathogenesis of rheumatoid arthritis". In: *European journal of immunology* 46.4, pp. 952–963.

Schultz, Heidi S, Louise M Nitze, et al. (2015). "Collagen induces maturation of human monocyte-derived dendritic cells by signaling through osteoclast-associated receptor". In: *The Journal of Immunology* 194.7, pp. 3169–3179.

Sedy, John R et al. (2005). "B and T lymphocyte attenuator regulates T cell activation through interaction with herpesvirus entry mediator". In: *Nature immunology* 6.1, pp. 90–98.

Serbina, Natalya V and Eric G Pamer (2006). "Monocyte emigration from bone marrow during bacterial infection requires signals mediated by chemokine receptor CCR2". In: *Nature immunology* 7.3, p. 311.

Shamamian, Peter et al. (2001). "Activation of progelatinase A (MMP-2) by neutrophil elastase, cathepsin G, and proteinase-3: A role for inflammatory cells in tumor invasion and angiogenesis". In: *Journal of cellular physiology* 189.2, pp. 197–206.

Shen, Meixiao et al. (2014). "Tumor-associated neutrophils as a new prognostic factor in cancer: a systematic review and meta-analysis". In: *PloS one* 9.6, e98259.

Sheppard, Kelly-Ann et al. (2004). "PD-1 inhibits T-cell receptor induced phosphorylation of the ZAP70/CD3ζ signalosome and downstream signaling to PKCθ". In: *FEBS letters* 574.1-3, pp. 37–41.

Shiroishi, Mitsunori, Kimiko Kuroki, et al. (2006). "Structural basis for recognition of the nonclassical MHC molecule HLA-G by the leukocyte Ig-like receptor B2 (LILRB2/LIR2/ILT4/CD85d)". In: *Proceedings of the National Academy of Sciences* 103.44, pp. 16412–16417.

Shiroishi, Mitsunori, Kouhei Tsumoto, et al. (2003). "Human inhibitory receptors Ig-like transcript 2 (ILT2) and ILT4 compete with CD8 for MHC class I binding and bind preferentially to HLA-G". In: *Proceedings of the National Academy of Sciences* 100.15, pp. 8856–8861.

Singhal, Sunil et al. (2016). "Origin and role of a subset of tumor-associated neutrophils with antigen-presenting cell features in early-stage human lung cancer". In: *Cancer Cell* 30.1, pp. 120–135.

Sly, Laura M et al. (2007). "The role of SHIP in macrophages". In: *Front Biosci* 12, pp. 2836–2848.

Smith, Isobel A et al. (2010). "BTN1A1, the mammary gland butyrophilin, and BTN2A2 are both inhibitors of T cell activation". In: *The Journal of immunology* 184.7, pp. 3514–3525.

Smith, Kathleen M et al. (1998). "Cutting edge: Ly-49D and Ly-49H associate with mouse DAP12 and form activating receptors". In: *The Journal of Immunology* 161.1, pp. 7–10.

Stafford, J.L. et al. (2006). "A novel family of diversified immunoregulatory receptors in teleosts is homologous to both mammalian Fc receptors and molecules encoded within the leukocyte receptor complex". In: *Immunogenetics* 58.9, pp. 758–773.

Steentoft, Catharina et al. (2013). "Precision mapping of the human O-GalNAc glycoproteome through SimpleCell technology". In: *The EMBO journal* 32.10, pp. 1478–1488.

Steevels, Tessa AM, Kristof Avondt, et al. (2013). "Signal inhibitory receptor on leukocytes-1 (SIRL-1) negatively regulates the oxidative burst in human phagocytes". In: *European journal of immunology* 43.5, pp. 1297–1308.

Steevels, Tessa AM, Robert Jan Lebbink, et al. (2010). "Signal inhibitory receptor on leukocytes-1 is a novel functional inhibitory immune receptor expressed on human phagocytes". In: *The Journal of Immunology* 184.9, pp. 4741–4748.

Sunderkötter, Cord et al. (2004). "Subpopulations of mouse blood monocytes differ in maturation stage and inflammatory response". In: *The Journal of Immunology* 172.7, pp. 4410–4417.

Sykulev, Yuri et al. (1996). "Evidence that a single peptide–MHC complex on a target cell can elicit a cytolytic T cell response". In: *Immunity* 4.6, pp. 565–571.

Takizawa, Hitoshi, Steffen Boettcher, and Markus G Manz (2012). "Demand-adapted regulation of early hematopoiesis in infection and inflammation". In: *Blood* 119.13, pp. 2991–3002.

Tamassia, Nicola et al. (2013). "Cutting edge: an inactive chromatin configuration at the IL-10 locus in human neutrophils". In: *The Journal of Immunology* 190.5, pp. 1921–1925.

Tamura, K. et al. (2011). "MEGA5: molecular evolutionary genetics analysis using maximum likelihood, evolutionary distance, and maximum parsimony methods". In: *Molecular biology and evolution* 28.10, pp. 2731–2739.

Taube, Janis M et al. (2012). "Colocalization of inflammatory response with B7-h1 expression in human melanocytic lesions supports an adaptive resistance mechanism of immune escape". In: *Science translational medicine* 4.127, 127ra37–127ra37.

Tazzyman, Simon, Claire E Lewis, and Craig Murdoch (2009). "Neutrophils: key mediators of tumour angiogenesis". In: *International journal of experimental pathology* 90.3, pp. 222–231.

Teichmann, S.A. and C. Chothia (2000). "Immunoglobulin superfamily proteins in Caenorhabditis elegans1". In: *Journal of molecular biology* 296.5, pp. 1367–1383.

Terashima, TAKESHI et al. (1996). "Polymorphonuclear leukocyte transit times in bone marrow during streptococcal pneumonia". In: *American Journal of Physiology-Lung Cellular and Molecular Physiology* 271.4, pp. L587–L592.

Testi, Râ, JOSEPH H Phillips, and LEWIS L Lanier (1989). "T cell activation via Leu-23 (CD69)." In: *The Journal of Immunology* 143.4, pp. 1123–1128.

Thompson, J.D., D.G. Higgins, and T.J. Gibson (1994). "CLUSTAL W: improving the sensitivity of progressive multiple sequence alignment through sequence weighting, position-specific gap penalties and weight matrix choice". In: *Nucleic acids research* 22.22, pp. 4673–4680.

Thompson, R Houston et al. (2007). "PD-1 is expressed by tumor-infiltrating immune cells and is associated with poor outcome for patients with renal cell carcinoma". In: *Clinical cancer research* 13.6, pp. 1757–1761.

Tivol, Elizabeth A et al. (1995). "Loss of CTLA-4 leads to massive lymphoproliferation and fatal multiorgan tissue destruction, revealing a critical negative regulatory role of CTLA-4". In: *Immunity* 3.5, pp. 541–547.

Turnbull, Isaiah R et al. (2006). "Cutting edge: TREM-2 attenuates macrophage activation". In: *The Journal of Immunology* 177.6, pp. 3520–3524.

Tvinnereim, Amy R, Sara E Hamilton, and John T Harty (2004). "Neutrophil involvement in cross-priming CD8+ T cell responses to bacterial antigens". In: *The Journal of Immunology* 173.3, pp. 1994–2002.

Untergasser, Andreas et al. (2012). "Primer3—new capabilities and interfaces". In: *Nucleic acids research* 40.15, e115–e115.

Van Avondt, Kristof et al. (2013). "Ligation of signal inhibitory receptor on leukocytes-1 suppresses the release of neutrophil extracellular traps in systemic lupus erythematosus". In: *PloS one* 8.10, e78459.

Vavassori, Stefano et al. (2013). "Butyrophilin 3A1 binds phosphorylated antigens and stimulates human [gamma][delta] T cells". In: *Nature immunology* 14.9, pp. 908–916.

Vitale, Massimo et al. (1998). "NKp44, a novel triggering surface molecule specifically expressed by activated natural killer cells, is involved in non–major histocompatibility complex–restricted tumor cell lysis". In: *The Journal of experimental medicine* 187.12, pp. 2065–2072.

Vogel, C., S.A. Teichmann, and C. Chothia (2003). "The immunoglobulin superfamily in Drosophila melanogaster and Caenorhabditis elegans and the evolution of complexity". In: *Development* 130.25, pp. 6317–6328.

Walunas, Theresa L et al. (1994). "CTLA-4 can function as a negative regulator of T cell activation". In: *Immunity* 1.5, pp. 405–413.

Walzer, Thierry et al. (2007). "Identification, activation, and selective in vivo ablation of mouse NK cells via NKp46". In: *Proceedings of the National Academy of Sciences* 104.9, pp. 3384–3389.

Wang, Yang et al. (2005). "The role of herpesvirus entry mediator as a negative regulator of T cell–mediated responses". In: *Journal of Clinical Investigation* 115.3, p. 711.

Welte, Stefan et al. (2006). "Mutual activation of natural killer cells and monocytes mediated by NKp80-AICL interaction". In: *Nature immunology* 7.12, p. 1334.

Wende, Hagen, Armin Volz, and Andreas Ziegler (2000). "Extensive gene duplications and a large inversion characterize the human leukocyte receptor cluster". In: *Immunogenetics* 51.8, pp. 703–713.

Williams, A.F. and A.N. Barclay (1988). "The immunoglobulin superfamily-domains for cell surface recognition". In: *Annual review of immunology* 6.1, pp. 381–405.

Wolf, Hermann M et al. (1994). "Human serum IgA downregulates the release of inflammatory cytokines (tumor necrosis factor-alpha, interleukin-6) in human monocytes". In: *Blood* 83.5, pp. 1278–1288.

Yawata, Makoto et al. (2008). "MHC class I–specific inhibitory receptors and their ligands structure diverse human NK-cell repertoires toward a balance of missing self-response". In: *Blood* 112.6, pp. 2369–2380.

Yoder, J.A. et al. (2001). "Immune-type receptor genes in zebrafish share genetic and functional properties with genes encoded by the mammalian leukocyte receptor cluster". In: *Proceedings of the National Academy of Sciences* 98.12, p. 6771.

Yoshinaga, Steven K et al. (1999). "T-cell co-stimulation through B7RP-1 and ICOS". In: *Nature* 402.6763, p. 827.

Youn, Je-In et al. (2008). "Subsets of myeloid-derived suppressor cells in tumor-bearing mice". In: *The Journal of Immunology* 181.8, pp. 5791–5802.

Zhang, Xiaoming et al. (2009). "Coactivation of Syk kinase and MyD88 adaptor protein pathways by bacteria promotes regulatory properties of neutrophils". In: *Immunity* 31.5, pp. 761–771.